EXPERIMENTAL MEASUREMENT OF COMBUSTION NOISE AND COMPARISON TO A PREDICTIVE MODEL

by

William J. Westerman III

Thesis submitted to the Faculty of the

Virginia Polytechnic Institute and State University

in partial fulfillment of the requirements for the degree of

Master of Science

in

Mechanical Engineering

APPROVED:

L. A. Roe, Chairman

J. R. Mahan

C. J. Hurst

June 1991

Blacksburg, Virginia

EXPERIMENTAL MEASUREMENT OF COMBUSTION NOISE AND COMPARISON TO A PREDICTIVE MODEL

by

William J. Westerman III

(ABSTRACT)

The acoustic emission from the combustion of turbulent mixtures of several gaseous fuels and oxygen was measured to determine the effect of burner diameters, flow velocities and reactant chemistries. The data are presented in the form of acoustic pressure spectra and over-all sound pressure levels.

The experiment consisted of a geometrically simple pre-mixed burner with five interchangeable nozzles whose diameters varied from 0.117 cm to 0.541 cm. The fuels examined in the experiment were acetylene, methane and propane. Three flow velocities were tested for each fuel. Methane was tested within a velocity range of 10 m/s to 25 m/s while propane was examined within a range of 20 m/s to 40 m/s. Acetylene was tested at somewhat higher velocities ranging from 50 m/s to 100 m/s.

The resulting data base consisted of 23 unique test conditions. The data were evaluated based on peak frequency and overall sound pressure level. The experimental data are also compared to a predictive model.

Acknowledgements

The author wishes to express his sincere appreciation to Dr. L. A. Roe for his encouragement, aid, and guidance throughout this work. He also wishes to thank Dr. J. R. Mahan and Dr. C. J. Hurst for serving on his advisory committee.

The author would also to thank Liat Zindorf for her love and encouragement and especially her "beyond the call of duty" assistance in taking data at odd hours of the night.

Finally, the author would like to thank his parents, Dr. and Mrs. W. J. Westerman II for their motivation and financial support. He is particularly indebted to his father who always expressed great interest in the work and offered many free engineering consultations.

Table of Contents

List of Illustrations

List of Tables

List of Symbols

a, b, c, d	Constants in the transition burning expression
c	Velocity of sound in air (m/s)
d	Distance of the field point from source (m)
D	Burner Diameter (m)
E	Expansion ratio (-)
f	Frequency (Hz)
f_c	Frequency of the maximum radiated sound power (Hz)
F	Fuel mass fraction (-)
H	Heat release rate (kJ/s)
n	The effective number of noise sources
OASPL	Over-All Sound Pressure Level (dB)
OAPWL	Over-All Sound Power Level (dB)
P	Acoustic pressure (N/m^2)
p	Nondimensional acoustic pressure (-)
Q	Volumetric flow rate (m^3/s)
R	Radius of the spherical cell (m)

r	Instantaneous radius of the spherical cell (m)
S_L	Laminar flame speed of the fuel (m/s)
S_P	Sound Power (W)
t	time (s)
t_i	Fuel injection time (s)
U	Convective velocity of the fuel (m/s)
V	Volume (m^3)

Greek Letters

β	Quantity used to nondimensionalize d^2V/dt^2 (m^3/s^2)
γ	Quantity used to nondimensionalize acoustic pressure (N/m^2), Eq. (4.34)
ρ	Density of air (kg/m^3)
τ	Nondimensional time (-)

Subscripts

b	Order of the frequency band
bl	Quantities associated with the lower frequency of the "b" band

bu	Refers to the quantities associated with the upper frequency of the "b" band
i	Refers to the initial value of the corresponding quantities
n	Refers to the order of frequency
s	Refers to the surface burning process
tr	Refers to the transition burning process
tt	Refers to the complete process of burning

1.0 Introduction

In many practical industrial and commercial systems, turbulent combustion is used as an energy source. In all cases, these flow systems become noisy due to the combustion process. In turbopropulsion applications, combustion noise has been recognized as a potential contributor to core engine noise. In the interest of minimizing the noise from these combustion processes, much research has been devoted to measuring and describing the acoustic emission of such systems.

An understanding of the noise production mechanism of turbulent combustion can suggest ways of reducing such noise. Recently, studies have been conducted to control combustion noise by introducing cancelling sound waves via a feedback control system.

However, perhaps the most important use of combustion noise may be as a diagnostic tool to determine operating conditions of a process. Evidence strongly suggests that the acoustic noise of a flame is a strong indicator of stability characteristics in the reacting flow system. Under extreme conditions, combustion noise can be extensive enough to be destructive to the combustion chamber.

Despite the research into combustion noise in the past twenty-five years, the details of the noise production are still unclear. From an experimental standpoint, only a

limited amount of work has been devoted to measuring the sound emission from turbulent combustion systems. Such data have indicated that several parameters strongly influence the noise from combustion. It has been shown that burner geometry, reactant flow velocity, flame speed, and flame temperature affect the sound spectra and overall sound pressure levels in a turbulent combustion process [2,3]. However, the available experimental data do not lend well to understanding the noise production mechanism due to either overly complicated burner configurations or, simply, too few test conditions to determine the effects of varying relevant experimental parameters. This also makes it difficult to evaluate theoretical explanations of combustion noise.

The goal of this study is to obtain an experimental data base of combustion noise measurements for a variety of relevant experimental inputs. In addition, it is desirable to utilize a simple experimental apparatus to allow the data to have a wide range of application for the evaluation of theoretical models. Yet to design such an experiment, it seemed necessary to consider the requirements of evaluating such models.

Because of its availability and its recent development, the theoretical model of Mahan-Nathani [1] was selected as a guide to designing the experiment and also to test the usefulness of the data base for modellers in general. This model addresses the physics of the noise generation process and relies, not in correlation to existing data, but in a simple explanation of the noise generation in turbulent flames. The model, which attempts to predict the sound spectrum and over-all sound pressure level of a reacting flow, appears to exhibit spectral trends which are in general agreement with existing data. However, the lack of a general data base of sound spectra prevents the merit of the theoretical model from being fully evaluated. This study also attempts to perform such an evaluation.

2.0 Literature Review

Past experimental efforts into the acoustic emission of turbulent flames concentrate on a particular aspect of some practical application. These results, however, are not applicable to a wide range of combustion situations. This lack of an experimental data base as a reference for theoretical comparison is the primary motivation for the work presented here. The greatest concern with most theoretical exercises in explaining the mechanisms of combustion noise is the lack of experimental evidence to support or dismiss such models. The experimental work which has been conducted is limited in scope and consistency between individual efforts. Overviews on the experimental and theoretical efforts of the past are presented in References 2 and 3. It is evident in more recent studies that the field of combustion acoustics is tending toward the use of sound emission as a diagnostic tool.

The relationship between combustion and acoustics has been recognized and reported since as early as 1802 in a technical note on singing flames [4]. In 1896, Lord Rayleigh [5] gave the first satisfactory theoretical explanation of such noise. He suggested that periodic heat supply from the flame induces upstream gases in a burner to vibrate at its characteristic organ-pipe frequency.

As noise pollution became exceedingly more important in the 1950's (with the dawn of jet propulsion), a renewed interest was taken in understanding and reducing the noise emission of combustion processes in commercial burners and jet engines. The foundation of much of this modern theory is based on Lighthill's theoretical treatment of sound radiated from a non-reacting fluid flow as a result of turbulence [6,7]. This work is the first to model the sound emission from a turbulent flow as a static distribution of fundamental acoustic noise sources. Lighthill showed that the fluctuating shear in the turbulence acts a quadrapole sound source.

Following Lighthill's treatment of sound radiated from turbulent flow, Gaydon and Wolfhard [8] reasoned that the noise from turbulent diffusion flames might be a result of continuous ignitions of "turbulent balls" of mixed air and fuel. This view appears to be consistent with research that soon followed.

A decade after Lighthill's turbulent flow noise model, Bragg (in 1963) [9] extended this rudimentary theory to apply to a combusting flow. He suggested that a small element of combusting fuel, burning at constant pressure, would displace surrounding gases due to the increased volume of products as a result of heat evolution. This spherical pressure wave would be followed by an expansion wave at the end of combustion, thereby bringing the surroundings to rest again. Bragg's example illustrated the characteristics of a simple monopole source. In this instance, the total sound energy radiated by the combustion process and the intensity at any point would depend on both the rate of change of volume evolution ($\frac{d^2V}{dT^2}$) and the rate of volume evolution itself ($\frac{dV}{dT}$). In addition, Bragg concluded that the noise produced directly by the non-reacting flow is negligible in comparison to the combustion source noise resulting from unsteadiness in local heat release rates. This direct acoustic noise of combustion was estimated to be about one millionth (10^{-6}) of the total energy release of the combustion. It is important

to note that this theory insists that a laminar flame would emit no combustion noise due to the steadiness of the reaction.

The theory of combustion noise as represented by a series of reacting monopole sources was reinforced by the work of Smith and Kilham [10] in 1963. Experimental observations allowed them to relate sound pressure to various geometrical and flow parameters using scaling laws. For premixed flames of propane, ethylene, and methane with air, they found that the acoustic power was proportional to UDS_L for various fuel-air mixtures; where U is the convective velocity of the mixture, D is the diameter of the nozzle, and S_L is the laminar flame speed. They concluded by showing that this relationship is similar to that of the acoustic output of a statistical distribution of simple monopole sources throughout the combustion zone.

In 1966, Thomas and Williams [11] performed an experimental study of the noise produced by the combustion of a spherical volume of homogeneous premixed gas contained in a soap bubble and ignited by a spark. The study considered both surface ignition and central ignition of the spherical volume. This experimental approach was chosen in an attempt to study the basic relationship between flame structure and sound radiation for a simple combustion system. They found that this combustion process acted as a simple monopole source whose strength is a function of the rate of volume variation ($\frac{d^2V}{dT^2}$). In addition, Thomas and Williams found a strong relationship between sound emission and flame speed. A thorough physical examination of the propagating flame was made using high speed motion picture photography and is presented in the paper. This experimental evidence indicated that the centrally ignited bubble does in fact act as a monopole source and the flame expansion ratio directly affects the noise output.

Giammar and Putnam [12] examined the acoustic output of two commercial turbulent diffusion burners, combusting natural gas. Both burners were impinging gas jet types. The first configuration consisted of two axially impinging jets, the second

burner being an "octopus" burner configuration with eight impinging jets pointed from eight corners of a geometric cube towards a common center. The effects of flow rate and burner diameter were examined. They identified various sources of combustion noise and, based on the acoustic pressure spectra, showed that this noise was dominant in the 160 to 1000 Hz range.

An extensive analysis of non-premixed flames was performed by Knott [13] in 1971. In particular, Knott considered non-resonating flames of hydrogen and ethylene with oxidizers of oxygen and air. The effects of burner diameter, equivalence ratio and flow rate on acoustic power were examined. It was determined that acoustic power is proportional to U^4_{fuel}. Finally, based on experimental results, Knott proposed a model comprised of monopole noise sources.

In 1975, Kumar [14] reviewed Knott's work and although he commends Knott on the bulk of his work, he questioned the method of premixing the fuel and oxidizer in Knott's apparatus and did not feel that fully developed pipe flow was achieved for the tests. However, Kumar does not cite why he believes this fault renders the data unreliable. In his own experiments, Kumar measured the sound spectra of premixed and nonpremixed methane and enriched air flames. He found "profound differences" between the two configurations with the sound power of the premixed flame proportional to U^3 and the nonpremixed flame output proportional to U^4. For the experimental tests performed, Kumar presents acoustic pressure spectra, time domain pressures and data relating to the directionality of the sound emitted from the flames.

Chiu and Summerfield [15] offered correlations between acoustic power and turbulence scales and intensities for open flames and liquid spray combustors. Furthermore, they examined the sound emission and resonance in ducted combustors. Data is presented in the form of acoustic pressure spectra for the combustion processes examined. Of particular interest was the comparison between near field and far field spectra which

showed identical frequency distributions. They concluded that the noise generation was attributed to various non-steady phenomena including turbulent fluctuations and acoustic instabilities inherent in the burner design.

Perhaps the most widely cited research of the 1970's belongs to Strahle [3,16,17,18]. He based his theory of combustion noise on Lighthill's [6,7] aeroacoustic model. Strahle proposed that the sound emitted from a turbulent flame is proportional to the reaction rate time derivative. In addition, he offered further evidence that the sound source possesses monopole behavior. Strahle was able to derive meaningful scaling rules, based on his own experimental evidence, to correlate the acoustic output of turbulent flames. Acoustic pressure spectra presented by Strahle indicate that most of the noise occurs in the range of 200 to 2000 Hz. Based on experimental data, Strahle developed a scaling law to predict the sound pressure levels to be

$$S_P = 0.625X10^{-5}U^{2.67}D^{2.81}S_L{}^{1.83}F^{-.026}\,, \tag{2.1}$$

where the convective velocity (U) and flame speed (S_L) are in feet per second, burner diameter (D) is in feet, and fuel mass fraction (F) is unitless. The standard deviation of these results was determined to be 37 percent.

Shivashankara et al. [19,20] considered flames with flow velocities to 600 fps and burner sizes ranging up to one inch in diameter. The data is presented in the form of pressure spectra in the time domain and frequency domain. Based on this experimental data and other published results, scaling laws were developed to predict acoustic output of turbulent flames. These scaling laws consider the fuel mass fraction to be independent of flame speed. In addition, the study notes that the directivity in the combustion noise source varies by less than 4 dB with the peak pressure recorded axially downstream of the flow. It should be emphasized that these scaling laws only predict the total sound

power output of the turbulent flame and do not address the spectral distribution of the combustion noise.

Mathews and Rekos [21] attempted to apply the analytical relationship of Strahle to several burner configurations and to a full-scale turbofan engine. Frequency spectra were examined for peak frequencies and over-all sound pressure levels. The predictions of Strahle for sound pressure level proved to be in good agreement with noise data obtained from the tested combustors. They conclude by discussing a number of relationships between experimental variables and measured acoustic data.

The work of Lighthill and Strahle was further advanced by Dowling [22] in 1978 to include the effect of variation of mean temperature and flow velocity at the flame front. In particular, he examined the refraction of sound waves as they pass through the combustion zone. His work offered an explanation of why Strahle's theory failed to predict the observed non-uniformities in the sound field of a turbulent flame.

In 1979, Ramohalli [23] considered the possibility of inferring information regarding the operating conditions of a flame through examination of the acoustic emission of the combustion system. Based on photographic observations and the frequency spectra of the tested flames, a simple model was developed to extract information regarding the acoustic field. The photographs of the flame explicitly show that large eddies form first and then break down into smaller and smaller eddies. This was an important step in using the sound spectra of a flame as a diagnostic tool to determine combustion details such as turbulence and reaction rates. In addition, the effect of air-fuel ratio on frequency spectra is presented.

Ho and Doyle [24] presented a parametric expression for the prediction of sound power levels. By applying the effective combustor discharge temperature, they found good agreement between their model and experimental data. Furthermore, the experimental data is presented as frequency spectra which show peak frequencies to be about

450 Hz for the experimental tests performed. The model was found to apply to a broad range of applications including gas turbine engines.

Ramachandra and Strahle [25] developed a nonintrusive acoustic technique to determine heat release rates and turbulent properties in an open premixed turbulent flame. This technique reinforces the importance of utilizing the acoustic emission of the flame as a diagnostic tool for determining operating conditions of the combustion system. Utilizing the optical emission of C_2 radicals as an indicator of heat release, they concluded that the fluctuating heat release rate can be deduced from the sound spectrum of the flame.

A thorough study of the effects of burner size and shape on over-all sound pressure levels and frequency spectra was conducted by Kotake and Takamoto [26]. The performance of rectangular, square and circular burner nozzles of various sizes was studied over a range of equivalence ratios. It was found that nozzle shape had little effect on the noise spectra for fuel rich flames; however an appreciable effect was observed for fuel lean flames. Correlations of the acoustic output were determined for flow velocity and effective burner diameter.

The acoustic emission of open turbulent diffusion flames was examined by Seshan [27] in 1986. The performance of two different diameter burners was examined as were two industrial furnaces. The two burners studied were tested for the combustion of methane. Upon examining the data, Seshan found a common spectral shape for a wide range of operating and burner configurations. Peak frequency ranges correlated well with the cold flow Reynolds number as predicted by theoretical estimations. He concluded by suggesting that an algorithm might be developed to monitor and control industrial burners through the acoustic output of the flame.

In 1987, Mahan [28] reconsidered the work of Thomas and Williams [11] and their examination of the surface ignition of combustible bubbles. His model assumed

that a stream of turbulent eddies, of initial diameters distributed about a specific mean value and standard deviation, enter the combustion zone and are burned via surface ignition. A Fourier analysis of the pressure-time series resulting from a continuous stream of these reacting eddies produced a line spectrum. When converted to a third-octave band pressure spectrum, the results closely resembled those obtained experimentally by Thomas and Williams. This study was perhaps one of the first successful attempts at predicting an acoustic spectrum of a turbulent combustion process.

In 1988, Mahan and Nathani [29] improved upon Mahan's original model. The previous model had not considered the convective velocity of the eddy while entering the flame front. Experimental evidence had shown that this is an important parameter in the noise production process. The improvement included a transition burning period during which the eddy enters the combustion zone. In a second phase,the eddy is assumed to burn uniformly as described in the original model.

Based on Mahan's work, Nathani [1], developed a model which more closely approximates reality. The model predicts a third-octave pressure spectra and over-all sound pressure levels based on burner diameter, flow velocity, laminar flame speed, flame temperature, and several parameters applying to the acoustic environment. From available data at the time, the model appeared to yield good results. Yet, to determine its validity, the model needs to be thoroughly exercised using consistent experimental data.

In general, past studies have concentrated on a particular application of combustion noise production; a complete and consistent data base which utilizes a simple burner and considers relevant variables does not exist. In addition, the theoretical studies cited consider, at best, the total sound output of the turbulent combustion process and do not attempt to predict the spectral distribution of this noise. The development of noise production theory has reached a stage where a consistent data base is necessary to aid in evaluation.

3.0 Experimental Design

To allow the data to be as useful as possible to theorists, the Mahan-Nathani model [1] was obtained as a guide in designing the experiment. The model then suggested the parameters to be examined. From the theory, discussed in Appendix A, relevant inputs were then determined to be burner diameter, flow velocity, and fuel chemistries.

3.1 Burner design

In keeping with the simplicity of the theoretical model, it was important to utilize a geometrically simple burner. For this reason, a Harris Model #85 (Serial number 0688) standard commercial type oxy-acetylene welding torch was chosen for mixing and regulating the fuel and oxygen flows. The torch was modified to accept a range of burner nozzles which threaded onto the torch handle, replacing the standard welding tips. Because the objective of the study was to exercise the theoretical model, it was necessary to be able to systematically adjust each theoretical variable independent of the other

model variables. This configuration allowed easy alteration of fuel type, flow velocities, and burner diameters thereby addressing all model parameters. The burner allowed for safety and portability which was also a fundamental requirement for the experiment.

The oxygen and fuel are mixed in a small chamber in the welding torch. From there, the flow is directed through a small orifice past which the passage diameter gradually increases until the mixture reaches the torch head. The small orifice acts as a flame arrester should the flame front propagate upstream to the mixing chamber. Nassau Rockmount resettable flashback arresters were also provided at the base of the torch for both fuel and oxidizer. From the torch head, the flow then passes through the chosen burner nozzle.

Five nozzles were constructed to thread into the torch head. The available nozzle inside diameters were 0.117 cm, 0.165 cm, 0.356 cm, 0.414 cm, and 0.541 cm. Each nozzle was 13.34 cm in length. For acetylene and propane, the three smallest burners were tested, and for methane, the three largest burners were used. For the fuels tested, the burners used were selected based on the limits of flashback and blow-off. The nozzles were constructed of ASTM 4140 steel tubing and a 3/8 inch bolt. The head of the bolt was drilled to match the outside diameter of the given tubing. After inserting the tubing into the machined bolt, the two pieces were silver soldered. A smoothly converging nozzle shape was machined into the base of each burner to aid in achieving developed flow. The burner construction allowed a range of nozzle diameters to be conveniently threaded into the torch head which accepted the 3/8 inch 28 thread.

3.2 *Oxidizer Selection*

Oxygen was selected as an oxidizer for the fuels tested although many past experimental efforts utilized air. The reason for this was that oxygen offers wider flammability limits for a given fuel. This allowed a wider range of conditions to be tested experimentally. In addition, oxygen allowed a more stable flame with the desired simple burner configuration without the need of external flame holders as air (as an oxidizer) would dictate.

Mixture ratios were based on the neutral flame concept (Appendix B) which provides for complete combustion via premixed oxygen and entrained atmospheric air. This was an important step in determining an overall stoichiometric fuel and oxidizer mixture.

3.3 *Flow Control*

Supply pressures for the various gases were controlled by two-stage regulators. The oxygen cylinder pressure was regulated by an Industrial Gas and Supply regulator (Model number 25-100). For acetylene and methane, an Industrial Gas and Supply regulator (Model number 25-15) was used. For the considerably lower pressure propane, a Matheson regulator (Model number 9) was used.

Gas flow was controlled and measured using three different flow meters: Brooks Instrument Division Model No. 1112CH11fE2AA; Cole Parmer Instrument Co. Model No. FM034-39; Cole Parmer Instrument Co. Model No. FM044-40. The Cole Parmer

Model FM044-40 was used exclusively for oxygen flow while the other two flow meters were used for fuel flows depending on the required flow rates.

The flow meters were calibrated using a Singer American Meter Division 802 (serial number K871130) gas meter. To allow for any pressure drop that may have occurred through the burner configuration, the flow from the burner exit was measured by the gas meter for a range of flow meter scale readings and the time was recorded for the given flow volume using a stop watch. This allowed calibration charts to be created for each meter with respect to the particular gas flow/pressure drop conditions.

3.4 Data Acquisition

A microphone was used in conjunction with a real-time analyzer to measure the acoustic signal. Sixteen samples of the acoustic emission were collected and averaged using a Spectrascope Model SD330A-7 Real-Time Analyzer (Serial Number 251) to produce a spectral distribution for each test point. The spectra were then digitized and stored on an IBM PC. A block diagram of the instrumentation is shown in Figure 1.

A Bruel and Kjaer 4133 microphone and Bruel and Kjaer Type 2801 power supply were used to convert the acoustical pressure output of the burner into an electrical signal. The signal was then amplified by a Realistic Pre-amplifier (Model 42-2101A) rated at 1.5 Watts. The output of the amplifier provided the required input signal for the spectrum analyzer.

The acoustical signal from the amplifier was converted into a frequency spectrum by the real-time analyzer. The analyzer utilizes a series of frequency-tuned bandpass filter to convert the input electrical signal from the time domain to the frequency domain.

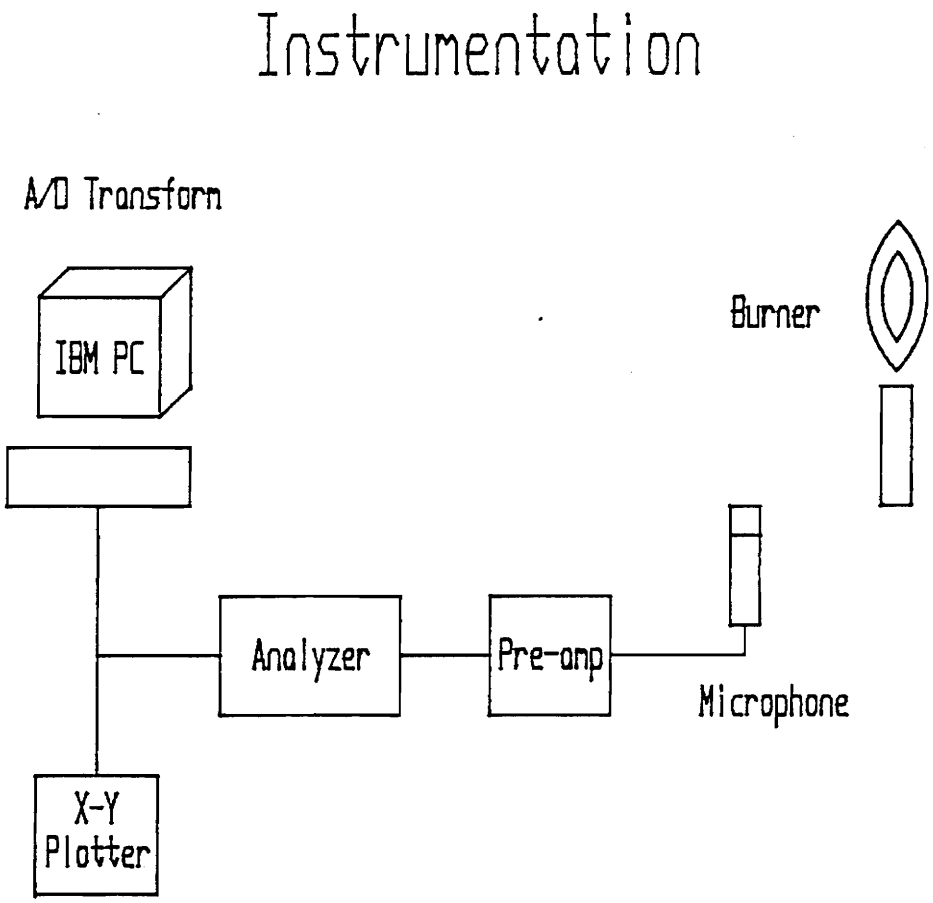

Figure 1. Block diagram of acoustic instrumentation

To achieve minimum analysis time, the analyzer employs time compression techniques. Following the compression, the input signal is frequency analyzed using 250 synthesized filter locations that are tuned by a built-in sweep generator. The analyzer range could be varied from 25 Hz to 20,000 Hz and a wide range of input bands and output gains could be selected to achieve maximum sensitivity. The analyzer also allowed for averaging to condition a noisy signal. In keeping with past experimental efforts, a frequency range of 0 to 10,000 Hz was used for experimental measurement. In addition, the signal was sampled and averaged 16 times to minimize time domain randomness encountered during testing.

The analyzer can store an averaged spectrum which may later be plotted via a 1 to 5 Volt output signal for both the X-axis (frequency) and Y-axis (pressure). These output signals were instead transformed to digital signals using a Data Translation Series DT2811 analog and digital I/O board. The board was configured for an analog to digital conversion and was installed in an IBM PC. This allowed the data to be stored digitally on 5 1/4 inch floppy diskettes. The signal board was controlled by a BASIC program written specifically for this application. The digital data were later converted from voltages to frequency and pressure and reduced for inspection and plotting. Calibration of the data acquisition system is discussed in the Procedure section.

3.5 Acoustic Environment

Although is was desirable to conduct the acoustic tests in an anechoic chamber, it was infeasible due to the possible fire hazard of running an open flame in a small room with walls of raw insulation. In addition, the soot generated by the acetylene flame

during initial start-up made running the tests in a confined area impractical. Because of these problems, it was decided to run the tests outside. This is a common method of running acoustic tests on large equipment that cannot be tested in an anechoic chamber. This method only requires an open space free of standing structures which might reflect generated sound waves. Generally, a microphone is placed at ground level, in accordance with ANSI standard S1.34-1980 (ASA 14-1980) and the true sound pressure is then half of the pressure measured by the microphone.

After considering several alternatives, it was decided to conduct the tests at Virginia Polytechnic Institute and State University's Prices Fork Research Center. The Mechanical Engineering Department's Rocket Testing Laboratory offered an instrumentation building at the base of a steep hill adjacent to a large flat field. The height of the roof of the building was just even with the field surface. This allowed the tests to be run on top of the building while the instrumentation was kept secure within the building. The nearest standing structure was another small building approximately 200 yards away.

A four-foot-square testing pad was constructed to allow the microphone to be mounted at ground level. The stage was constructed of two-by-fours and half-inch plywood such that the height of the platform was about four inches. The platform with the mounted microphone was placed flat on the roof of the test building with the burner placed upon the platform. The microphone was placed one meter below the burner exit and one meter away from the point where the burner axis intersected the platform. This gave the microphone a total distance of just over 1.4 meters from the noise source, as shown in Figure 2, such that far-field sound waves could be assumed down to approximately 350 Hz.

It was readily observed in preliminary testing that a breeze could cause instabilities in the reacting flow. Since this did not reflect the true noise of the combustion process,

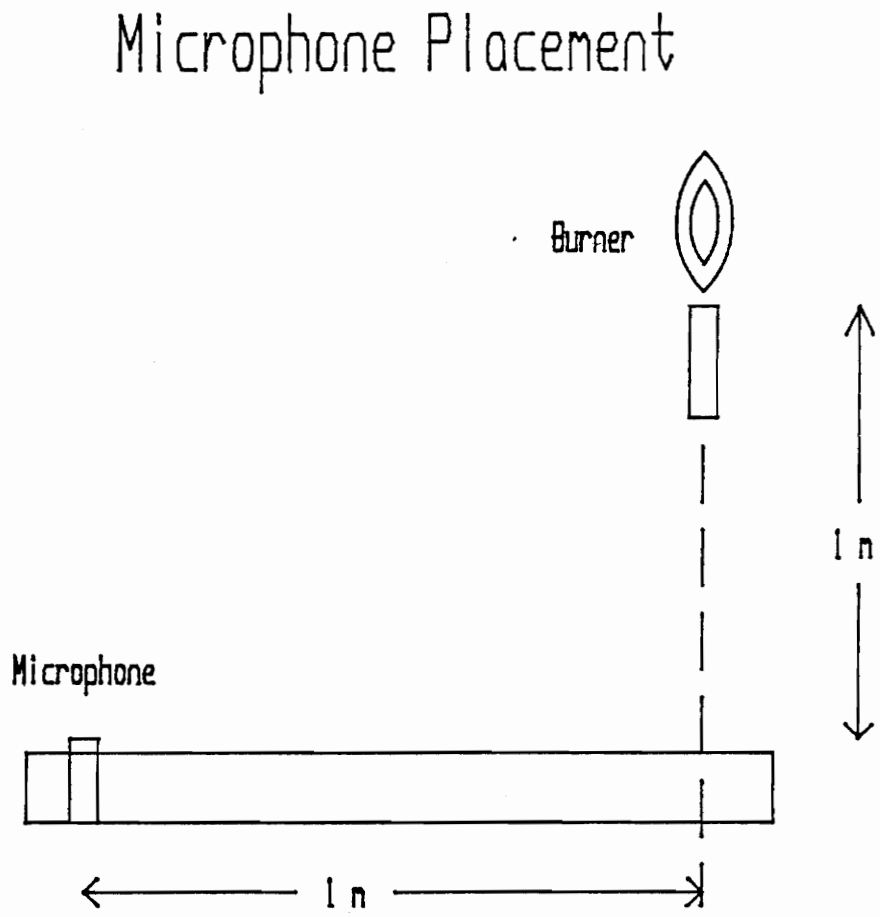

Figure 2. Microphone placement relative to the burner

it was desirable to conduct the tests under very calm weather conditions. During daylight hours, a breeze was consistently blowing off the barren field next to the test site. However, a few hours after sunset each day, much calmer conditions generally prevailed. In addition, at night fewer disturbances from Prices Fork Road, approximately a quarter of a mile away, were evident. It was therefore obvious that the most reliable data could be collected on very calm nights.

Acetylene data was collected in the early morning of July 4, 1990; Propane data was collected late night on July 5, 1990; Methane data was collected late night on July 23, 1990.

Once the experimental apparatus was obtained, the experimental procedure was next designed. The next chapter discusses the determination of test points to be examined, the calibration of the instrumentation and the experimental method which was followed.

4.0 Experimental Procedure

4.1 Determination of Test Matrix

4.1.1 Equivalence Ratio

Initially, the possible range of burner diameters, flow velocities and mixture ratios for each fuel had to be determined. It was noticed at preliminary stages of the experimental work that a premixed stoichiometric flow of fuel and oxygen caused high-frequency instabilities. It was theorized that the flame might in fact be over-oxidized due to entrained atmospheric air. These instabilities had to be avoided if the true direct noise of the combustion process was to be measured. This necessitated the use of a different criterion for determining fuel-oxygen mixtures.

Mixture ratios were chosen based on the neutral flame concept (Appendix B) which provides for complete combustion of the fuel via premixed oxygen and entrained atmospheric air using visual inspection. The mixture for each fuel was adjusted until

only two flames zones were visible and this ratio was applied to all tests for that fuel. This was an important step in determining an overall stoichiometric fuel and oxidizer mixture.

4.1.2 Burner Diameter and Flow Velocity

To determine the range of flow velocities to be tested, each burner was examined for a given fuel. The flow velocity of the reacting mixture was decreased until flash-back occurred. This velocity was the lower limit for the fuel and burner combination. Next, the flow velocity of the reacting mixture was gradually increased until blow-off occurred. This velocity was the upper limit for the fuel and burner combination. Another such limiting factor for the fuels tested was the limited flow rate that could be generated using the given pressure regulators and flow meters. For acetylene and propane, this limiting factor dictated the use of only the smallest three burner nozzles. Conversely, stable methane flames were not attainable for the smallest two diameters and only the three largest burner nozzles were tested.

Once the stability limits for the given fuels were determined, a range of three flow velocities was selected, the highest and lowest being slightly within the indicated velocity limits. It is not surprising that all burner sizes tested for a given fuel exhibited very similar flash-back and blow-off flow velocities as these are directly related by the laminar flame speed of a given mixture.

4.2 *Acoustic Calibration*

The acoustical instrumentation was calibrated using a General Radio Company Type 1567 Sound Level Calibrator (Serial number 15480) with an output of 114 dB at 1000 Hz. The sound level calibrator output was confirmed using a Columbia Model SPL-103 Sound Level Meter (Serial number E2223). The microphone was placed in the calibrator with the proper adaptor and the resulting pressure-frequency spectrum was determined by the spectrum analyzer. This spectrum was then routed to the x-axis and y-axis pen plotter outputs, converted to two digital signals by the A/D board, and recorded as a single data set of voltages representing coordinates of the pressure-frequency spectrum. This was repeated for all possible analyzer input range and output gain combinations. The calibration procedure was performed a total of 22 times for the different input range/ output gain combinations and a 95 percent confidence interval showed an uncertainty of +/- 0.289 percent for the pressure amplitude output. With the known analog microphone pressure and frequency inputs and the recorded digital output, the output voltage signal from the microphone could be determined for the known input sound source. This allowed for the raw voltages to be converted to the corresponding frequency and pressure data by applying the calibration results when experimental measurements were later taken.

The integrity of the analyzer was tested using a Bruel and Kjaer Sweep/Function Generator (Serial number 89-09556) in conjunction with a Hewlett Packard 5314A Universal Counter (Serial number 2204A09094). Various periodic signals were applied to the analyzer at known frequencies and the frequency spectra were verified.

A white noise generator was used to assure a flat response for the microphone.

4.3 *Test Procedure*

The test matrices used for the experiments are shown in Tables 1-3. These tables indicate the flow velocities for the fuel and oxygen and the indicated flow meter scale readings to obtain the desired flows for the given burners.

The experimental procedure consisted of connecting the test fuel to the flow meters and selecting the desired burner nozzle. An initial flow of fuel only was ignited and the two flow meters were then adjusted until the proper flow velocities of the fuel and oxygen were achieved. Next, the input range and output gain of the real time analyzer were adjusted to achieve maximum resolution without overloading the analyzer input. The acoustic signal was then averaged 16 times and the resulting spectral distribution was stored in the analyzer memory.

The analog-to-digital (A/D) board control program was prepared to begin receiving data from the analyzer by selecting the plotting function on the analyzer. The analyzer's X and Y plotter outputs were in fact connected to the A/D board. The analyzer transferred the stored averaged frequency spectrum to the digital A/D board over a period of about one minute. Because the pen plotter outputs are intentionally rate-controlled to limit pen speed, a high sampling rate was chosen on the A/D board to ensure faithful replication of the spectrum. Essentially, then, the acquisition of the spectral data can be interpreted as the determination of 250 pressure-frequency data points by the analyzer, the fitting of an analog curve to form a spectral shape, the transmission of this analog function to an A/D board, and the conversion to discrete points again. The sampling rate chosen produced about 2000 coordinate points for each spectrum. The data was stored on disk under a file name unique to the given test condition. This procedure was repeated for all experimental test points. The background

Table 1. Acetylene Test Matrix

Fuel and Burner Parameters		Volumetric Flow Rate	
D (cm)	U_{mix} (m/s)	$Q_{C_2H_2}$ (l/min)	Q_{O_2} (l/min)
0.117	50	1.61	1.61
0.117	75	2.41	2.41
0.117	100	3.22	3.22
0.165	50	3.21	3.21
0.165	75	4.82	4.82
0.165	100	6.42	6.42
0.356	50	14.9	14.9
0.356	75	22.3	22.3

Table 2. Methane Test Matrix

Fuel and Burner Parameters		Volumetric Flow Rate	
D (cm)	U_{mix} (m/s)	Q_{CH_4} (l/min)	Q_{O_2} (l/min)
0.356	10	3.58	2.38
0.356	20	7.15	4.77
0.414	10	4.85	3.23
0.414	20	9.69	6.46
0.414	25	12.1	8.08
0.541	10	8.28	5.52
0.541	20	16.6	11.0
0.541	25	20.7	13.8

Table 3. Propane Test Matrix

Fuel and Burner Parameters		Volumetric Flow Rate	
D (cm)	U_{mix} (m/s)	$Q_{C_3H_8}$ (l/min)	Q_{O_2} (l/min)
0.117	20	0.429	0.858
0.117	30	0.643	1.29
0.117	40	0.858	1.73
0.165	20	0.857	1.71
0.165	30	1.28	2.57
0.165	40	1.71	3.43
0.356	20	3.97	7.94
0.356	30	5.96	11.9

noise was measured on each date of testing as a reference for any possible variation that might have existed. In addition, the spectra for several non-reacting flows were measured for reference.

4.4 Data Reduction

4.4.1 Constant Bandwidth Spectra

Each file of raw data consisted of up to 2,000 spectral samples due to the high sampling rate of the A/D board. The analyzer, however, generated only 250 discrete frequency coordinates with its band-pass filters. The raw data did not perfectly reveal these discrete points. The closest coordinates to the center frequencies measured by the analyzer were then selected for the reduced data file. At frequencies below 2000 Hz, where the spectrum was rather complicated and the analyzer transferred data at a relatively slow rate, the raw data files contained a high density of frequency-pressure coordinates. For these lower frequencies, the analyzer center frequencies could generally be matched within 0.5 percent by the raw data frequencies. At frequencies above 5000 Hz, where the spectrum was relatively flat, the analyzer center frequency could be matched within 3 percent. A BASIC program was written to perform this reduction and is shown in Appendix C.

4.4.2 Overall Sound Pressure Level

The overall sound pressure level was generated from the constant percentage bandwidth data. Because each of the 250 points generated in this data represents a RMS pressure value, the overall sound pressure level was calculated by also taking an RMS pressure of all of the constant bandwidth pressure components. This reduction was performed by a BASIC program shown in Appendix C.

4.4.3 Third Octave Band Spectra

The constant percentage bandwidth data was reduced to third octave band spectra by applying an RMS summation of the pressures within each third octave band. These pressures were then matched to the appropriate central frequency of the respective band. This reduced the constant bandwidth spectrum to 19 third-octave bands. A BASIC program was written to perform this reduction procedure and is presented in Appendix C.

5.0 Results and Discussion

An experimental data base of combustion noise was collected to aid in the development and appraisal of predictive models. Specifically, the theoretical model of Mahan-Nathani (Appendix A) was chosen to examine trends found in the experimental data. The model was evaluated by addressing all inherent input parameters including burner diameter, flow velocity and chemical inputs. The acoustic emission from the combustion of turbulent mixtures of several gaseous fuels and oxygen was recorded. Oxygen was selected as an oxidizer to allow wider stability limits than could be achieved with air as an oxidizer. Acetylene, methane and propane were each examined with three burner diameters and three flow velocities as shown in Tables 1, 2 and 3. The fuel-oxygen mixture ratios were determined based on the concept of a "neutral flame" (Appendix B). This is the condition upon which the fuel is completely oxidized by the pre-mixed oxygen and entrained air from the surroundings. Upon applying this criterion, the following fuel-oxygen ratios (volumetric) were obtained for the three fuels:

acetylene	1:1
methane	2:3
propane	1:2

Section 5.1 discusses the constant-bandwidth frequency spectra that were measured experimentally. This data can be seen in Appendix D. The peak frequencies and overall sound pressure levels for all spectra were identified and are tabulated in Table 4. These two parameters were chosen as useful characteristics to allow quantitative comparisons to be made regarding input variable effects. In addition, these parameters will be used for the comparison of experimental data to model predictions.

In Section 5.2, model predictions are compared to the experimental results. For constant- bandwith spectra, the model predicts spectra that show an unrealistic peak frequency of 0 Hz. For increasing frequencies, the predictions show a series of harmonics. To allow a more reliable comparison, the experimental data is converted from constant-bandwidth spectra to third-octave-bandwidth spectra. The converted experimental data is presented in Appendix E. The peak frequency and overall sound pressure level for this data is shown in Table 5.

5.1 Experimental Results

All acoustic spectra were measured using a frequency scale of 0 to 10,000 Hz while pressure scales were adjusted to allow maximum resolution. The operation of the spectrum analyzer using the 10 kHz band allows a useful frequency range above 120 Hz; lower frequencies are limited by the uncertainty in the analyzers' first measurement step. The spectral plots which follow typically show a low frequency content (below 120 Hz) which is an artifact of the spectral analysis procedure and does not represent the true frequency content in this range. Therefore, the peak frequencies reported in Table 4 consider the first identifiable peak above this range. Preliminary measurements on the

Table 4. OASPL and Peak Frequency for Constant-Bandwidth Data

Fuel and Burner Parameters			Experimental Results	
Fuel (-)	D (cm)	U (m/s)	OASPL (dB)	f_P (Hz)
Acetylene	0.117	50	79.50	84.3
Acetylene	0.117	75	86.14	521
Acetylene	0.117	100	87.59	648
Acetylene	0.165	50	86.52	226
Acetylene	0.165	75	87.36	521
Acetylene	0.165	100	88.37	690
Acetylene	0.356	50	87.02	1721
Acetylene	0.356	75	87.34	560
Methane	0.356	10	76.85	880
Methane	0.356	20	86.60	575
Methane	0.414	10	83.06	595
Methane	0.414	20	87.64	529
Methane	0.414	25	90.46	558
Methane	0.541	10	84.31	534
Methane	0.541	20	92.18	536
Methane	0.541	25	93.25	555
Propane	0.117	30	74.90	1466
Propane	0.117	40	76.23	1891
Propane	0.165	20	61.38	658
Propane	0.165	30	81.81	1915
Propane	0.165	40	83.07	1720
Propane	0.356	20	86.33	680
Propane	0.356	30	91.79	724

250 Hz band indicated no significant spectral content below this limiting 120 Hz associated with the 10 kHz band.

The effects of each input variable are described in the following discussion. Comparison spectral plots show the effects of a single variable while holding others constant. The constant parameters represent the median values.

1. Burner Diameter: Figures 3, 4, and 5 show the effect of burner diameter on the frequency spectra of methane, propane and acetylene respectively while holding all other experimental parameters constant. In general, the data presented in the figures and in Table 4 reveal that the peak frequency is not significantly affected by changing diameter. The slight effects that are seen appear to be random.

   The tabulated data show an interesting exception to this trend which supports past theoretical efforts. For propane flowing at 20 m/s through the 0.117 cm burner, a peak frequency was measured which is much lower than those found for the 0.165 cm and 0.356 cm burner diameters tested at the same flow velocity. It is apparent that this is caused by a low turbulence condition. The calculated Reynolds number for this case is about 1600 and is the only test point considered which might not be turbulent. This finding supports Braggs' [9] theory which predicts no noise for laminar flames. Although the reaction was clearly audible, it is suspected that the acoustic mechanism at this point was in a transitory phase between a noiseless laminar flame and a steady turbulent reaction. Because the noise mechanism in this reaction is likely different than that found in the rest of the data, this test condition will not be considered in the discussion which follows.

   Other inconsistencies in the spectral trends for diameter might be wrongly assumed by only considering the data in Table 4. In several cases, the peak frequency occurs in a region where the spectrum is somewhat flat and does not contain a

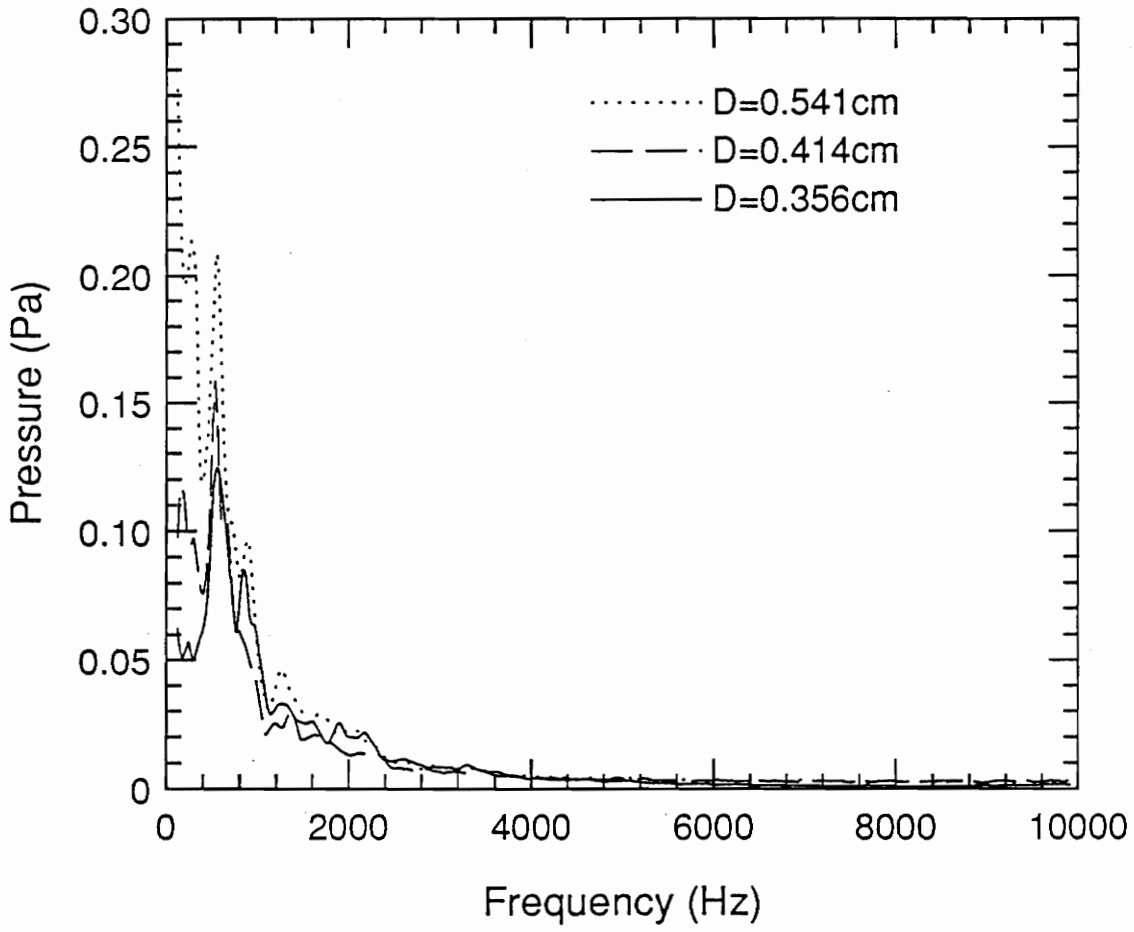

Figure 3. Spectra for Methane with varying burner diameter: U = 20 m/s

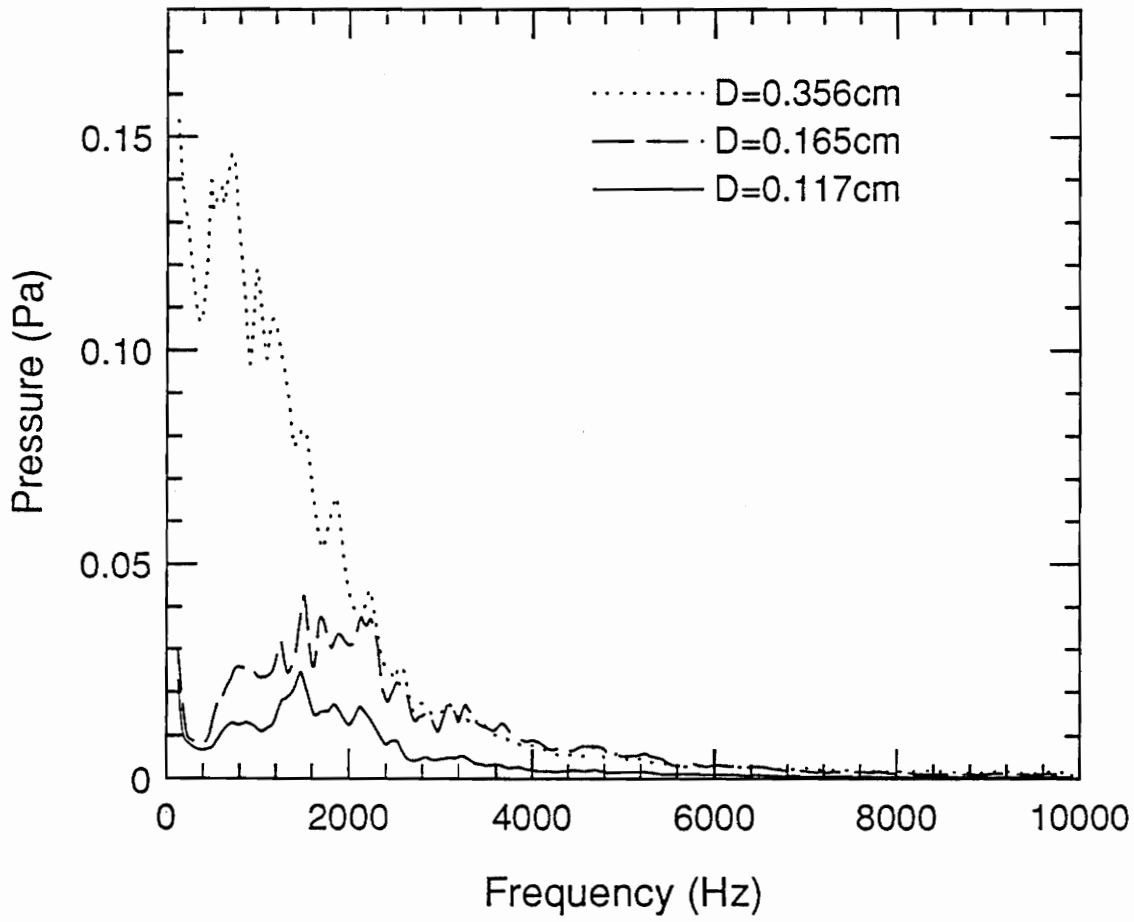

Figure 4. Spectra for Propane with varying burner diameter: U = 30 m/s

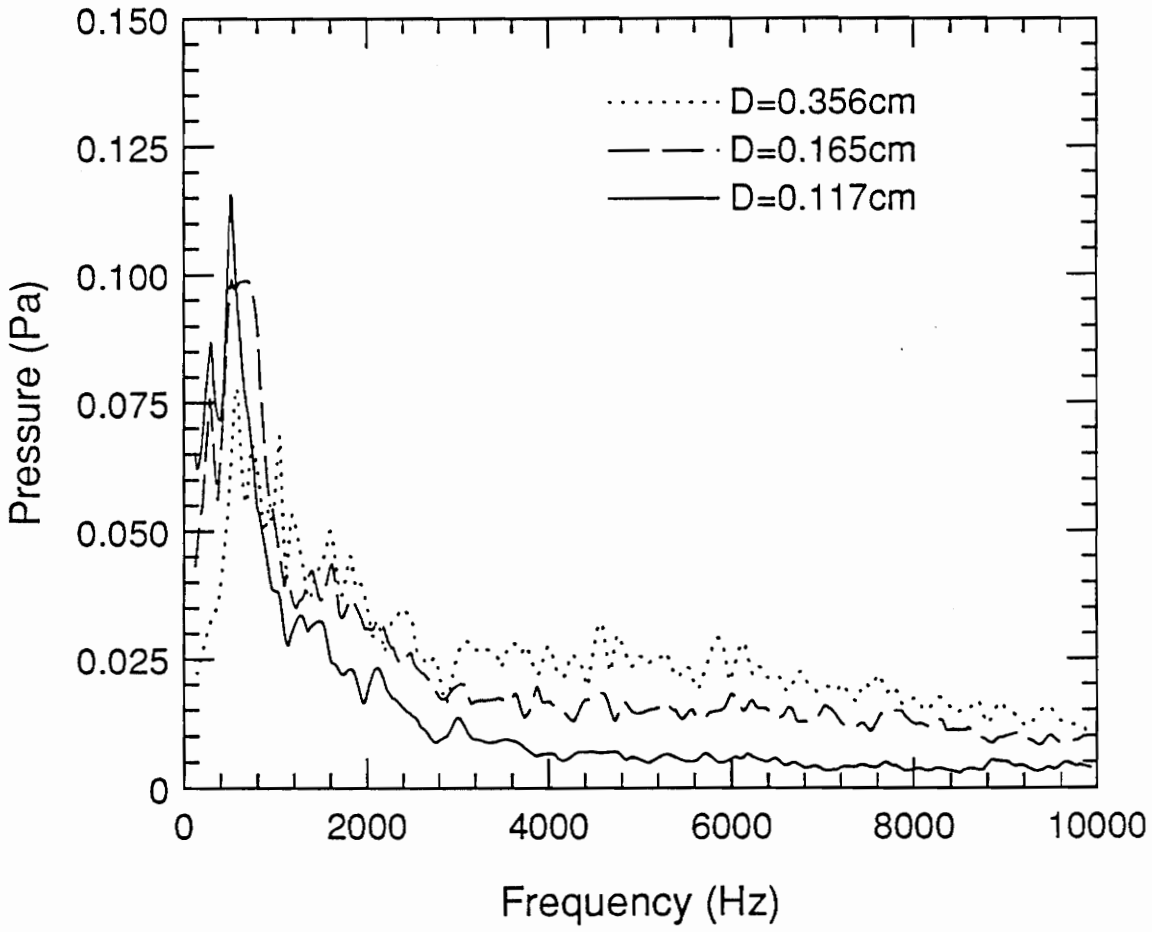

Figure 5. Spectra for Acetylene with varying burner diameter: U = 75 m/s

dominant peak. Upon considering the spectral shapes in these cases, the spectral content of the data show the general trends seen in the rest of the data set.

Finally, the data from Table 4 clearly show that the overall sound pressure levels increase with increasing burner diameters.

As discussed previously, the model predicts decreasing peak frequencies with increasing burner diameters. However, this trend is not exhibited in the experimental data. Perhaps the range of experimental burner diameters examined is not wide enough to expose an underlying trend. The model would also predict increasing overall sound pressure levels with increasing burner diameters, simply due to the larger sound sources associated with larger burner diameters. This predicted trend is supported by the experimental data.

2. Flow Velocity: Figures 6, 7 and 8 show the effect of flow velocity on frequency spectra with burner diameter and chemistry held constant. These figures show velocity to have little effect on peak frequency. Yet, examination of the data in Table 4 shows peak frequency to increase for eleven out of the possible fifteen direct comparisons allowed by the experimental data. This general trend would then be in agreement with the theoretical model which predicts increasing peak frequencies with increasing flow velocities. The data presented in Table 4 also shows that overall sound pressure level increases with increasing flow velocity. This trend is also predicted by the theoretical model.

3. Chemical Inputs: Only one direct comparison could be made regarding the reactant chemistry. Figure 9 shows a spectral comparison of propane and methane for flow through a burner diameter of 0.356 cm at a velocity of 20 m/s. The figure shows that the two spectra are remarkably similar. The theoretical model only considers two parameters which would differentiate between fuels; namely, flame speed and flame temperature. Flame speed and flame temperature data as presented by Gaydon and

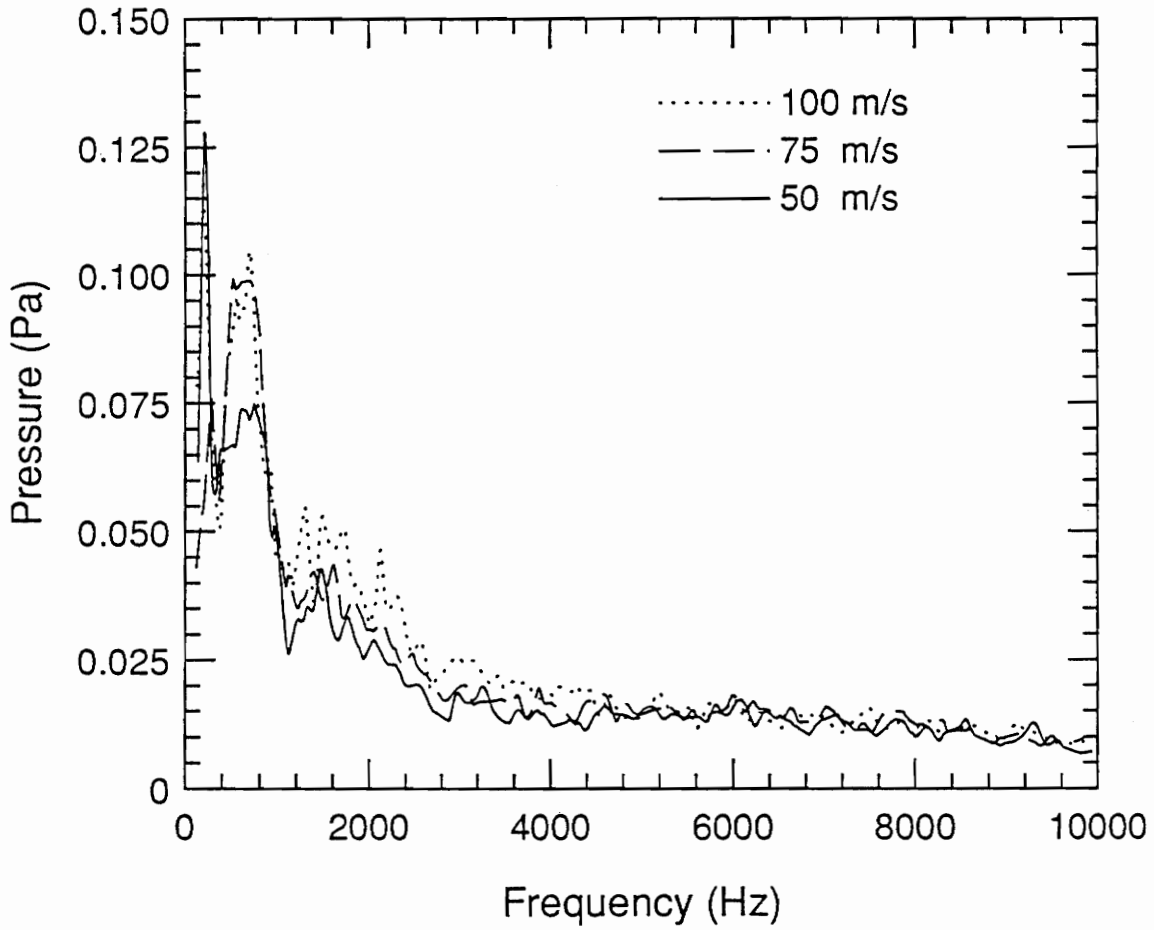

Figure 6. Spectra for Acetylene with varying flow velocity: D = 0.165 cm

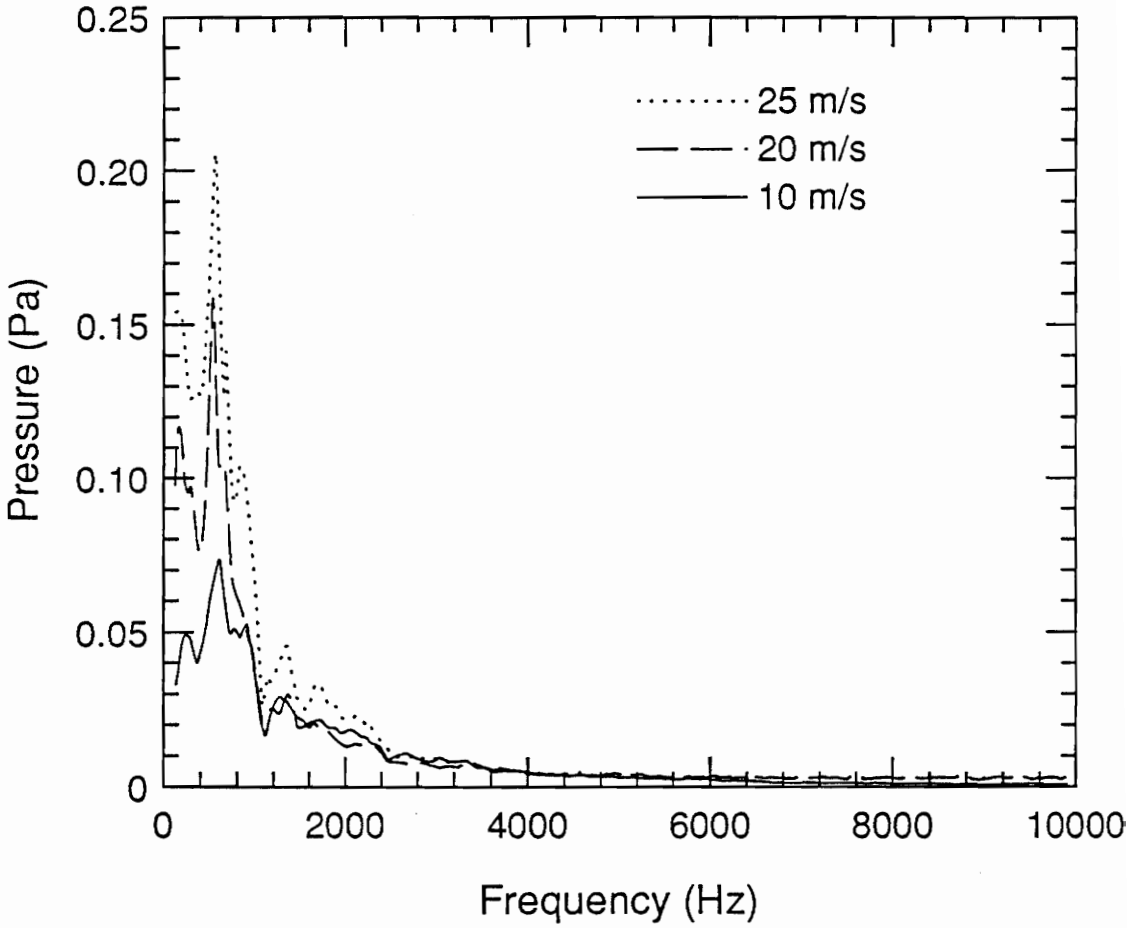

Figure 7. Spectra for Methane with varying flow velocity: D = 0.414 cm

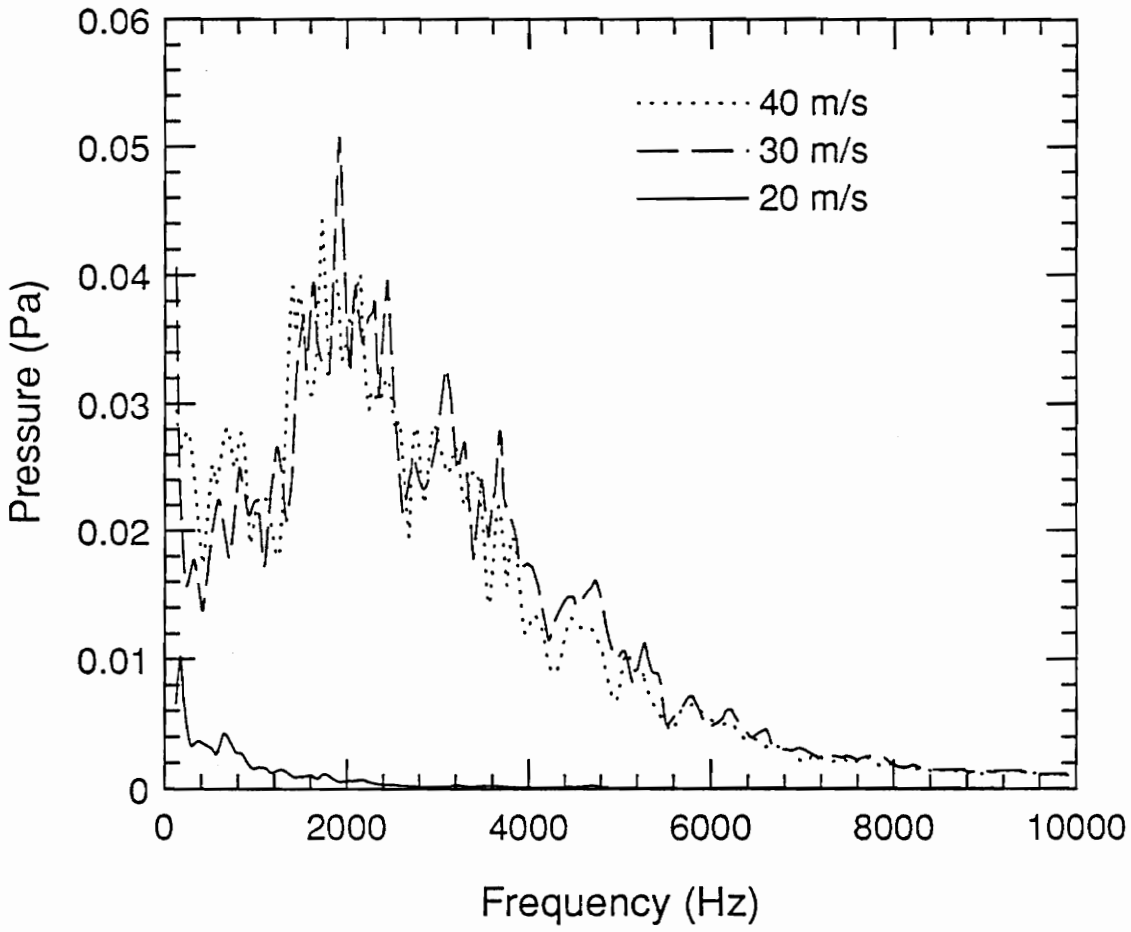

Figure 8. Spectra for Propane with varying flow velocity: D = 0.165 cm

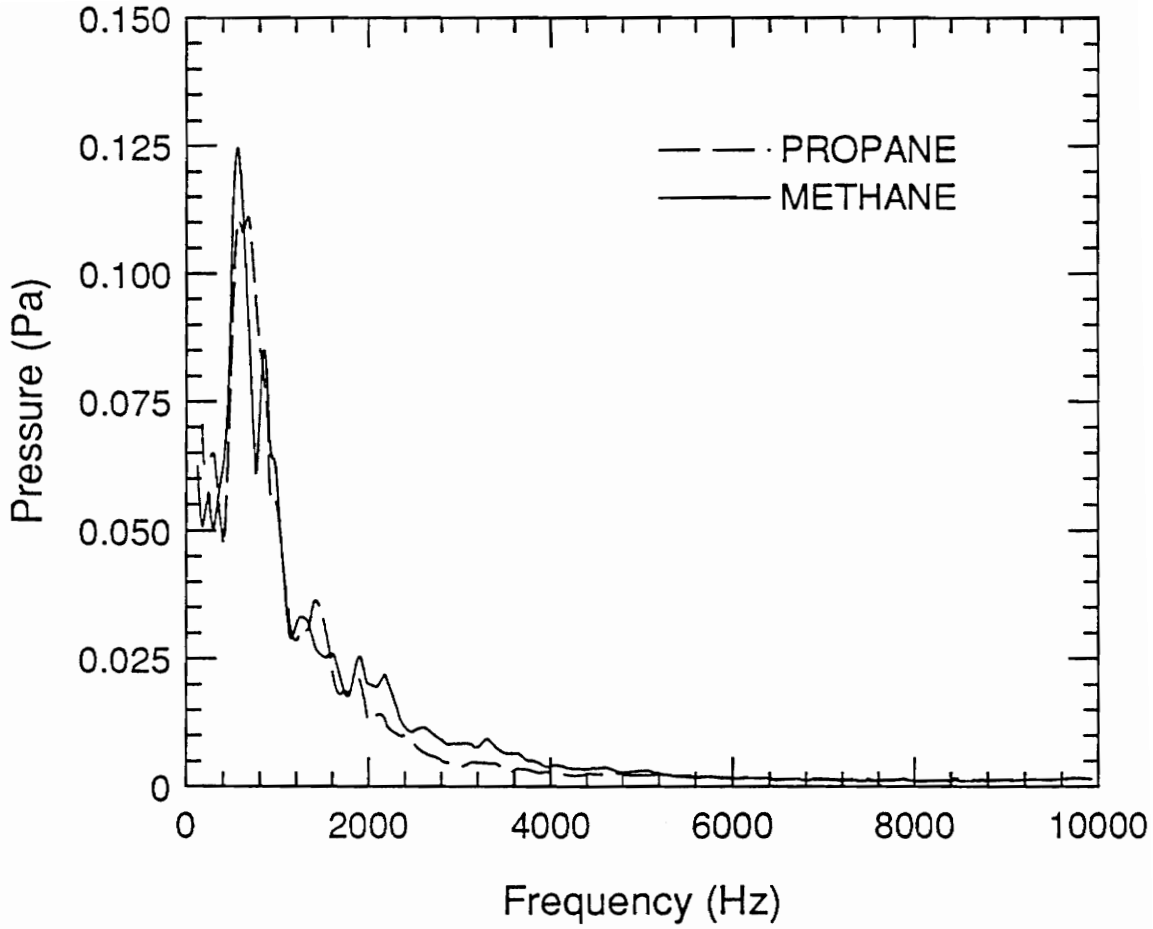

Figure 9. Spectra for Methane and Propane: D = 0.356 cm, U = 20 m/s

Wolfhard [8] show methane and propane to be comparable regarding these two parameters. Hence, the model would also predict very similar acoustic spectra.

The noise attributed to the experimental surroundings is shown in Figure 10. The reader should note the pressure scale is less than 10 percent of scales used to show reacting flows. It is clear that the background noise present during experimental testing is insignificant when compared to the sound emission from the combusting fuel-oxygen mixtures.

Figure 11 shows the spectra of a non-reacting methane flow of 20 m/s through the 0.414 cm burner. The figure clearly demonstrates that the non-reaction flow noise contributes less than 10 percent to the overall sound pressure level of the reacting flow case. This result is also consistent with the theory of Bragg [9]. In addition, it should be remembered that this noise also includes the background noise present during testing.

Data points in the test matrix were found to be quite repeatable as shown in Figures 11 and 12. Figure 12 shows three spectra of reacting acetylene at 75 m/s through a 0.165 cm diameter nozzle. Initial experimental tests were conducted to determine if successive measurements for a given condition were repeatable. It was shown that in fact they were. Yet to quantify a confidence level, one test point for each of the fuels was repeated three times. This allowed a T-test to be performed with nine degrees of freedom. This analysis yielded a 95 percent confidence level of +/- 18 percent for the peak frequency and +/- 12 percent for the overall sound pressure level.

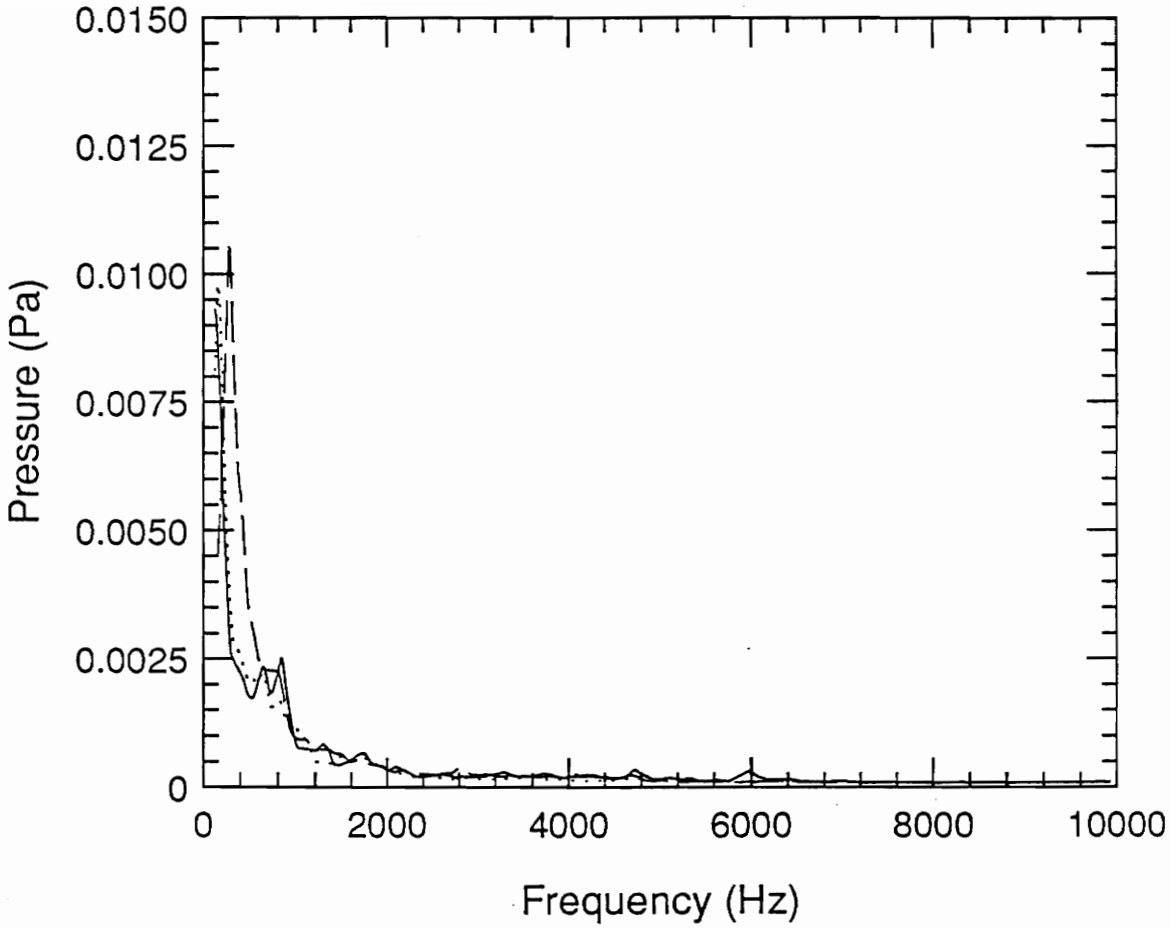

Figure 10. Spectrum of Background Noise

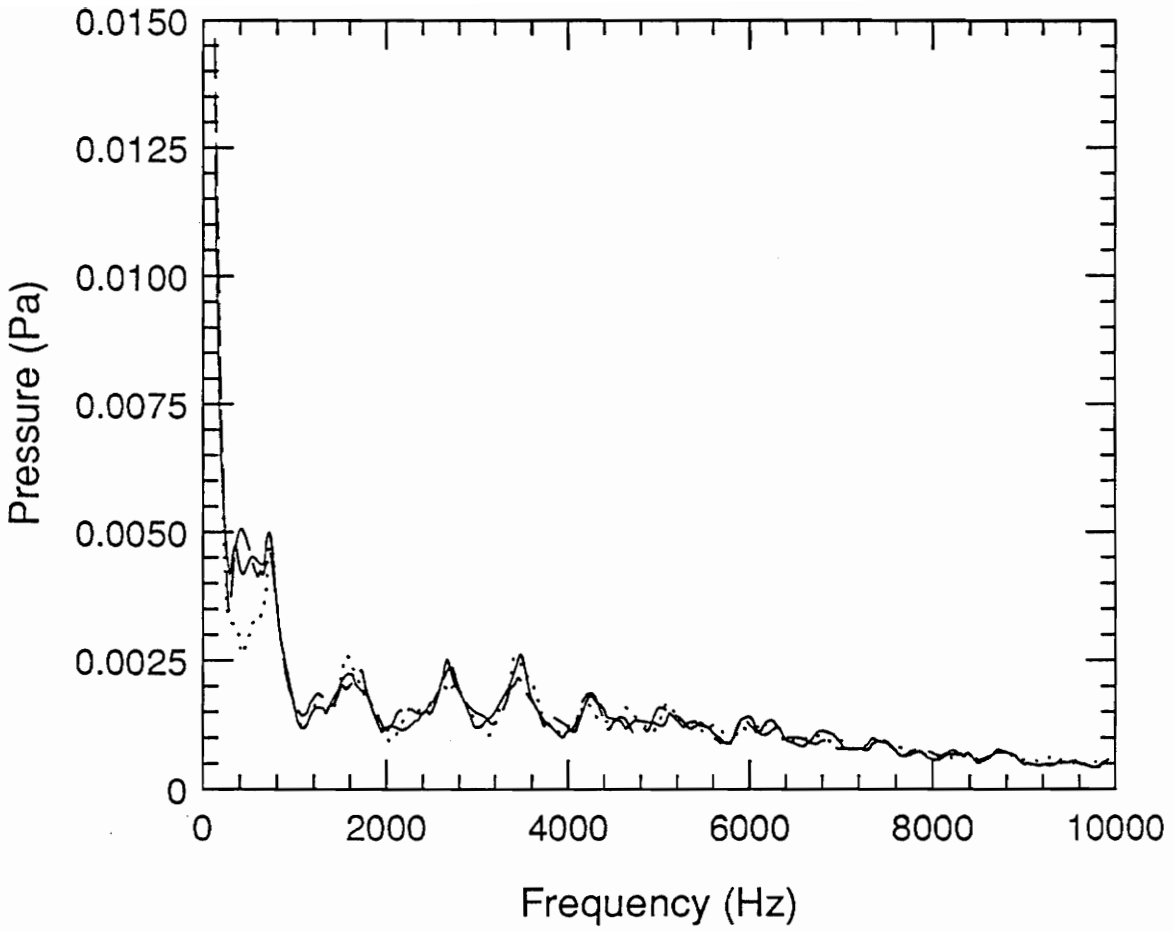

Figure 11. Spectrum of non-reacting Methane flow: U = 20 m/s, D = 0.414 cm

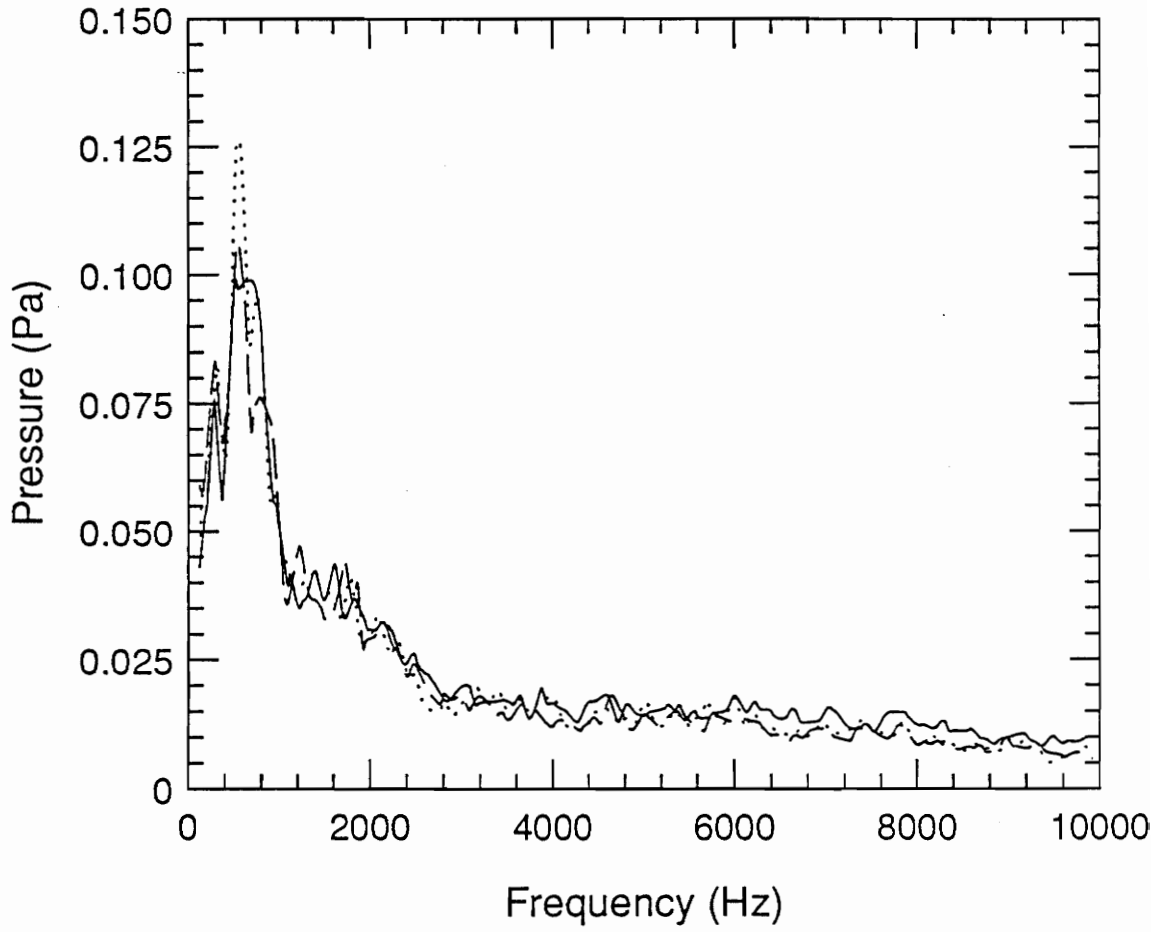

Figure 12. Spectra for Acetylene: U = 75 m/s, D = 0.165 cm

5.2 *Comparison To Theoretical Model*

The study has now reached a point where the performance of the Mahan-Nathani theoretical model may be considered. As with the experimental data just presented, peak frequency and overall sound pressure level will be used as criteria for evaluating the model. As discussed previously, the model predicts an unrealistic peak frequency of 0 Hz for constant-bandwidth spectra. To allow a more meaningful comparison between the model predictions of peak frequency and those determined experimentally, the experimental constant-bandwidth data is converted to third-octave-bandwidth spectra. Upon applying this conversion to the theory, the model will then predict non-zero peak frequencies, and a direct comparison can be made to the peak frequencies determined experimentally. Also, since third-octave-bandwidth spectra reduce the data to seventeen center frequencies in a 10 kHz frequency range, more general insight into the frequency content of the acoustic spectra is allowed. This conversion then avoids the mundane task of evaluating the intricacies of the experimental data when compared to the relatively simple third-octave-bandwidth data as predicted by the model. The converted experimental data appears in Appendix E. The tabulated peak frequencies and overall sound pressure levels appear in Table 5.

5.2.1 Determining Model Input Requirements

Recall that the model requires input parameters which include burner diameter, flow velocity, flame speed and flame temperature. Since flame speeds and flame temperatures were not measured experimentally, their values must be estimated. However,

the two stage reaction of the neutral flame (Appendix B) dictates two different reactions with unique flame speeds and flame temperatures to each stage. To further complicate matters, the true reaction encountered experimentally is certainly more complicated than this assumed two-step reaction. In light of these uncertainties, estimating these chemical parameters becomes necessary.

As a first approximation, an attempt was made to run the model for flame speeds and flame temperatures as obtained from literature [8,29]. These values were obtained for the fuel-oxygen ratios used experimentally. Arguably, these values were measured for a complete reaction with oxygen and ignore the entrained air encountered experimentally. The model predictions based on these inputs provided poor results when compared to the experimental results.

Upon considering the flame speed data from Gaydon and Wolfhard [8], it was seen that flame speed is very sensitive to the fuel-oxygen ratio in the combustible mixture. For example, the flame speeds for methane were found to vary from approximately 25 cm/s for the fuel-rich, stage one reaction of the neutral flame (1:1 fuel-oxygen ratio) to 330 cm/s for the combustion of a stoichiometric mixture of methane and oxygen (1:2 fuel-oxygen ratio). These flame speeds apply to the complete combustion of the fuel-oxygen mixture, yet the neutral flame reaction (which determined the experimental mixtures) considers the partial reaction of a methane molecule in oxygen followed by continuing reaction with entrained air.

The model clearly failed to predict the experimental data under these conditions. A close examination of these data revealed that the model may produce useful results however, if the flame speed and flame temperature are adjusted from the data of Gaydon and Wolfhard [8] (which were measured under completely different conditions), to those which might realistically exist in these experiments.

The model was next examined to determine its sensitivity to flame speed and flame temperature. It was noted that flame temperature only affects amplitude, and consequently overall sound pressure level, and not the frequency distribution of the predicted acoustic spectra. Higher flame temperatures resulted in higher acoustic pressures at all frequencies. It was revealed, though, that flame speed affects the frequency distribution, with higher flame speeds resulting in higher-frequency spectral distributions.

This evidence suggested that the model might be forced to match the frequency content of the experimental data by adjusting the flame speed. Flame temperature inputs could then be adjusted to match the overall sound pressure levels measured in the experimental tests. Because the model predicts a non-zero peak frequency in a third-octave-band spectrum, a force fit of the model could be made with two distinct and necessary requirements; a match of both peak frequency and overall sound pressure level.

This exercise in forcing the data might then lend some insight into what flame speeds and flame temperatures might actually be occurring experimentally. In addition, if the required force fit data appeared to be unrealistic, this flaw could then be addressed.

The resulting flame speeds and flame temperatures required to force fit the model to the experimental data are shown in Table 6. The data for flame speeds is fairly consistent for all three fuels. However, the necessary flame temperatures required to match the overall sound pressure levels vary considerably throughout the range of test conditions. In fact, the true flame speeds and flame temperatures for a given fuel should be similar as the chemistry (mixture) is constant for all cases. The data presented in Table 6 reveal no obvious trends for required flame speeds and flame temperatures yet it does suggest what flame speeds and flame temperatures might be used to model a given fuel. In addition, if the theoretical model is correct, the data suggest what the true flame speeds and flame temperatures encountered in the experimental tests might be.

Table 5. Third-Octave Band Results for Experimental Data

Fuel and Burner Parameters			Experimental Results	
Fuel (-)	D (cm)	U (m/s)	OASPL (dB)	f_P (Hz)
Acetylene	0.117	50	79.50	158
Acetylene	0.117	75	86.14	497
Acetylene	0.117	100	87.59	497
Acetylene	0.165	50	86.52	625
Acetylene	0.165	75	87.36	625
Acetylene	0.165	100	88.37	625
Acetylene	0.356	50	87.02	4894
Acetylene	0.356	75	87.34	4894
Methane	0.356	10	76.85	785
Methane	0.356	20	86.60	625
Methane	0.414	10	83.06	625
Methane	0.414	20	87.64	497
Methane	0.414	25	90.46	625
Methane	0.541	10	84.31	625
Methane	0.541	20	92.18	315
Methane	0.541	25	93.25	250
Propane	0.117	30	74.90	1560
Propane	0.117	40	76.23	1960
Propane	0.165	20	61.38	625
Propane	0.165	30	81.81	1960
Propane	0.165	40	83.07	1960
Propane	0.356	20	86.33	785
Propane	0.356	30	91.79	785

Table 6. Requirements to Force Fit the Model to Experimental Results

Fuel and Burner Parameters			Fit Requirements	
Fuel (-)	D (cm)	U (m/s)	T_o (K)	S_L (cm/s)
Acetylene	0.117	50	3300	140
Acetylene	0.117	75	5000	140
Acetylene	0.117	100	5500	120
Acetylene	0.165	50	3500	220
Acetylene	0.165	75	2750	200
Acetylene	0.165	100	2530	200
Acetylene	0.356	50	2125	115
Acetylene	0.356	75	1150	200
Methane	0.356	10	1440	245
Methane	0.356	20	5000	210
Methane	0.414	10	2300	245
Methane	0.414	20	5250	190
Methane	0.414	25	4800	240
Methane	0.541	10	1275	315
Methane	0.541	20	2950	345
Methane	0.541	25	6750	110
Propane	0.117	30	2464	230
Propane	0.117	40	2480	200
Propane	0.165	20	1175	85
Propane	0.165	30	4000	310
Propane	0.165	40	3000	300
Propane	0.356	20	3850	270
Propane	0.356	30	4775	260

5.2.2 Estimating Flame Speed and Flame Temperature

Based on the flame speed and flame temperature data of Gaydon and Wolfhard [8], the values of these parameters required to match the model prediction to the experimental results do not appear to be unrealistic. It seems that a reasonable estimate of flame speed and flame temperature might be made be by considering both the force fit requirements and the published values.

It is likely that the true flame speeds for the fuel-oxygen mixtures examined experimentally must fall between the flame speed indicated for the fuel lean mixture in the primary stage reaction of the neutral flame and that for a stoichiometric fuel-oxygen mixture. From Gaydon and Wolfhard, the range of possible flame speeds for the fuels tested are then:

Acetylene:	$300 < S_L < 1100$ cm/s
Methane:	$30 < S_L < 330$ cm/s
Propane:	$60 < S_L < 400$ cm/s

These respective flame speeds set limits on what the true values can be in the experimental tests.

The adiabatic flame temperatures were calculated for the experimental fuel-oxidizer mixtures to suggest a limit on the possible flame temperature which might be present in the experimental tests. The calculated adiabatic flame temperatures for each fuel were determined to be:

Acetylene:	T = 4637 K
Methane:	T = 2873 K
Propane:	T = 2827 K

Due to convective heat transfer and radiative heat transfer, the true flame temperature is expected to be lower than the calculated adiabatic flame temperature.

From the possible flame speeds and flame temperatures presented for experimental fuels, and based on the flame speeds and flame temperatures necessary to force the model (Table 6), specific flame speeds and flame temperatures were assumed for each fuel. These estimates are as follows:

Acetylene:	T = 4000 K	S_L = 500 cm/s
Methane:	T = 2400 K	S_L = 240 cm/s
Propane:	T = 2750 K	S_L = 260 cm/s

The outcome of the assumed flame speed and flame temperatures as applied to the theoretical model yielded some interesting results, yet also exposed some possible weaknesses in the theory. Table 7 shows the predicted peak frequency and the overall sound pressure level for each experimental test point. The model proved to match methane the most accurately and acetylene the least accurately of the three fuels tested. This is partially an artifact of the method of estimating the flame speed and flame temperature parameters. Furthermore, several anomalies in the model code results were noted and will be discussed in Section 6.2.3.

Figure 13 shows the model prediction for the third octave band spectrum of a 10 m/s methane flow through a 0.414 cm burner diameter. The similarity in the results through the first frequency peak is because the assumed flame speed is very close to the force fit required flame speed. However, the spectral shape of the model closely approximates the experimental results. In particular, the second frequency spike at approximately 2000 Hz is almost the same in both spectra and is not directly an artifact of the model being forced. A comparison of a higher flow velocity (25 m/s) through the same burner is shown in Figure 14. In this case, the model fails to predict even the shape of the experimental spectra

Table 7. Model Results for Assumed Chemical Parameters

Fuel and Burner Parameters			Model Results	
Fuel (-)	D (cm)	U (m/s)	OASPL (dB)	f_P (Hz)
Acetylene	0.117	50	84.90	4894
Acetylene	0.117	75	88.73	4894
Acetylene	0.117	100	91.77	4894
Acetylene	0.165	50	87.90	3894
Acetylene	0.165	75	93.96	3894
Acetylene	0.165	100	97.25	3894
Acetylene	0.356	50	98.56	1559
Acetylene	0.356	75	104.2	1559
Methane	0.356	10	81.70	625
Methane	0.356	20	80.24	785
Methane	0.414	10	83.07	625
Methane	0.414	20	81.61	625
Methane	0.414	25	83.81	625
Methane	0.541	10	85.44	497
Methane	0.541	20	84.10	497
Methane	0.541	25	86.20	497
Propane	0.117	30	73.46	2464
Propane	0.117	40	77.68	2464
Propane	0.165	20	74.25	1960
Propane	0.165	30	78.26	1960
Propane	0.165	40	82.33	1960
Propane	0.356	20	82.48	785
Propane	0.356	30	86.56	785

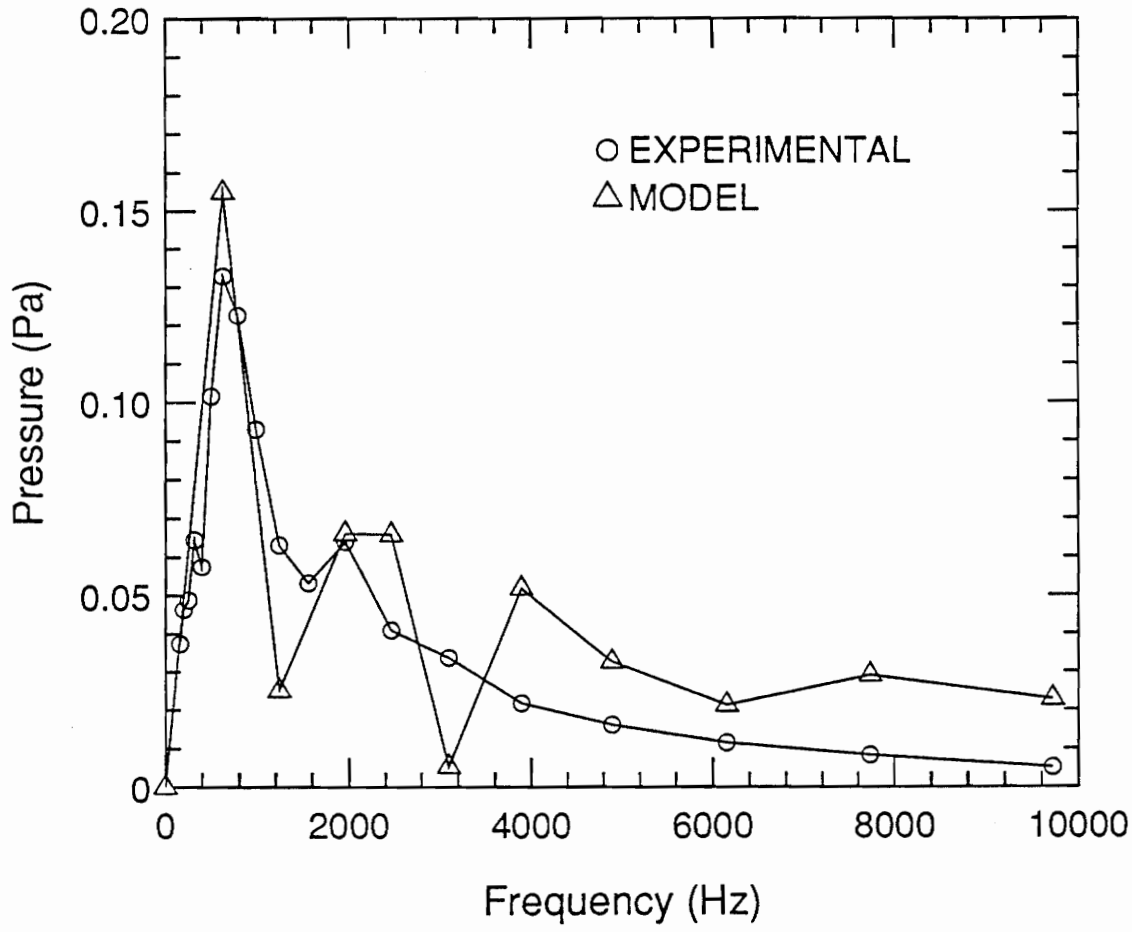

Figure 13. 1/3-Octave Spectrum for Methane: U = 10 m/s, D = 0.414 cm

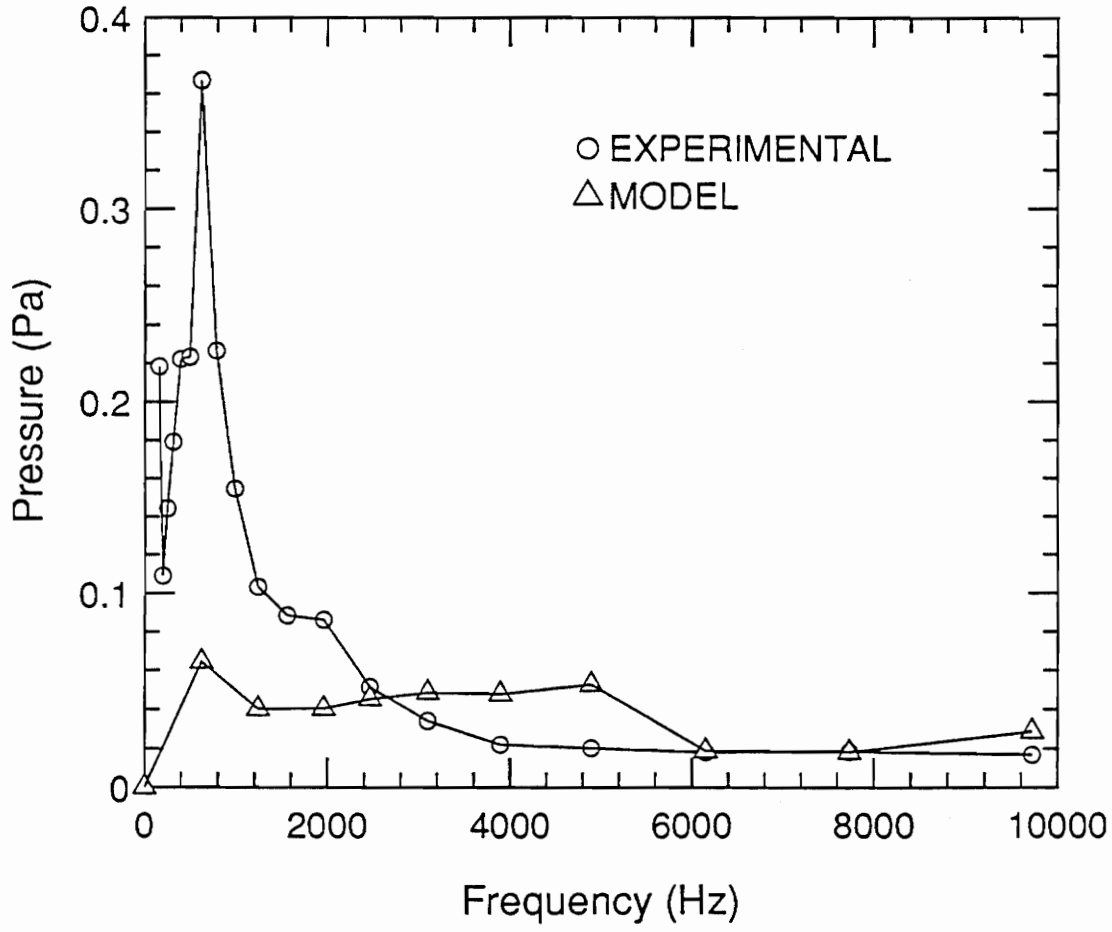

Figure 14. 1/3-Octave Spectrum for Methane: U = 25 m/s, D = 0.414 cm

Figure 15 shows a prediction for acetylene with the largest tested burner diameter of 0.356 cm. The results clearly show that the predicted spectrum shape closely resembles that determined experimentally. However, the overall sound pressure level predicted is much higher than the experimental data indicates.

Some apparently anomalous behavior was observed in the results obtained from the computer model. These are detailed and discussed in Appendix A.

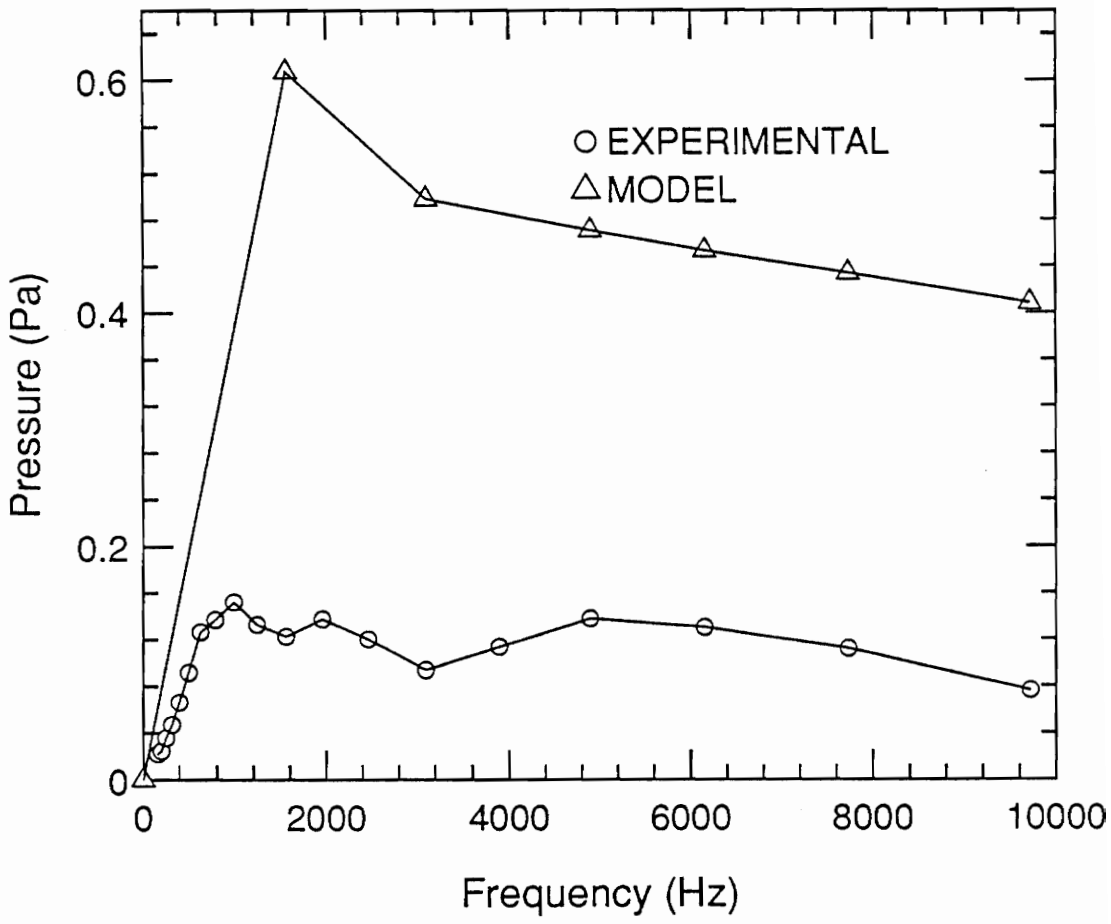

Figure 15. 1/3-Octave Spectrum for Acetylene: U = 75 m/s, D = 0.356 cm

6.0 Conclusions and Recommendations

6.1 Conclusions

An experimental data base of acoustic spectra was collected for the noise emission of turbulent combustion process. Unlike the limited number of past experimental efforts, the experiment utilizes a geometrically simple burner configuration and uses a consistent method of addressing known relevant input parameters.

Increasing burner diameters and flow velocities were found to have little effect on frequency content yet caused increasing overall sound pressure levels. The effects of alternate fuels and consequently, flame speed and flame temperature, could only be examined for one case between methane and propane. The overall sound pressure level and the acoustic spectra were very similar, as might be expected due to similar laminar flame speeds and adiabatic flame temperatures. For all cases, the peak frequency was determined to fall between 80 Hz and 2000 Hz. Overall sound pressure levels fell between 61 dB and 93 dB.

To test the usefulness of the data base to theories in general, the data was compared to the turbulent combustion noise model of Mahan-Nathani [1]. Initially, the model code was run using flame speed and flame temperature data as published in combustion literature. Upon application of these values, the model predicted acoustic spectra which were inconsistent with experimental data. Because of the complex nature of the reaction present in the experimental tests it was probable that these published values did not accurately represent the physical process encountered experimentally. Therefore, flame speed and flame temperature data were assumed based on the likely range of these variables and the required values to approximate the experimental results. In general, when applied to the model code, the assumed flame speeds and flame temperatures yielded acoustic spectra which closely resembled the spectral shapes found experimentally. Several discrepancies in the code were identified including the calculation of the number of sound sources (Appendix A). Also, limitations in the model were apparent for high velocities and high flame speeds as found with acetylene.

The study indicates that the model results for low velocity, low flame speed conditions in some cases closely approximate the experimental results. In addition, it reveals that combustion noise may have a wide range of diagnostic applications. These applications include the possibility of using acoustic emission of a flame as a means as a means of determining fuel-oxidizer mixture ratios, flame speeds and flame temperatures as well as methods for combustion noise reduction. With refinement, the model might be used to more practically determine flame speeds and flame temperatures of fuel-oxidizer mixtures under atmospheric pressures.

6.2 *Recommendations*

The present study reveals the need for further examination in both experimental noise measurement and theoretical predictive methods. The experimental data and the model predictions show tremendous potential for a clear understanding of the true noise mechanism of combustion.

The following recommendations are made for future experimental work.

1. Additions to the existing data base of acoustic spectra might offer more insight into the effects of the four input variables. A wider range of burner diameters and flow velocities could show slight trends not apparent in the present study. However, this would require a burner design with flame holders to overcome stability limits. This type of experimental configuration would add further complications which the model does not provide for. In addition, more fuels should be examined to offer insight into chemical effects (flame speed and flame temperature) on the acoustic spectra; as the present study only allows one direct comparison. The effect of equivalence ratio might also be examined.
2. To address the uncertainty in overall fuel-oxidizer ratios, a burner might be utilized which includes a coflow of non-reacting gas around the reacting mixture. This would eliminate the possibility of entrained air as occurred with the present experimental design. The true mixture of fuel and oxygen would then be assured and a better estimate of flame speed and flame temperature data could be made. However, this method will still allow for some energy loss to the non-reacting gas, resulting in lower temperatures than the adiabatic flame temperature.

The following recommendations are made for further study of Nathani's theoretical model.

1. The possibility of incomplete combustion should be addressed in the model.
2. A more plausible reaction should be modelled to include more than one reaction step. Simply considering a two step reaction may lead to considerably better model results.
3. A statistical distribution of cell sizes, rather than the constant diameter employed in the present model, might favorably affect the models' predicted frequency distribution. As the model stands, the spectral content is determined simply by the combustion of one reacting cell.
4. The discontinuities in input variable trends should be addressed. It is suspected that the problem lies not in the supporting theory, but in the numerical integrations which occur in the model code.
5. The calculation of the number of sound sources in the model code should be corrected to properly follow the theory. Presently, this error is slight (about 9 percent) and only affects the calculation of overall sound pressure levels.

References

1. Nathani, Arun, "A Turbulent Combustion Noise Model." MS Thesis. Viginia Polytechnic Institute and State University, 1989.

2. Putnam, A., and L. Faulkner, "An Overview of Combustion Noise", AIAA Paper No. 82-0927, 1982.

3. Strahle, W. C., "A Review of Combustion Generated Noise", AIAA Paper No. 75, 1975.

4. Higgins, B., "On the Sound Produced by a Current of Hydrogen Gas Passing Through a Tube", Journal of National Philosophy, Chimistry, and the Arts, Vol. 1, 1802, pp. 129-131.

5. Rayleigh, Lord, Theory of Sound, Macmillan, London, 1896, p. 103.

6. Lighthill, M. J., "On Sound Generated Aerodynamically. I. General Theory,", Proceedings of the Royal Society of London, Series A, Vol. 211, 1952, pp. 564-587.

7. Lighthill, M. J., "On Sound Generated Aerodynamically. II. Turbulence as a Source of Sound,", Proceedings of the Royal Society of London, Series A, Vol. 222, 1954, pp. 1-23.

8. Gaydon, A. G., and H. G. Wolfhard, Flames, 3rd ed., Chapman and Hall, London, 1970, p. 163.

9. Bragg, S. L., "Combustion Noise," Journal of the Institute of Fuel, Vol. 35, No. 264, January 1963, pp. 12-16.

10. Smith, T. J. B., and J. K. Kilham, "Noise Generation by Open Turbulent Flames," Journal of the Acoustical Society of America, Vol. 35, No. 5, May 1963, pp. 715-724.

11. Thomas, A., and G. T. Williams, "Flame Noise: Sound Emission from Spark-Ignited Bubbles of Combustible Gas," Proceedings of the Royal Society of London, Series A, Vol. 294, 1966, pp. 449-466.

12. Giammar, R. D., and A. A. Putnam, "Combustion Roar of Turbulent Diffusion Flames," ASME Transactions, Series A, Jounal of Engineering for Power, Vol. 92, No. 2, April 1970, pp. 157-165.

13. Knott, P. R., "Noise Generation by Turbulent Nonpremixed Flames," AIAA paper No. 71-732, 1971.

14. Kumar, R. N., "Further Experimental Results on the Structure and Acoustics of Turbulent Jet Flames" AIAA paper No. 75-523, 1975.

15. Chiu, H. H., and M. Summerfield, "Theory of Combustion Noise" Acta Astronautica Vol. 1, 1974, pp. 967-984.

16. Strahle, W. C., "Convergence of Theory and Experiment in Direct Combustion-Generated Noise," AIAA Paper No. 75-522, 1975.

17. Strahle, W. C., "On Combustion Generated Noise," Journal of Fluid Mechanics, Vol. 49, part 2, 1971, pp. 399-414.

18. Strahle, W. C., "Some Results in Combustion Generated Noise," Journal of Sound and Vibration, Vol. 23, 1972, pp. 113-125.

19. Shivashankara, B. N., W. C. Strahle, and J. C. Handley, "Combustion Noise Radiation by Open Turbulent Flames," AIAA Paper No. 73-1025, AIAA Aeroacoustics Conference, Seattle, WA, October 15-17, 1973.

20. Shivashankara, B. N., W. C. Strahle, and J. C. Handley, "Evaluation of Combustion Noise Scailing Laws by an Optical Technique," AIAA Journal, Vol. 13, No. 5, 1975, pp. 623-627.

21. Mathews, D. C., and N. F. Rekos, "Prediction and Measurement of Direct Combustion Noise in Turbopropulsion Systems," Journal of Aircraft, Vol. 14, No. 9, 1977, pp. 850-859.

22. Dowling, A. P., "Mean Temperature and Flow Effects on Combustion Noise," AIAA paper No. 78-XXX, 1978.

23. Ramohalli, K., "Acoustic Diagnostics of the Nonpremixed Turbulent Jet Flames," AIAA Paper No. 79-0591, 1979.

24. Ho, P. Y., and V. L. Doyle, "Combustion Noise Prediction," AIAA paper No. 79-0588, 1979.

25. Ramachandra, M. K., and W. C. Strahle, "Acoustic Signature from Flames as a Combustion Diagnostic Tool," AIAA Journal, Vol. 21, No. 8, August 1983.

26. Kotake, S., and K. Takamota, "Combustion Noise: Effects of the shape and Size of Burner Nozzle," Journal of Sound and Vibration, No. 112, 1987, pp. 345-354.

27. Seshan, P. K., "Reynolds Number Effects in Combustion Noise," Combustion Science and Technology, Vol. 49, 1986, pp. 263-275.

28. Mahan, J. R., "A New Turbulent Combustion Noise Model," Proceedings of NOISE-CON 87, The Pennsylvania State University, PA, June 8-10, 1987, pp. 201-206.

29. Mahan, J. R., and A. Nathani, "An Improved Turbulent Combustion Noise Model," Proceedings of INTER-NOISE 88, International Conference on Noise Control Engineering, Avignon, France, August 30 - September 1, 1988, pp. 891-894.

30. Koenigsberger, F., Welding Technology, Cleaver-Hume Press Ltd., London, 1953, p. 6.

31. Giachino, W., Welding Technology, American Technical Society, Chicago, 1968, p. 1-3.

32. Althouse, A.D., Modern Welding, The Goodheart-Willcox Co. Inc., South Holland Ill., 1972, p. 11.

Appendix A. The Mahan-Nathani Model

A1. The Mahan-Nathani Model

Based on the work of Mahan [28], Nathani [1] proposed a new model which addresses the physics of the noise generation process, allowing the prediction of the acoustic emission from a turbulent flame. The model simplifies the combustion process by assuming that the flow of combustibles from the burner breaks down into small spherical cells of reactants whose initial diameter is dependent on the diameter of the burner. The subsequent combustion of one of these cells produces a sound pressure wave which is sensed in the form of combustion noise. By methodically adding up the effects of a continuous stream of these cells, the total noise generation of a turbulent combustion system can be predicted. The model considers the following parameters to predict the overall sound pressure level and the frequency spectrum of the flames' sound emission:

Burner	U = Mixture Convective Velocity
	D = Burner Diameter
Fuel	S_L = Laminar Flame Speed
	E = Expansion Ratio (Volumetric)

A1.1 Modeling the Noise Sources

For a turbulent jet of combusting fuel-oxidizer mixture, turbulent eddies of reactants and hot products are formed which are subsequently burned upon entering the flame zone. Nathani reasons that the flow of these complex eddies might be modeled as

a single continuous stream of spherical cells whose initial diameters were fixed at a constant value with no deviation.

Given a pre-mixed flow of fuel-oxidizer through a burner of diameter D, the volumetric flow rate of the mixture is given by

$$Q = \frac{\pi}{4} D^2 U \,, \tag{A1.1}$$

where U is the reactant mixtures' convective velocity. If R_i is the initial radius of a combustible cell, then the the initial volume of a single cell is

$$V_i = \frac{4}{3} \pi R_i^3 \,. \tag{A1.2}$$

Assuming the continuous stream of injected mixture breaks up uniformly into a single stream of the theoretical noise sources, then the injection time, in which a single cell is formed is given by

$$t_i = \frac{2R_i}{U} \,. \tag{A1.3}$$

Because the model considers only a single stream of reacting cells, the volumetric flow rate, Q, can be written as

$$Q = \frac{V_i}{t_i} \,. \tag{A1.4}$$

Substituting Eq. (A1.2) and Eq. (A1.3) into Eq. (A1.4) yields

$$Q = \frac{2}{3} \pi R_i^2 U \,. \tag{A1.5}$$

Finally, equating Eqs. (A1.1) and (A1.5) gives

$$R_i = \sqrt{\frac{3}{8}}\, D \,. \qquad (A1.6)$$

It is of particular interest to note that the above result was derived without any reference to turbulence scales. The correctness of this result awaits the scrutiny of the experimental data.

A1.2 The Burning Process

The model hypothesizes that two distinct burning processes occur as the spherical cell of reactants propagates through the flame front boundary. The transition process begins at time zero when the cell initially comes in contact with the flame front, and ends when the cell has just completely entered the reaction zone. The transition time t_{tr} is then determined to be

$$t_{tr} = \frac{2R_i}{U} \,. \qquad (A1.7)$$

The surface burning process begins when the cell has completely entered the reaction zone, and ends when the fuel in the cell has been completely consumed. Assuming a uniform combustion occurring radially toward the center of the cell, the surface burning time t_S is given by

$$t_s = \frac{R_s}{S_L} \,. \qquad (A1.8)$$

where R_r is the initial radius at the beginning of the surface burning process (the radius at the end of the transition process) and S_L is the laminar flame speed of the mixture. Hence, the total burning time of one cell of reactants is determined to be

$$t_{tt} = t_{tr} + t_s \,. \tag{A1.9}$$

A1.3 The Acoustic Pressure Expression

The primary goal of the analysis is to evaluate an expression for dV/dt as a function of time for both the surface and transition burning processes. This is necessary because the total acoustic energy radiated by the combustion process is dependent on the time rate of change of the volume evolution d^2V/dt^2, as shown by Bragg [10]. For the surface burning process, it can be shown that

$$\left.\frac{d^2V}{dt^2}\right|_s = 8\pi(E-1)(t-t_{tt})S_L^{\,3} \,. \tag{A1.10}$$

where E is the expansion ratio (volume occupied by the products of combustion divided by the volume occupied by the unburned mixture at the same pressure).

Determining d^2V/dt^2 for the transition burning process is somewhat more complicated than for the surface burning process. The following four boundary conditions have been identified for the process:

$$\left.\frac{dV}{dt}\right|_{tr=0} \text{ and } \left.\frac{d^2V}{dt^2}\right|_{tr=0}, \quad \text{at } t=0 \,. \tag{A1.11}$$

and

$$\left.\frac{dV}{dt}\right|_{tr} = \left.\frac{dV}{dt}\right|_{s} \quad \text{and} \quad \left.\frac{d^2V}{dt^2}\right|_{tr} = \left.\frac{d^2V}{dt^2}\right|_{s}, \quad \text{at} \quad t = t_{tr} . \tag{A1.12}$$

These four boundary conditions suggest that dV/dt might be represented by the following third-degree quadratic expression

$$\left.\frac{dV}{dt}\right|_{tr} = at^3 + bt^2 + ct + d . \tag{A1.13}$$

Upon applying the boundary conditions, it can be shown that

$$a = \frac{-8\pi(E-1)t_s t_{tt} S_L{}^3}{t_{tr}{}^3} . \tag{A1.14}$$

$$b = \frac{4\pi(E-1)t_s S_L{}^3}{t_{tr}{}^2}(t_s + 2t_{tt}) . \tag{A1.15}$$

$$c = d = 0 . \tag{A1.16}$$

A1.4 Evaluation of the Radius at the Beginning of Surface Burning

At this point the only unknown remaining is the radius of the cell at the beginning of the surface burning process R_S. Since R_S is implicitly used in determining expressions for both transition and surface burning processes, it must be evaluated in terms of the four basic fuel and burner parameters. Following the logic of the model thus far, an expression containing R_s is determined as

$$\frac{at_{tr}{}^4}{4} + \frac{bt_{tr}{}^3}{3} = \frac{4}{3}\pi(E-1)\left(R_i{}^3 - R_s{}^3\right) . \tag{A1.17}$$

Both expressions for a and b are nonlinear functions, therefore it is not possible to obtain an explicit expression for R_S. However, equation (A1.17) may be solved iteratively with equations (A1.7), (A1.8), (A1.9), (A1.14) and (A1.15) to obtain R_S.

A1.5 Development of the Acoustic Pressure Expression

An expression for the acoustic pressure due to a single burning cell in terms of fundamental burner and fuel variables is now presented. Nathani shows that the non-dimensional acoustic pressure for surface burning is

$$P_s = \tau - 1 \,, \tag{A1.18}$$

where τ is the non-dimensional time

$$\tau = \frac{t}{t_{tt}} \tag{A1.19}$$

P_S is defined as

$$P_s = \frac{p_S}{\gamma} \,, \tag{A1.20}$$

$$\gamma = \frac{\rho}{4\pi d}\beta \,, \tag{A1.21}$$

$$\beta = 8\pi t_{tt}(E-1)S_L{}^3 \,, \tag{A1.22}$$

where ρ is the density of air. The non-dimensional acoustic pressure for the transition period is found to be

$$P_{tr} = \frac{1}{\beta}\left(3at_{tt}^{\,2}\tau^2 + 2bt_{tt}\tau\right) . \qquad (A1.23)$$

The non-dimensional acoustic pressure as a function of time for the burning of one cell is given by equations (A1.18) and (A1.23). Nathani uses a Fourier series of the periodic function of period $\tau = 1$ to apply these equations to a continuous stream of combustible cells and to obtain the pressure spectra. The reader is referred to this work (Nathani [1]) for further explanation.

A1.6 Third-Octave Band Spectra

The Fourier series solution discussed in the previous section generates a line spectrum for the acoustic emission of a turbulent flame. The line spectrum is converted into a third-octave band spectrum by applying an RMS to the pressures within a given third-octave band.

The first 1/3-octave band extends from 0 to 45 Hz with a center frequency of 20 Hz

$$0 < f_1 < 45 \text{ Hz}, \text{ and } f_{1c} = 20 \text{ Hz} . \qquad (A1.24)$$

The lower frequencies of the remaining b^{th} bands are given by

$$f_{bl} = 45 \text{ x } 2^{(b-2)/3}, \qquad (A1.25)$$

the upper frequencies of the b^{th} bands are given by

$$f_{bu} = 45 \text{ x } 2^{(b-1)/3}, \qquad (A1.26)$$

and the center frequencies of these bands are given by

$$f_{bc} = 45 \text{ x } 2^{(2b-3)/6}. \qquad (A1.27)$$

The pressure amplitude in each band is calculated by applying an RMS sum of the pressures within each third-octave band

$$|P_b| = \sqrt{\sum_{n=f_{bl}t_{tt}}^{n=f_{bu}t_{tt}} |P_n|^2} \quad , \quad b = 1,2,....\infty. \qquad (A1.28)$$

A1.7 The Effective Number of the Noise Sources

The solution for the acoustic pressure developed thus far only reflects a single burning cell. Therefore, an expression for the number of such reacting cells at a given time is developed in terms of fundamental burner and fuel parameters.

Nathani shows that the number of effective noise sources at any given instant is

$$n = \sqrt{\frac{2}{3}} \frac{Ut_{tt}}{D} \quad . \qquad (A1.29)$$

From this result, an expression for the total sound power can be obtained by multiplying the power expressions for the noise generated by a single cell by the instantaneous number of cells in the combustion zone.

A1.8 Evaluating Pressure and Power

A1.8.1 Sound Pressure

The total sound pressure amplitude generated by a single cell is obtained by taking the root-mean square of the sum of the pressure amplitudes in each band, that is,

$$P_{si} = \sqrt{|P_1|^2 + |P_2|^2 + |P_3|^2 + ... + |P_b|^2 + ... + |P_\infty|^2} \quad . \qquad (A1.30)$$

The overall sound pressure level (OASPL) is given by

$$OASPL = 20 \log\left(\frac{P}{P_{ref}} \right) , \qquad (A1.31)$$

where

$$P_{ref} = 2 \text{ x } 10^{-5} \text{ N/m}^2 . \qquad (A1.32)$$

A1.8.2 Sound Power

The sound power is shown to be the product of the pressure amplitude produced by a single cell and the instantaneous number of the combustible cells in the combustion zone:

$$S_P = 4\pi d^2 n\left(\frac{P_{si}^{\ 2}}{2\rho c} \right) , \qquad (A1.33)$$

where ρ is the density of air and c is the velocity of sound. The overall sound power level (OAPWL) is expressed as

$$OAPWL = 10 \log\left(\frac{S_P}{S_{Pref}} \right), \qquad (A1.34)$$

where,

$$S_{Pref} = 10^{-13} \text{ W}. \qquad (A1.35)$$

A1.9 Computer Code

All calculations cited in this section have be coded to be performed by a FORTRAN program. The program implements regression routines to determine the coefficients for the acoustic pressure expression during the transition burning process. Output options include third-octave band predictions and calculated overall sound pressure levels. The computer code is included in Appendix A2.

A2. Model FORTRAN Code

```
C                FORTRAN PROGRAM FOR
C
C          "A TURBULENT COMBUSTION NOISE MODEL"
C
C                   (THESIS)
C
C                   SUBMITTED TO
C
C          DEPARTMENT OF MECHANICAL ENGINEERING
C
C     VIRGINIA POLYTECHNIC INSTITUTE AND STATE UNIVERSITY
C
C                BLACKSBURG, VIRGINIA
C
C                      BY
C
C                   ARUN NATHANI


C          THE FOLLOWING PROGRAM EVALUATES CURVES FOR
C          DV/DT AND ACOUSTIC PRESSURE GENERATED BY A
C          SINGLE BURNING CELL IN THE COMBUSTION ZONE.
C          IT ALSO GENERATES LINE SPECTRA, 1/3 OCTAVE BAND
C          SPECTRA FOR THE TOTAL SOUND PRESSURE PRODUCED IN
C          THE COMBUSTION ZONE.  IN ADDITION, THIS PROGRAM
C          GIVES THERMOACOUSTIC EFFICIENCY, SOUND POWER,
C          PEAK FREQUENCY AND OVER-ALL SOUND PRESSURE LEVEL.
C          FINALLY, THE PROGRAM DEVELOPS A EMPIRICAL
C          CORRELATION FOR THE SOUND POWER PRODUCED IN
C          TERMS OF FUNDAMENTAL BURNER AND FUEL PARAMETERS


C               INPUT BURNER PARAMETERS
C
C          U ..... CONVECTIVE VELOCITY OF FUEL INJECTION (M/S)
C          D ..... BURNER DIAMETER (M)


C               INPUT FUEL PARAMETERS
C
C          SL ..... LAMINAR FLAME SPEED (M/S)
C          E ..... EXPANSION RATIO  (RATIO BETWEEN THE VOLUME
C                  OCCUPIED BY BURNT GASES TO UNBURNT GASES
C          QQ ..... CALORIFIC VALUE OF THE FUEL (J/M**3)
C          FR ..... AIR-FUEL VOLUMETRIC RATION
C          FLTP..... FLAME TEMPERATURE (KELVINS)


C               EXPERIMENTAL PARAMETERS
C
```

```
C       DOP,DP... DISTANCE OF OBSERVATION POINT FROM SOURCE (M)
C       RHO ..... DENSITY OF AIR (KG/M**3)
C       CSOU..... VELOCITY OF SOUND IN AIR (M/S)
C       FLIN..... PREIGNITION REACTANT TEMPERATURE


C            PARAMETERS EVALUATED
C
C       DVT  .... DV/DT (M**3/S), (RATE OF CHANGE OF VOLUME
C             FOR A SINGLE BURNING CELL AS A FUNCTION
C             OF TIME)
C       D2VT .... D**V/DT**2 (M**3/S**2), (DERIVATIVE  OF
C             DV/DT AS A FUNCTION OF TIME)
C       PST..... ACOUSTIC PRESSURE (N/M**2) AS A FUNCTION
C             OF TIME FOR A SINGLE BURNING CELL
C       SPL..... SOUND PREESSURE LEVEL SPECTRUM, (NONDIMEN
C             -SIONAL LINE SPECTRUM AS A FUNCTION
C             OF FREQUENCY)
C       OASPL ... OVER-ALL SOUND PRESSURE LEVEL, (NONDIMEN
C             SIONAL)
C       ETA ..... THERMOACOUSTIC EFFICIENCY
C       POWW  ... ACOUSTIC POWER (WATTS)


C       INTERMEDIATE PARAMETERS
C
C       RI ..... INITIAL RADIUS OF THE CELL (M)
C       RS ..... CELL RADIUS AT THE BEGINING OF
C             SURFACE BURNING (M)
C       NI ..... INSTANTANEOUS NUMBER OF CELLS
C       A,B ..... CONSTANTS IN THE DV/DT EXPRESSION
C       TTR ..... TRANSITION TIME (S)
C       TS ..... SURFACE BURNING TIME (S)
C       TTT ..... TOTAL BURNING TIME (S)
C       AN,BN ... FREQUENCY DEPENDENT VARIABLES USED TO
C             EVALUATE SPL SPECTRUM
C       H ..... HEAT PRODUCTION RATE


C          INDEPENDENT PARAMETERS
C
C       CF ..... CENTRAL FREQUENCIES IN 1/3 OCTAVE BAND (HZ)
C       F ..... FREQUENCY (HZ)
C       T ..... TIME (S)
C       PR ..... REFERENCE ACOUSTIC PRESSURE (N/M**2)
C       BF ..... FREQUENCIES ENVELOPING THE 1/3 OCTAVE BANDS
C       PI ..... 22./7.
C       NN ..... NUMBER OF HARMONICS WHERE CALCULATIONS STOP
C       IA,IB,IC,ID,IE..... INTEGERS TO IDENTIFY THE USER PROMTS
```

```
C            REGRESSION ARRAYS INVOLVED
C
C          UUU,UU....ARRAYS FOR CONVECTIVE VELOCITY
C          DDD,DD....ARRAYS FOR BURNER DIAMETER
C          EEE,EE....ARRAYS FOR EXPANSION RATIO
C          SLLL,SLL..ARRAYS FOR FLAME SPEED
C          PPP .....ARRAY OF PREDICTED POWER
C          PRWW.....ARRAY OF REGRESSION POWER
C          BB.....SOLUTION OF REGRESSION
C          X,DBD,R,SCPE,XMAX,XMIN...EXTERNAL ARRAYS FOR RGIVN


C          THIS PART OF THE PROGRAM WILL GIVE DIMENSIONS TO ALL
C          ARRAYS INVOLVED IN THE SOLUTION

      DIMENSION DV(500),PST(500)
      DIMENSION FN(900),AN(900),BN(900)
      DIMENSION PF(900),PSF(900),PAF(900)
      DIMENSION BF(900),CF(900),CFK(900),PBAND(900),DB(900)
      DIMENSION POWER(200),BCF(200),UN(200),UA(200)
      DIMENSION POGIL(200)
      DIMENSION DDD(6,6,6,6),UUU(6,6,6,6),SLLL(6,6,6,6),EEE(6,6,6,6)
      DIMENSION PPP(6,6,6,6),FFF(6,6,6,6),POWR(6,6,6,6)
      DIMENSION UU(4),EE(4),SLL(4),DD(4)
      DIMENSION X(81,5),BB(5,1),DBD(5),R(5,5),SCPE(1,1),XMAX(5),XMIN(5)

c          FOLLOWING STEP DEFINES THE EXTERNAL SUBROUTINES
C          WHICH SUBSEQUENTLY WILL BE USED TO EVALUATE THE
C          REGRESSION FIT FOR SOUND POWER

      EXTERNAL AMACH,RGIVN,UMACH,WRRRN

C          FOLLOWING STEPS PROMPT THE USER TO FEED IN THE
C          INFORMATION FOR WHICH THE PROGRAM IS DESIRED TO RUN.
C          ACCORDING TO THE INFORMATION FED IN, THESE STEPS TAKE
C          AN EXIT TO EXECUTE THE DESIRED ACTIONS OR FURTHER
C          THE USER FOR MORE INFORMATION.

 10   CONTINUE
      STDE=0.
      CFFP=0.
      WRITE(6,*)
      WRITE(6,*)'       DO YOU WANT TO...'
      WRITE(6,*)'       DEVELOP REGRESSION FIT FOR SOUND POWER?'
      WRITE(6,*)
      WRITE(6,*)'       ENTER: <1> FOR YES, <2> FOR NO'
      READ(5,*)IA
      RHO=1.21
      FR=9.47
      DP=1.
      CSOU=343.
```

```
      QQ=3.58*10.**7
      WRITE(6,*)
      IF (IA .EQ. 1) GO TO 11
      WRITE(6,*)'       DO YOU WANT TO...'
      WRITE(6,*)'       EVALUATE POWER, THERMOACOUSTIC EFFICIENCY'
      WRITE(6,*)'       PEAK FREQUENCY AND OASPL FOR A SINGLE CASE'
      WRITE(6,*)
      WRITE(6,*)'       ENTER: <1> FOR YES, <2> FOR NO'
      READ(5,*)IB
      WRITE(6,*)
      WRITE(6,*)'       DO YOU WANT TO...'
      WRITE(6,*)'       OBTAIN LINE SPECTRUM FOR A SINGLE'
      WRITE(6,*)'       BURNING CELL?'
      WRITE(6,*)
      WRITE(6,*)'       ENTER: <1> FOR YES, <2> FOR NO'
      READ(5,*)IC
      WRITE(6,*)
      WRITE(6,*)'       DO YOU WANT TO...'
      WRITE(6,*)'       OBTAIN 1/3 OCTAVE BAND FOR A SINGLE'
      WRITE(6,*)'       BURNING CELL?'
      WRITE(6,*)
      WRITE(6,*)'       ENTER: <1> FOR YES, <2> FOR NO'
      READ(5,*)ID
      WRITE(6,*)
      WRITE(6,*)'       DO YOU WANT TO...'
      WRITE(6,*)'       OBTAIN DV/DT VS. TIME, AND PRESSURE'
      WRITE(6,*)'       VS. TIME PLOTS FOR A SINGLE BURNING CELL?'
      WRITE(6,*)
      WRITE(6,*)'       ENTER: <1> FOR YES, <2> FOR NO'
      READ(5,*)IE
      WRITE(6,*)
      IF (IA .EQ. 2) GO TO 12
   11 CONTINUE
      WRITE(6,*)'        PLEASE ENTER U(MIN),U(MAX) '
      WRITE(6,*)'  (BOUNDARY VALUES OF CONVECTIVE VELOCITY (IN M/S))'
      READ(5,*)UMIN,UMAX
      WRITE(6,*)
      UU(1)=UMIN
      UU(2)=(UMIN+UMAX)/2.
      UU(3)=UMAX
      DO 13 K=1,3
      DO 14 L=1,3
      DO 15 M=1,3
      DO 16 N=1,3
      UUU(K,N,M,L)=UU(N)
   16 CONTINUE
   15 CONTINUE
   14 CONTINUE
   13 CONTINUE

      WRITE(6,*)'       PLEASE ENTER D(MIN),D(MAX)'
```

```
      WRITE(6,*)'   (BOUNDARY VALUES OF BURNER DIAMETER, (IN CM))'
      READ(5,*)DMIN,DMAX
      WRITE(6,*)
      DD(1)=DMIN/100.
      DD(2)=(DMIN+DMAX)/(2.*100.)
      DD(3)=DMAX/100.
      DO 17 K=1,3
      DO 18 L=1,3
      DO 19 N=1,3
      DO 20 M=1,3
      DDD(K,N,M,L)=DD(M)
   20 CONTINUE
   19 CONTINUE
   18 CONTINUE
   17 CONTINUE

      WRITE(6,*)'       PLEASE ENTER SL(MIN),SL(MAX)'
      WRITE(6,*)'     (BOUNDARY VALUES OF FLAME SPEED (IN CM/S))'
      READ(5,*)SLMIN,SLMAX
      WRITE(6,*)
      SLL(1)=SLMIN/100.
      SLL(2)=(SLMIN+SLMAX)/(2.*100.)
      SLL(3)=SLMAX/100.
      DO 21 K=1,3
      DO 22 M=1,3
      DO 23 N=1,3
      DO 24 L=1,3
      SLLL(K,N,M,L)=SLL(L)
   24 CONTINUE
   23 CONTINUE
   22 CONTINUE
   21 CONTINUE

      WRITE(6,*)'       PLEASE ENTER E(MIN),E(MAX)'
      WRITE(6,*)'   (BOUNDARY VALUES OF EXPANSION RATIO)'
      READ(5,*)EMIN,EMAX
      WRITE(6,*)
      EE(1)=EMIN
      EE(2)=(EMIN+EMAX)/2.
      EE(3)=EMAX
      DO 25 M=1,3
      DO 26 N=1,3
      DO 27 L=1,3
      DO 28 K=1,3
      EEE(K,N,M,L)=EE(K)
   28 CONTINUE
   27 CONTINUE
   26 CONTINUE
   25 CONTINUE

      WRITE(6,*)' U   D    E   SL    SP    ETA  OSPL   FREQP'
```

```
      WRITE(6,*)

      MM = 1
      DO 29 L = 1,3
      DO 30 M = 1,3
      DO 31 K = 1,3
      DO 32 J = 1,3

C           THIS PART OF THE PROGRAM WILL GIVE VALUES TO ALL
C           THE EXPERIMENTAL PARAMETERS USED
C
      U = UUU(K,L,M,J)
      D = DDD(K,L,M,J)
      SL = SLLL(K,L,M,J)
      E = EEE(K,L,M,J)


C           THIS PART OF THE PROGRAM WILL GIVE INPUT VALUES OF
C           THE BURNER AND FUEL PARAMETERS

      IF (IA .EQ. 1)THEN
      GO TO 33
      ENDIF
   12 WRITE(6,*)'       ENTER CONVECTIVE VELOCITY U (M/S)'
      READ(5,*)U
      WRITE(6,*)
      WRITE(6,*)'       ENTER BURNER DIAMETER D (CM)'
      READ(5,*)D
      D = D/100.
      WRITE(6,*)
      WRITE(6,*)'       PLEASE ENTER INITIAL REACTANT TEMP. IN KELVINS'
      WRITE(6,*)'       (ENTER <1> FOR DEFAULT (298 K))'
      READ(5,*)GG
      WRITE(6,*)

      IF (GG .EQ. 1) THEN
      FLIN = 298.
      ELSE
      FLIN = GG
      ENDIF

      WRITE(6,*)'       PLEASE ENTER SOUND VELOCITY IN MEDIUM'
      WRITE(6,*)'       (ENTER <1> FOR DEFAULT (343 M/S))'
      READ(5,*)HH
      WRITE(6,*)

      IF (HH .EQ. 1) THEN
      CSOU = 343.
      ELSE
      CSOU = HH
      ENDIF
```

```
WRITE(6,*)'      PLEASE ENTER MEDIUM DENSITY'
WRITE(6,*)'      (ENTER <1> FOR DEFAULT (1.21 KG/M**3))'
READ(5,*)RR
WRITE(6,*)

IF (RR .EQ. 1.) THEN
RHO=1.21
ELSE
RHO=RR
ENDIF

WRITE(6,*)'      PLEASE ENTER DISTANCE OF OBSERVATION POINT'
WRITE(6,*)'      (ENTER <1> FOR DEFAULT (1 M))'
READ(5,*)DOP
WRITE(6,*)

IF (DOP .EQ. 1.) THEN
DP=1.
ELSE
DP=DOP
ENDIF

WRITE(6,*)'      ENTER FUEL TYPE FROM THE FOLLOWING OPTIONS...'
WRITE(6,*)'      ENTER <1> FOR METHANE'
WRITE(6,*)'      ENTER <2> FOR CARBON MONOXIDE'
WRITE(6,*)'      ENTER <3> FOR HYDROGEN'
WRITE(6,*)'      ENTER <4> FOR ACETYLENE'
WRITE(6,*)'      ENTER <5> FOR OTHER THAN ABOVE'
READ(5,*)IF
IF (IF .EQ. 1) THEN
SL=.5
FR=9.47
FLTP=2210.
QQ=3.58*10.**7
ENDIF

IF (IF .EQ. 2) THEN
SL=.4
FR=2.38
FLTP=2400.
QQ=5.86*10.**6
ENDIF

IF (IF .EQ. 3) THEN
SL=2.5
FR=2.88
FLTP=2400.
QQ=1.08*10.**7
ENDIF
```

```
      IF (IF .EQ. 4) THEN
      SL = 1.4
      FR = 11.9
      FLTP = 2600.
      QQ = 5.61*10.**7
      ENDIF

      IF (IF .EQ. 5) THEN
      WRITE(6,*)' PLEASE ENTER THE FOLLOWING INFORMATION ABOUT THE
      WRITE(6,*)
      WRITE(6,*)'       LAMINAR FLAME SPEED? (IN CM/S)'
      READ(5,*)SL
      SL = SL/100.
      WRITE(6,*)
      WRITE(6,*)'       STOCHIOMETRIC AIR-FUEL RATIO (VOLUMETRIC)?'
      READ(5,*)FR
      WRITE(6,*)
      WRITE(6,*)'       FLAME TEMPERATURE? (IN KELVINS)'
      READ(5,*)FLTP
      WRITE(6,*)
      WRITE(6,*)'       HEAT OF REACTION (IN J/M**3) X 10 ** -7 ?'
      READ(5,*)QQ
      QQ = QQ*10.**7
      WRITE(6,*)
      ENDIF

      E = FLTP/FLIN

      WRITE(6,*)
      WRITE(6,*)'OUTPUT.....'
      WRITE(6,*)
   33 CONTINUE
      NN = 500
      NNN = 50.
      PI = 22./7.

C          THIS PART OF THE PROGRAM EVALUATES THE INTERMEDIATE
C          PARAMETERS WHICH ARE DIRECTLY RELATED TO
C          BURNER AND FUEL VARIABLES

      RI = SQRT(3./8.)*D
      TTR = 2.*SQRT(3./8.)*D/U
      H = (PI/4.)*U*D**2*QQ/FR
      CN = U/(2.*SL)


C          1. IN THIS FIRST PHASE OF PROGRAMMING, THE
C             RADIUS "RS" AT THE BEGINING OF SURFACE
C          BURNING IS EVALUATED.
```

```
C       1.1  IN THE FIRST STEP THE INITIAL VALUES OF
C            HIGHEST POSSIBLE RS (RSH) AND LOWEST
C            POSSIBLE RS (RSL) ARE GIVEN.  ALSO A
C            INITIAL VALUE OF RS (RSG) IS GUESSED.

      RSH = RI
      RSL = 0.
      RSG = RI

C       1.2  LOOP FOR THE CALCULATION OF "RS" BEGINS
C            IN THIS STEP.  THE FIRST STEP IS TO CHECK
C            THE CONVERGENCE OF GUESSED VALUE OF "RS".

 34   IF (RSG .GT. RI .OR. RSG .LT. 0.1*RI) THEN
      WRITE(6,*)'PROGRAM NOT CONVERGING. INPUT DATA
      GO TO 35
      ENDIF

C       1.3  SURFACE BURNING TIME AND TOTAL BURNING TIME
C            ARE EVALUATED IN TERMS OF THE GUESSED VALUE
C            OF RADIUS AT THE BEGINING OF SURFACE BURNING

      TS = RSG/SL
      TTT = TTR + TS
      EPS = TTR/TTT

C       1.4  CONSTANTS A AND B ARE EVALUATED.

      A = -8.*PI*(E-1.)*TS*TTT*SL**3/(TTR**3)
      B = 4.*PI*(E-1.)*TS*SL**3*(TS + 2.*TTT)/(TTR**2)

C       1.5  THE DIFFERNCE "RSD" BETWEEN THE GUESSED VALUE OF RS
C            AND THE CALCULATED VALUE OF RS (FROM THE GUESS)
C            IS EVALUTED.  THIS DIFFERENCE IS CHANGED INTO
C            PERCENTAGE DEVIATION FROM THE GUESS.  IF THE CHANGE
C       , THEN CONTROL IS TAKEN FROM THE LOOP
C            AND THE CURRENT GUESS OF "RS" IS ACCEPTED AS THE
C            FINAL VALUE OF "RS".

      RSD = RSG-(RI**3-3.*TTR**3*(A*TTR/4. + B/3.)/(4.*(E-1.)*PI))**.333
      PD = RSD/RSG
      IF (PD .LT. 0.)THEN
      PD = -1.*PD
      ENDIF
      IF (PD .LE. .01) THEN
      RS = RSG
      GO TO 36
      ENDIF

C       1.6  IF THE GUESSED VALUE OF "RS" IS LESS THAN THE
C            CALCULATED VALUE, THEN
```

```
C       1.6.1  LOWEST POSSIBLE VALUE OF "RS" IS EQUATED TO
C              THE GUESS,
C       1.6.2  A NEW GUESS IS MADE AS A MEAN OF PREVIOUS
C              GUESS AND THE HIGHEST ACCEPTABLE VALUE OF "RS".

      IF (RSD .LT. .0) THEN
      RSL = RSG
      RSG = (RSG + RSH)/2.
      ENDIF

C       1.7  IF THE GUESSED VALUE OF "RS" IS GREATER THAN THE
C            CALCULATED VALUE, THEN
C       1.7.1  HIGHEST POSSIBLE VALUE OF "RS" IS EQUATED TO
C              THE GUESS,
C       1.7.2  A NEW GUESS IS MADE AS A MEAN OF PREVIOUS
C              GUESS AND THE LOWEST POSSIBLE VALUE OF "RS".
C       1.7.3  GO BACK TO THE START OF LOOP

      IF (RSD .GT. .0) THEN
      RSH = RSG
      RSG = (RSG + RSL)/2.
      ENDIF
      GO TO 34
   36 CONTINUE
      BETA = 8.*PI*TTT*(E-1.)*SL**3

C             THE FOLLOWING STEPS EVALUATE DV/DT AND RATE
C             OF CHANGE OF DV/DT AS A FUNCTION OF TIME
C             FOR A SINGLE BURNING EDDY

      IF (IA .EQ. 1) GO TO 37
      IF (IE .EQ. 2) GO TO 37
      GB = RHO/(4.*PI*DP)
      IF (IE .EQ. 1) THEN
      WRITE(6,*) 'DV/DT AND PRESSURE VS TIME FOR A SINGLE BURNING
      WRITE(6,*)
      WRITE(6,*) 'NONDIMEN. TIME     DV/DT (M**3/S)    PRESS. (N/M**2)'
      WRITE(6,*)
      ENDIF
      DO 38 I = 1,NNN
      TAU = FLOAT(I-1)/(NNN-1)
      T = TAU*TTT
      IF(TAU.LT.EPS)THEN
      DV(I) = A*T**3 + B*T**2
      PST(I) = GB*(3.*A*T**2 + 2.*B*T)
      ENDIF
      IF(TAU.GT.EPS)THEN
      DV(I) = 4.*PI*(E-1.)*(TTT-T)**2*SL**3
      PST(I) = GB*8.*PI*(E-1.)*(T-TTT)*SL**3
      ENDIF
      III = 1
```

```
      IF (IA .EQ. 1) GO TO 39
      IF (IE .EQ. 1) THEN
      WRITE(6,1000) TAU,DV(I),PST(I)
      WRITE(6,*)
 1000 FORMAT(1X,3(F15.6,3X))
      ENDIF
   39 CONTINUE
   38 CONTINUE
   37 CONTINUE
      IF (IA .EQ. 1) GO TO 40
      IF (IB .EQ. 2 .AND. IC .EQ. 2 .AND. ID .EQ. 2 ) GO TO 35
      IF (IC .EQ. 1) THEN
      WRITE(6,*)
      WRITE(6,*)' LINE SPECTRUM DUE TO A SINGLE BURNING EDDY'
      WRITE(6,*)
      WRITE(6,*)' FREQ. (KHZ)    PRESS (N/M**2)'
      WRITE(6,*)
      ENDIF
   40 CONTINUE

C       2. THIS PART OF THE PROGRAM OBTAINS LINE SPECTRUM
C          PRODUCED BY A SINGLE CONTINUOUS TRAIN OF EDDIES.

C       2.1 A LOOP IS STARTED FOR THE ORDER N OF THE LINE
C          SPECTRUM. ALL THE VARIABLES DEPENDENT ON "N"
C          TO BE USED FOR THE EVALUATION OF CONSTANTS "AN"
C          AND "BN" ARE EVALUATED.

    41 CONTINUE
      PSUM = 0.
      DO 42 N = 1,NN
      XX = N
      Q = XX*PI
      TH = Q*EPS
      S = SIN(2.*TH)
      C = COS(2.*TH)
      FN(N) = N/TTT
      IF (FN(N) .GT. 13000.) GO TO 43

C       2.2 "AN" AND "BN" FOR THE GIVEN VALUE OF
C          N ARE EVALUATED.

      AN(N) = 3.*A*TTT**2/BETA*((EPS**2/(2.*Q)-1./(4.*Q**3))*S
     1 + EPS/(2.*Q**2)*C)
     1 + 2.*B*TTT/BETA*(EPS/(2.*Q)*S-1./(4.*Q**2) + 1./(4.*Q**2)*C)
     1 -EPS/(2.*Q)*S-1./(4.*Q**2)*C + 1./(4.*Q**2)
     1 -1./(2.*Q)*S

      BN(N) = 3.*A*TTT**2/BETA*((-(EPS)**2/(2.*Q) + 1./(4.*Q**3))*C
     1 + EPS/(2.*Q**2)*S-1./(4.*Q**3))
     1 + 2.*B*TTT/BETA*(-EPS/(2.*Q)*C + 1./(4.*Q**2)*S)
```

```
     1  + EPS/(2.*Q)*C-1./(2.*Q)-1./(4.*Q**2)*S
     1 -1./(2.*Q) + 1./(2.*Q)*C

C          THIS STEP CALCULATES ACOUSTIC PRESSURE
C          AMPLITUDE AT EACH OF THE FREQUENCIES
C          ORDER "N" FOR A SINGLE BURNING CELL.  THESE
C          PRESSURE AMPLITUDES ARE THEN MULTIPLIED BY
C          THE NUMBER OF COMPACT NOISE SOURCE REGIONS
C          TO OBTAIN THE TOTAL ACOUSTIC PRESSURE AT EACH
C          HARMONIC FREQUENCY.  FINALLY THE LINE SPECTRUM FOR THE
C          SOUND PRESSURE VERSUS FREQUENCY IS PLOTTED.

     PF(N) = 2.*SQRT(AN(N)**2 + BN(N)**2)
     PSF(N) = RHO*PF(N)*BETA/(4.*PI*DP)
     YYY = 0.00
     ZZZ = FN(N)/1000.
     IF (IA .EQ. 1) GO TO 44
     IF (IC .EQ. 1) THEN
     WRITE(6,2000)ZZZ,PSF(N)
 2000 FORMAT(2X,F7.3,10X,F8.6)
     ENDIF
  44  CONTINUE

C          SUM OF THE SQUARES OF THE PRESSURE AMPLITUDES
C          AT EACH FREQUENCY

     PSUM = PSUM + PSF(N)**2
  42  CONTINUE
  43  CONTINUE
     IF (IB .EQ. 2 .AND. ID .EQ. 2 .AND. IA .EQ. 2) GO TO 35

C          THE FOLLOWING STEPS EVALUATE PRESSURE AMPLITUDE
C          OVERALL SOUND PRESSURE LEVEL, SOUND POWER
C          PRODUCED, AND THERMOACOUSTIC EFFICIENCY

     PAMP = SQRT(PSUM)
     PDB = 20.*LOG10(PAMP/.00002)
     ASPL = 20.*LOG10(PAMP* SQRT(CN)/.00002)
     PRW = 4.*PI*DP**2*PAMP*PAMP*CN/(2.*RHO*CSOU)
     TAE = PRW/H
     IF (IA .EQ. 1) GO TO 45
     IF (IB .EQ. 1 .OR. ID .EQ. 1) GO TO 46
  45  CONTINUE

C          THIS SECTION COVERTS THE ARRAYS OF PREDICTED POWER
C          AND INPUT PARAMETERS INTO CORRESPONDING ARRAYS TO
C          BE USED LATER AS INPUT FOR IMSL SUBROITINE RGIVN

     PPP(K,L,M,J) = PRW
     X(MM,1) = LOG10(UUU(K,L,M,J))
     X(MM,2) = LOG10(DDD(K,L,M,J))
```

```
      X(MM,3)=LOG10(SLLL(K,L,M,J))
      X(MM,4)=LOG10(EEE(K,L,M,J))
      X(MM,5)=LOG10(PPP(K,L,M,J))
      MM=MM+1
      NNNN=1
   46 CONTINUE

C          THIS PART OF THE PROGRAM CONVERTS THE LINE SPECTRUM
C          GIVEN EARLIER INTO 1/3 OCTAVE BANDS.

C          IN THIS PART BOUNDARY FREQUENCIES OF THE
C          1/3 OCTAVE BANDS ARE DEFINED

      BF(1)=16.
      BF(2)=20.
      DO 47 N=3,32
      BF(N)=45.*2.**(.33*(N-3))
   47 CONTINUE

C          EVALUATION OF CENTRAL FREQUENCIES OF 1/3 OCTAVE BANDS

      CF(1)=8.
      DO 48 N=2,32
      CF(N)=SQRT(BF(N-1)*BF(N))
   48 CONTINUE
      CFP=0.
      PMAX=0.

C          INITIALIZATION OF PRESSURE AMPLITUDES IN EACH BAND

      DO 49 N=1,32
      PBAND(N)=0.
   49 CONTINUE

C          IN THIS SECTION NET PRESSURE AMPLITUDE IN EACH
C          1/3 OCTAVE IS EVALUATED AS THE MEAN SQUARE
C          ROOT OF THE PRESSURES LYING INSIDE EACH OCTAVE
C          ALSO THIS AMPLITUDE IS NONDIMENSIONALIZED
C          EXPRESSED IN DECIBELS

      DO 50 I=1,31
      DO 51 N=1,500
      IF(FN(N).GE.BF(I) .AND. FN(N).LE.BF(I+1)) THEN
      PBAND(I)=PBAND(I)+PSF(N)**2
      ENDIF
   51 CONTINUE
   50 CONTINUE
      IF (IA .EQ. 1) GO TO 52
      IF (ID .EQ. 1) THEN

C          THIS SECTION GIVES HEADINGS TO THE 1/3 OCTAVE RESULTS
```

```
      WRITE(6,*)
      WRITE(6,*)'       1/3 OCTAVE.....'
      WRITE(6,*)
      WRITE(6,*)' FREQ (KHZ)   PRESS (DB)   PRESS (N/M**2)'
      WRITE(6,*)
      ENDIF
   52 CONTINUE
      DO 53 N=1,31
      PBAND(N)=SQRT(PBAND(N))
      IF(PBAND(N).EQ.0.)THEN
      GO TO 53
      ENDIF
      DB(N)=20.*LOG10(PBAND(N)/.00002)

C           THIS SECTION PLOTS THE 1/3 OCTAVE BAND
C           FOR 1) PRESSURE AMPLITUDES 2) PRESSURE
C           AMPLITUDES IN DECIBELS VERSUS THE
C           CORRESPONDING CENTRAL FREQUENCIES

      CFK(N)=CF(N)/1000.
      IF (IA .EQ. 1) GO TO 54
      IF (ID .EQ. 1) THEN
      WRITE(6,3000)CFK(N),DB(N),PBAND(N)
      WRITE(6,*)
   3000 FORMAT(2X,F7.4,6X,F6.2,6X,F6.4)
      ENDIF
   54 CONTINUE

C           THIS SECTION EVALUATES THE PEAK FREQUENCY AND
C           THE CORRESPONDING PRESSURE AMPLITUDE

      IF(PBAND(N).GE.PMAX)THEN
      PMAX=PBAND(N)
C     PCF=CF(N)
C     CFP=1./TTT
      CFP=CF(N)
      ENDIF
   53 CONTINUE

C           THIS SECTION WRITES DOWN THE OVERALL SOUND PRESSURE
C           LEVEL, TOTAL SOUND PRESSURE, THE ACOUSTIC
C           POWER AND PEAK FREQUENCY FOR A SINGLE RUN.

      IF (IA .EQ. 1) GO TO 55
      IF (IB .EQ. 1) THEN
      WRITE(6,*)
      WRITE(6,*)'SOUND POWER =',PRW,'W'
      WRITE(6,*)
      WRITE(6,*)'THERMOACOUSTIC EFFICIENCY =',TAE
      WRITE(6,*)
```

```
      WRITE(6,*)'OVER-ALL SOUND PRESSURE LEVEL =',ASPL,'DB'
      WRITE(6,*)
      WRITE(6,*)'PEAK FREQUENCY =',CFP,'HZ'
      ENDIF
   55 CONTINUE

C           THIS SECTION WRITES DOWN THE OVERALL SOUND PRESSURE
C           LEVEL, TOTAL SOUND PRESSURE, THE ACOUSTIC
C           POWER AND PEAK FREQUENCY FOR MULTIPLE RUNS

      IF (IA .EQ. 1) THEN
      TAE=TAE*10.**8
      D=D*10.**2+.5
      SL=SL*10.**2+.5
      CFFP=CFP+CFFP
      NU=U
      ND=D
      NSL=SL
      NE=E
      NC=CFP
      NA=ASPL
      NT=TAE
      NP=PRW
      WRITE(6,4000)NU,ND,NE,NSL,PRW,NT,NA,NC
   4000 FORMAT(2X,I2,4X,I1,4X,I2,4X,I2,4X,F6.4,4X,I3,4X,I3,4X,I4)
      WRITE(6,*)
      ENDIF
C     FFF(K,L,M,J)=CFP
C     X(MM,5)=LOG10(FFF(K,L,M,J))
C     MM=MM+1
      IF (IA .EQ. 2) GO TO 35
      PMAX=0.
   32 CONTINUE
   31 CONTINUE
   30 CONTINUE
   29 CONTINUE

C           THIS SECTION PERFORMS THE REGRESSION FOR THE
C           SOUND POWER FOR 81 RUNNING SETS AS SPECIFIED
C           IN THE INPUT.  SUBROUTINE RGIVN FROM IMSL
C           PERFORMS THE REGRESSION

      IDO=0
      NROW=81
      NCOL=5
      LDX=81
      INTCEP=1
      IIND=-4
      IDEP=-1
      IFRQ=0
      IWT=0
```

```
      ISUB = 1
      TOL = 100.0*AMACH(4)
      LDB = 5
      LDR = 5
      LDSCPE = 1
      NDEP = 1
      CALL RGIVN (IDO, NROW, NCOL, X, LDX, INTCEP, IIND, INDIND, IDEP,
     1          INDDEP, IFRQ, IWT, ISUP, TOL, BB, LDB, R, LDR, DBD,
     1          IRANK, DFE, SCPE, LDSCPE, NRMISS, XMIN, XMAX)

C         THIS SECTION COMPARES THE PREDICTED RESULTS WITH THE
C         LITERATURE.  IT ALSO GIVES THE MEAN PEAK FREQUENCY
C         OF THE PREDICTED REGRESSION.  FINALLY IT GIVES THE
C         ACTUAL PREDICTED RESULTS AND THE CORRESPONDING
C         REGRESSION RESULTS FOR SOUND POWER

      BB(1,1) = 10.**BB(1,1)
      WRITE(6,*)
      WRITE(6,*)'CONSTANT MULTIPLIER = ',BB(1,1)
      WRITE(6,*)
      WRITE(6,*)'EXPONENT OF VELOCITY = ',BB(2,1)
      IUR = (BB(2,1)-3.)*100./3.
      IUL = (BB(2,1)-2.67)*100./2.67
      WRITE(6,*)'% FROM LITER. FOR FUEL-LEAN PREMIXED FLAME = ',IUL
      WRITE(6,*)'% FROM LITER. FOR FUEL-RICH PREMIXED FLAME = ',IUR
      WRITE(6,*)
      WRITE(6,*)'EXPONENT OF BURNER DIAMETER = ',BB(3,1)
      IDR = (BB(3,1)-2.00)*100./2.00
      IDL = (BB(3,1)-2.81)*100./2.81
      WRITE(6,*)'% FROM LITER. FOR FUEL-LEAN PREMIXED FLAME = ',IDL
      WRITE(6,*)'% FROM LITER. FOR FUEL-RICH PREMIXED FLAME = ',IDR
      WRITE(6,*)
      WRITE(6,*)'EXPONENT OF FLAME SPEED = ',BB(4,1)
      ISL = (BB(4,1)-1.83)*100./1.83
      WRITE(6,*)'% FROM LITER. FOR FUEL-LEAN PREMIXED FLAME = ',ISL
      WRITE(6,*)
      WRITE(6,*)'EXPONENT OF EXPANSION RATIO = ',BB(5,1)
      WRITE(6,*)
      CFFP = (CFFP)/81.
      WRITE(6,*)'MEAN PEAK FREQUENCY = ',CFFP
      WRITE(6,*)
      WRITE(6,*)' CALCULATED SP    REGRESSION SP'
      WRITE(6,*)
      DO 56 L = 1,3
      DO 57 M = 1,3
      DO 58 K = 1,3
      DO 59 J = 1,3
      U = UUU(K,L,M,J)
      D = DDD(K,L,M,J)
      SL = SLLL(K,L,M,J)
      E = EEE(K,L,M,J)
```

```
      IJ = 1
      POWR(K,L,M,J) = BB(1,1)*U**BB(2,1)*D**BB(3,1)*SL**BB(4,1)*E**BB(5,1)
      WRITE(6,5000)PPP(K,L,M,J),POWR(K,L,M,J)
      WRITE(6,*)
 5000 FORMAT(2X,F10.6,6X,F10.6)
      STDE = (PPP(K,L,M,J)/POWR(K,L,M,J)-1.)**2 + STDE
   59 CONTINUE
   58 CONTINUE
   57 CONTINUE
   56 CONTINUE

C          THIS SECTION GIVES THE STANDARD DEVIATION IN THE
C          LITERATURE, AND THAT GIVEN BY THIS MODEL

      STDE = SQRT(STDE/81.)*100.
      WRITE(6,*)'STANDARD DEVIATION = ',STDE,'PERCENT'
      WRITE(6,*)
      WRITE(6,*)'STANDARD DEVIATION IN LITERATURE = 43 PERCENT'
   35 WRITE(6,*)

C          THIS SECTION PROMPTS THE USER FOR A SECOND RUN

      WRITE(6,*)'    DO YOU WANT TO RUN AGAIN'
      WRITE(6,*)
      WRITE(6,*)'    ENTER <1> FOR YES, <2> FOR NO'
      READ(5,*)IRUN
      IF(IRUN .EQ. 1) GO TO 10
      STOP
      END
```

A3. Anomalies In the Model Code

The results as presented in Table 7 expose a flaw in the model code. In particular, it is seen that for methane, the overall sound pressure level decreases in all cases when the velocity is increased from 10 m/s to 20 m/s. This is in sharp disagreement with the results that would be suggested by the actual Mahan-Nathani theory. However, the expected trend in overall sound pressure level is resumed when velocity is further increased to 25 m/s. Therefore, it appears that the results determined for a velocity of 10 m/s might be erroneous.

To investigate this discrepancy, the model code was run for all integer values of velocity between 5 m/s and 25 m/s for a fixed diameter of 0.356 cm. Figure 16 shows the response of overall sound pressure level as velocity is increased. The model shows that overall sound pressure levels decrease as velocity is increased from 5 m/s to 17 m/s. This is clearly in disagreement with the purely theoretical aspect of the model. Upon increasing velocity further, overall sound pressure levels increase as would be expected from the theory. These questionable results are apparently originating in the model code and are not due to the theory itself.

Another problem found was that the model code results for the smallest two burner diameters of acetylene yielded only two data points for the third-octave-band spectra. Hence, difficulty arose in trying to infer any conclusions regarding frequency content for acetylene. An examination of the model revealed that these results are due to a limitation in the fundamental theory. For very low burning times, as found with acetylene, the model will generate few data points. This indicates that the model should then be used only for low velocity, low flame speed cases.

With the assumed flame speed and flame temperature inputs, the shapes of the spectra predicted by the model are in general agreement with the experimental data.

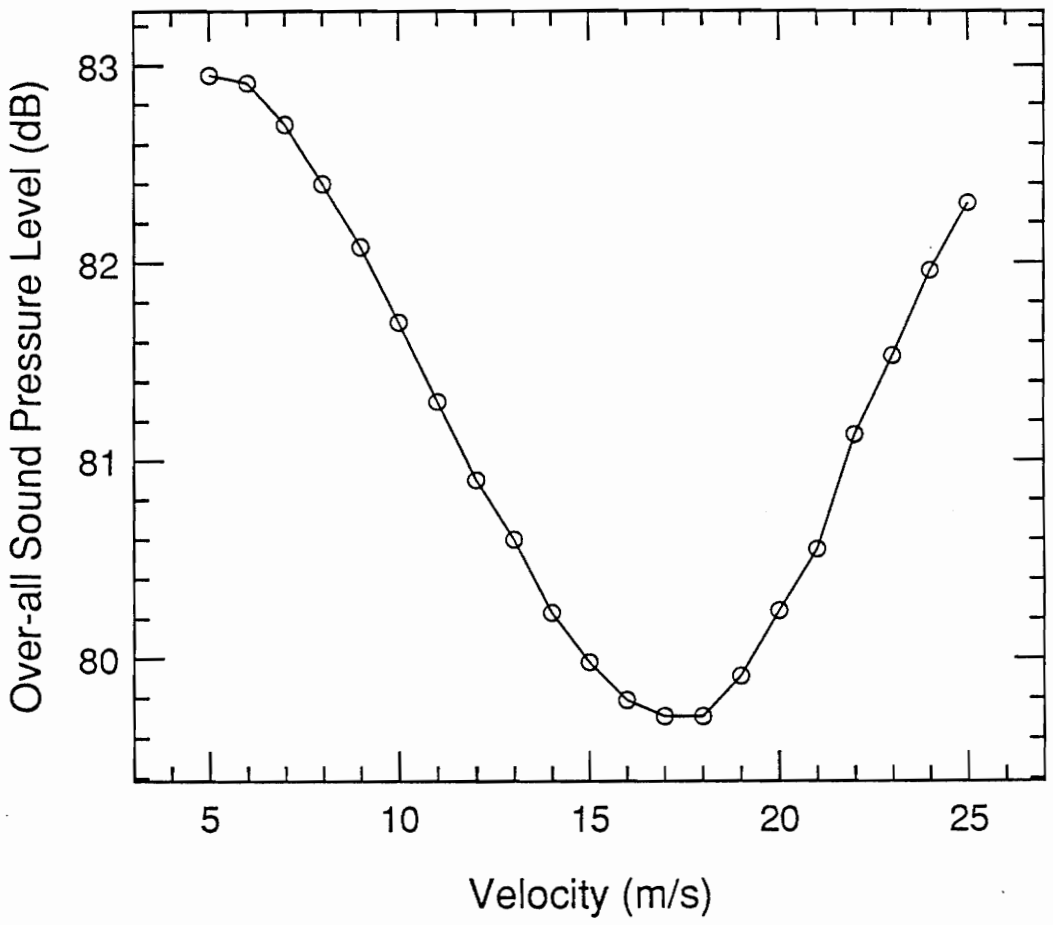

Figure 16. Predicted Overall Sound Pressure Level vs. Velocity: Methane, D = 0.356 cm

However, the model responds inconsistently to flame speed input. In particular, the model will respond to increasing flame speed with incremental increases in predicted peak frequency. Yet, at certain input levels, the model will predict an inconsistently large peak frequency change in a discrete manner. Continuing with incremental flame speed increases will then result in peak frequencies which again follow the continuous increasing peak frequency trend exhibited by the data prior to the discontinuity. This inconsistency acts in a similar manner as the inconsistency noted for overall sound pressure level response to velocity. Yet, in those results, the inconsistency was noted for overall sound pressure and not peak frequency.

It should be stressed here that these discontinuities in the code behavior did not occur often, but once discovered were sought out. In particular, for all experimental test points, only the case of methane flowing at 10 m/s showed unexpected results and it is believed that the rest of the computer code results reflect the true theoretical model results. The noted discrepancies were primarily seen in peak frequencies and not in overall sound pressure levels. The only exception was seen for overall sound pressure level response to velocity for the specific case of methane. However, the relatively low velocity of 10 m/s makes these test points unique among the rest of the data. Perhaps the low velocity does not allow the model code to converge to a solution when iterations occur.

Any further study concerning this code should examine the convergence criteria and the numerical integration process. Perhaps a different integration routine would alleviate the problems. Another possible solution might be to include a warning flag if the number of iterations to convergence is either unreasonably high or low. The model results obtained could then be questioned as to their validity. An increase in the number of integration steps may also reduce the occurrence of the problem.

Finally, an inconsistency in the code was noted in the calculation of the number of sound sources. Recall that the number of sound sources is used only in calculating

sound pressure levels. Therefore, the shape of the acoustic spectra is not affected by this calculation. To determine the extent of the error, the correct calculation was introduced into the code along with the erroneous calculation. A comparison of the results revealed that the code consistently underestimates the number of sound sources by about 9 percent which in turn results in about a 3 percent under-prediction of overall sound pressure levels compared to the theoretical calculation. It is apparent that this error is not the source of the anomalies cited previously and only results in slight discrepancies. When discontinuities in the model results were noted, the number of sound sources calculated in the code remained continuous. However, it is suggested that any further study regarding this model should correct this error.

Appendix B. Neutral Flame

Difficulty arose when trying to determine acceptable experimental fuel-oxygen mixture ratios for the combustible gases examined. In particular, the possible entrainment of surrounding air into the mixture added considerable uncertainties. Initial experiments showed that stoichiometric and fuel lean mixtures exhibited (based on premixed reactant flows) high frequency instabilities which tended to mask the true combustion noise. In view of past experimental data, it seemed apparent that the initial mixture should be fuel rich to avoid the undesirable combustion instabilities.

Insight into the reactions that occur when a premixed fuel-oxygen mixture is combusted in air was necessary to determine experimental fuel-oxygen ratios. In addition, an understanding of the underlying chemistry would reveal how to properly apply the model to the experimental results. Because of its wide use in industrial applications, the extensive literature on acetylene as used in welding processes was examined.

The concept of a "neutral flame" [30,31,32] is widely used in welding and is the condition upon which the fuel is completely oxidized by premixed oxygen and diffused air. Thus, the complete reaction occurs in two distinct combustion zones. In the primary reaction zone, the fuel reacts with oxygen to form products of CO and H_2. For acetylene, the following chemical equation results for the primary reaction zone:

$$C_2H_2 + O_2 \equiv 2CO + H_2$$

In the secondary reaction zone, the carbon monoxide and the hydrogen produced in the first reaction are oxidized by atmospheric air being entrained into the turbulent flame. For acetylene, the following chemical equation results for the secondary reaction zone:

$$2CO + H_2 + 1.5O_2 + 5.64N_2 \equiv 2CO_2 + H_2O + 5.64N_2$$

Therefore, the complete combustion of one mole of acetylene results from one mole of oxygen provided in the mixture and one-and-a-half moles of oxygen provided by the entrainment of surrounding atmosphere.

A neutral flame is characterized by two distinctly visible flame zones at the burner exit. The primary reaction zone consists of a brilliant blue inner come which will generally be well defined. The secondary reaction zone consists of a roughly defined orange flame surrounding the inner cone.

The neutral flame can be obtained by visually inspecting the flame as the fuel and oxidizer flows are adjusted. If initially the flame is under-oxidized, three visible flame zones will be apparent. As more oxygen is bled into the mixture, the middle reaction zone will be reduced until just two flame zones are evident. This will be the neutral flame and for acetylene a fuel-oxygen ratio of about 1:1 will result. However, if oxygen flow is further increased, the primary reaction zone, characterized by the well defined inner cone, will "neck" down and an over-oxidized flame will result. Therefore, to obtain a neutral flame by visual inspection, it is desirable to begin with an under-oxidized mixture and increase oxygen flow until only two flame zones result.

For propane and methane, the chemical reactions are more complicated although it seems apparent that a fuel-rich pre-mixture is necessary for experimental tests. The visual process to determine a neutral flame for acetylene was applied to the flames of propane and methane. The fuel-oxygen mixture was adjusted until two distinct reaction zones were achieved. Using this approach, the following fuel-oxygen mixtures were achieved and were used for experimental tests:

Acetylene	1:1
Methane	2:3
Propane	1:2

Appendix C. Reduction Programs

Program To Convert Raw Data To Constant-Bandwidth

```
10 REM ** THIS PROGRAM REDUCES THE RAW VOLTAGES FROM THE
20 REM ** INTO THE CORRESPONDING FREQUENCIES AND PRESSURES **
30 CLS : CLEAR
35 INPUT "INPUT ANALYZER VOLTAGE RANGE";A
40 DR$ = "C:\RDATA\"
45 REM ** OPEN THE FILE TO BE REDUCED **
50 INPUT "DATA FILE TO BE REDUCED";DT$
60 FD$ = DR$ + DT$
70 OPEN FD$ FOR INPUT AS #1
75 REM ** NAME THE REDUCED DATA FILE **
80 INPUT "REDUCED DATA FILE";REDD$
85 CC$ = "C:\DATA\"
90 FR$ = CC$ + REDD$
100 OPEN FR$ FOR OUTPUT AS #2
105 INPUT "NUMBER OF DATA POINTS";PT
110 FOR P = 1 TO PT
120 INPUT #1,X,Y
125 REM ** SELECT THE DATA POINTS AT 60 HZ INTERVALS **
130 IF X < 120 THEN 200
140 IF X < Z THEN 200
150 LET Z = X + 60
152 REM ** CALCULATE THE CORRESPONDING PRESSURE **
154 REM ** BASED ON 1 V INPUT TO ANALYZER = 1.4192 PA **
```

```
156 REM ** AND DIVIDE BY 2 TO CORRECT FOR THE REFLECTION AT MIC
160 PR=Y/5*A*1.4192/2
170 PRINT #2, USING"####.##### ";X;PR
200 NEXT P
220 END
```

Program To Calculate Overall Sound Pressure Level

```
1 REM ** PROGRAM TO CALCULATE THE OASPL **
10 CLS : CLEAR
15 REM ** INDICATE FILE TO BE REDUCED **
17 REM ** FILE NAME CODED TO EXPERIMENTAL PARAMETERS **
20 DR$="C:\DATA\R"
30 INPUT "BURNER NUMBER";BN$
40 INPUT "FLOW LETTER";F$
50 INPUT "FUEL LETTER";FL$
60 EX$=".DAT"
70 FD$=DR$+BN$+F$+FL$+EX$
80 OPEN FD$ FOR INPUT AS #1
100 GOSUB 500
130 INPUT "NUMBER OF DATA POINTS";PT
140 FOR P=1 TO PT
150 INPUT #1,X,Y
155 REM ** CALCULATE OASPL IN PASCALS **
160 XP=XP+Y**2
170 NEXT P
180 OP=XP**.5
185 REM ** CONVERT TO DB **
190 COG=LOG(OP/.00002)/LOG(10)
200 DBOP=20*COG
201 REM ** REPORT THE RESULTS FOR EXPERIMENTAL TEST POINTS **
```

```
203 LPRINT
206 LPRINT
208 LPRINT
210 LPRINT "FILE: ";BN$+F$+FL$
220 LPRINT "FUEL: ";FUEL$
230 LPRINT USING"BURNER DIAMETER = #.### cm";BD
240 LPRINT "FLOW VELOCITY   = ";F" m/s"
250 LPRINT USING "OASPL = #.#### Pa";OP
260 LPRINT USING "      = ##.### dB";DBOP
270 CLOSE 1
400 END
500 REM ** SUBROUTINE TO INTERPRET FILE NAME FOR FINAL REPORT **
505 IF FL$="A" THEN 600
510 IF FL$="P" THEN 700
520 REM      SET MEHTANE PARAMETERS
530 IF BN$="3" THEN BD=.356
540 IF BN$="4" THEN BD=.414
550 IF BN$="5" THEN BD=.541
560 IF F$="A" THEN F=10
570 IF F$="B" THEN F=20
580 IF F$="C" THEN F=25
585 FUEL$="METHANE"
590 GOTO 1000
600 REM      SET ACETYLENE PARAMETERS
610 IF BN$="1" THEN BD=.117
620 IF BN$="2" THEN BD=.165
```

```
630 IF BN$="3" THEN BD=.356
640 IF F$="A" THEN F=50
650 IF F$="B" THEN F=75
660 IF F$="C" THEN F=100
670 FUEL$="ACETYLENE"
680 GOTO 1000
700 REM       SET PROPANE PARAMETERS
710 IF BN$="1" THEN BD=.117
720 IF BN$="2" THEN BD=.165
730 IF BN$="3" THEN BD=.356
740 IF F$="A" THEN F=20
750 IF F$="B" THEN F=30
760 IF F$="C" THEN F=40
770 FUEL$="PROPANE"
1000 RETURN
```

Program To Convert To Third-Octave-Bandwidth

```
10 REM ** CONVERT PRESSURE SPECTRUM INTO 1/3 OCTAVE BANDS **
20 CLS : CLEAR
30 REM **  EVALUATE BOUNDARY FREQUENCIES OF 1/3 OCTAVE **
40 BF(1)=14.1:BF(2)=17.8:BF(3)=22.4:BF(4)=28.2:BF(5)=35.5
50 FOR I=6 TO 30
60 BF(I)=45*2**(.33*(I-6))
70 NEXT I
90 REM ** EVALUATE CENTRAL FREQUENCIES OF 1/3 OCTAVE **
110 FOR I=2 TO 30
120 CF(I-1)=(BF(I-1)*BF(I))
130 NEXT I
140 DR$="C:\DATA\"
150 DE$=".DAT"
160 INPUT "DATA FILE TO BE REDUCED";DT$
170 FD$=DR$+DT$+DE$
180 OPEN FD$ FOR INPUT AS #1
190 REM ** READ IN DATA FILE TO BE REDUCED **
200 INPUT "NUMBER OF DATA POINTS";PT
210 FOR P=1 TO PT
220 INPUT #1,X,Y
230 X(P)=X:Y(P)=Y
240 NEXT P
250 INPUT "REDUCED DATA FILE";REDD$
```

```
260 CC$="C:\TDATA\"
270 FR$=CC$+REDD$+DE$
280 OPEN FR$ FOR OUTPUT AS #2
290 REM ** CALCULATE THE RMS PRESSURE FO EACH BAND **
300 FOR I=1 TO 30
310 FOR P=1 TO PT
320 IF X(P)>BF(I) AND X(P)<BF(I+1) THEN 340
330 GOTO 350
340 PSUM(I)=PSUM(I)+Y(P)**2
350 NEXT P
360 NEXT I
370 FOR N=1 TO 30
380 PBAND(N)=(PSUM(N))**.5
390 NEXT N
400 REM ** PRINT THE CENTRAL FREQUENCY VS PRESSURE TO FILE **
410 FOR N=1 TO 30
420 IF CF(N)>10000 THEN 460
430 IF CF(N)<130 THEN 460
440 IF PBAND(N)=0 THEN PBAND(N)=(PBAND(N-1)+PBAND(N+1))/2
450 PRINT #2, USING"####.#### ";CF(N);PBAND(N)
460 NEXT N
480 END
```

Appendix D. Constant-Bandwidth Data

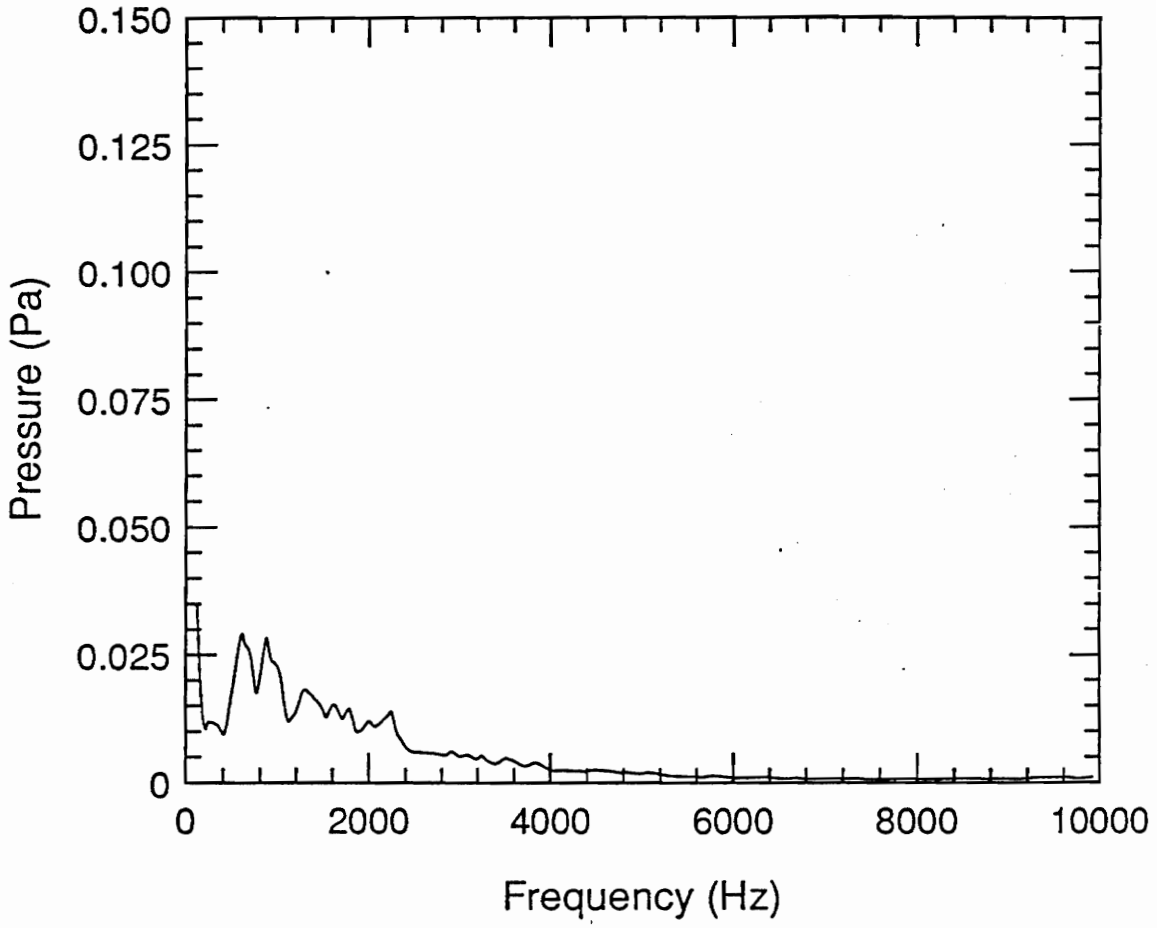

Figure 17. Spectrum for Methane: U = 10 m/s, D = 0.356 cm

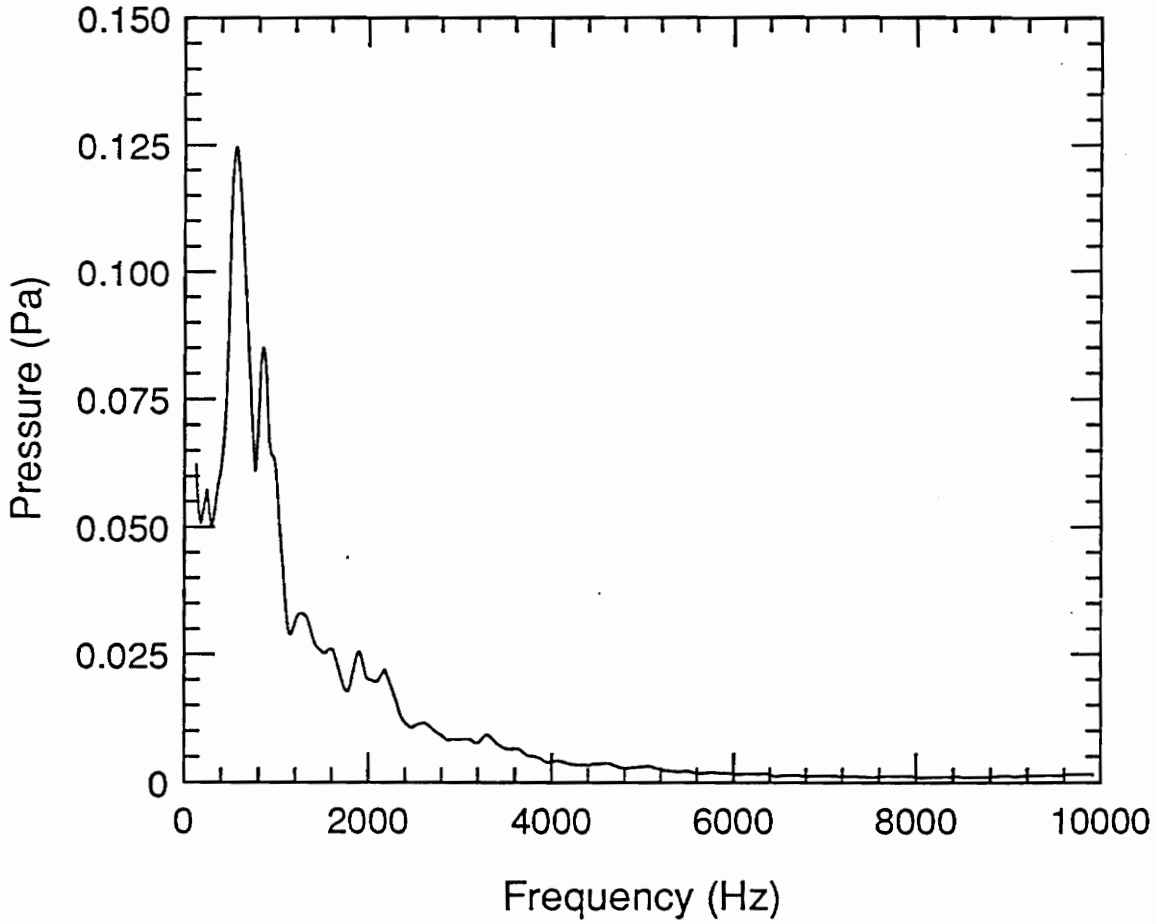

Figure 18. Spectrum for Methane: U = 20 m/s, D = 0.356 cm

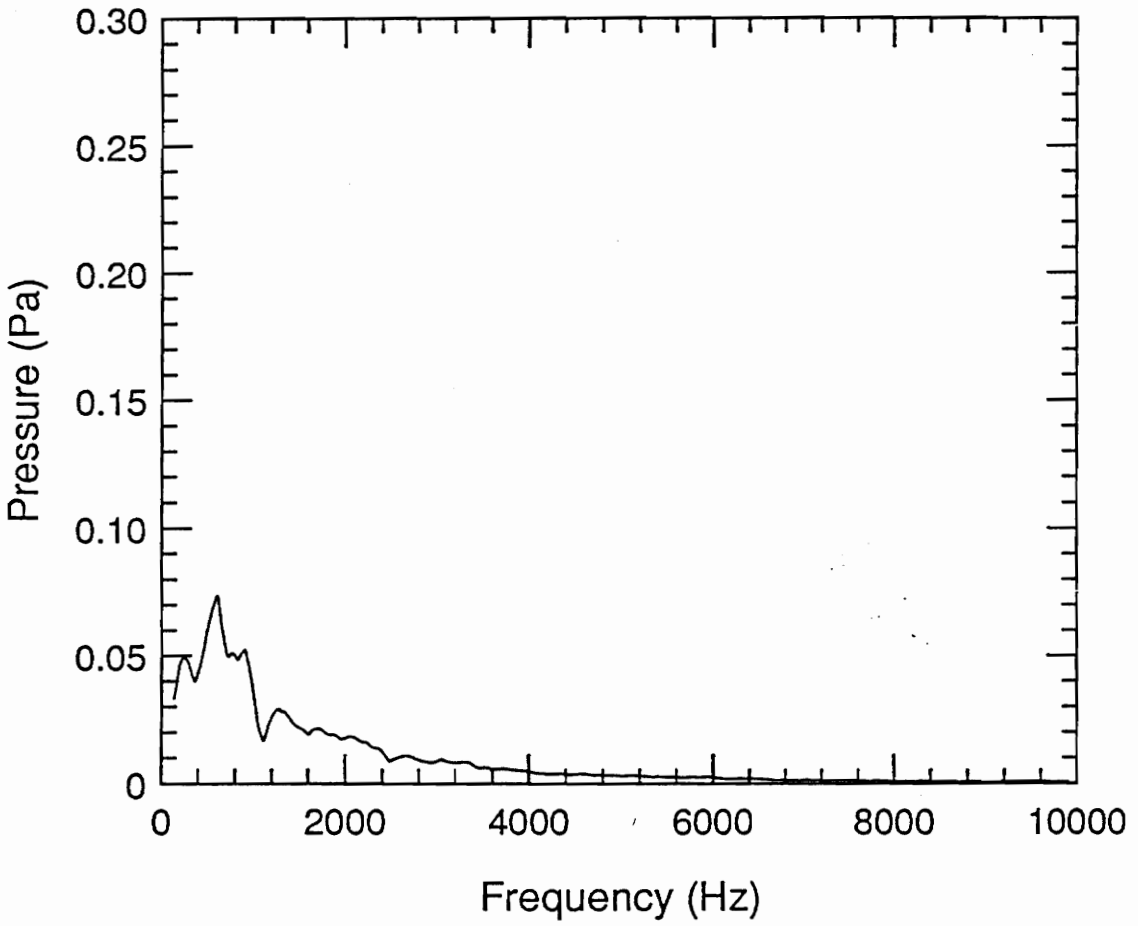

Figure 19. Spectrum for Methane: U = 10 m/s, D = 0.414 cm

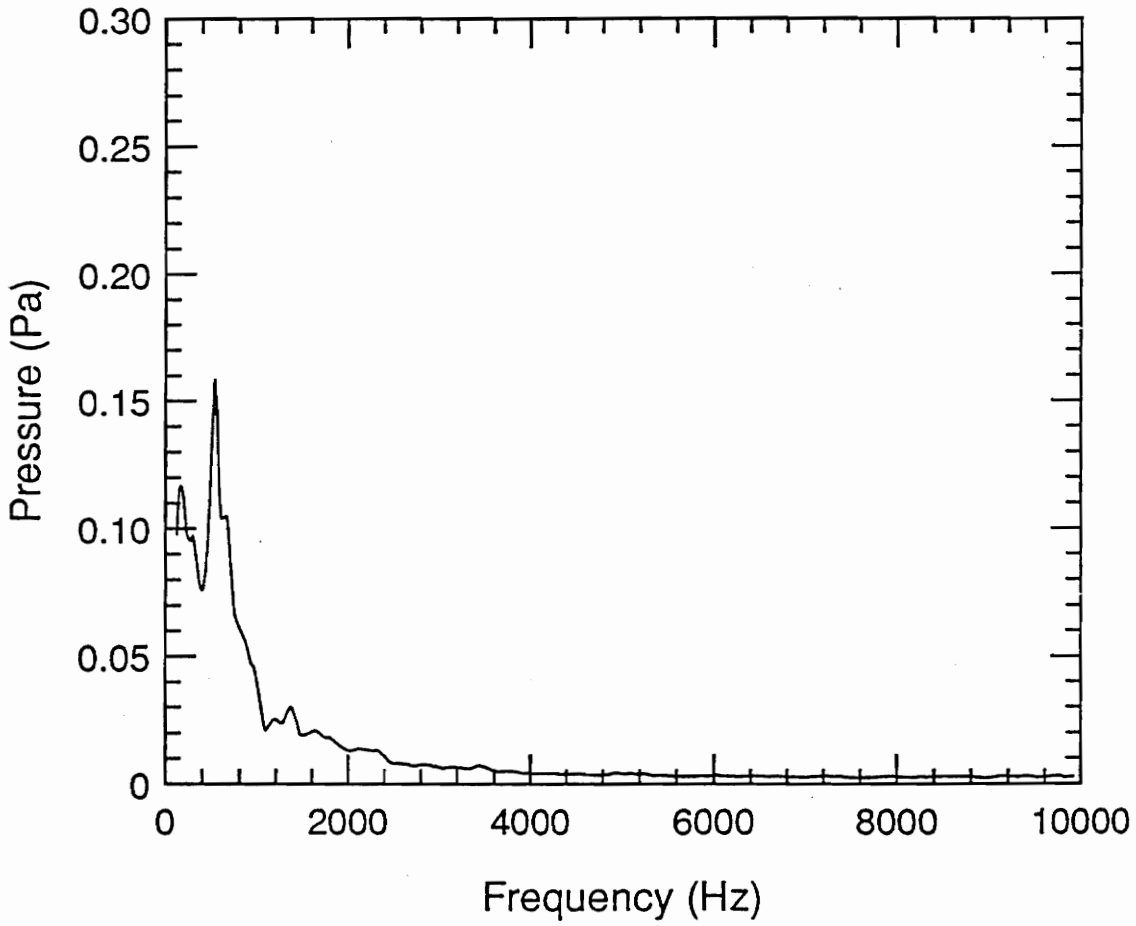

Figure 20. Spectrum for Methane: U = 20 m/s, D = 0.414 cm

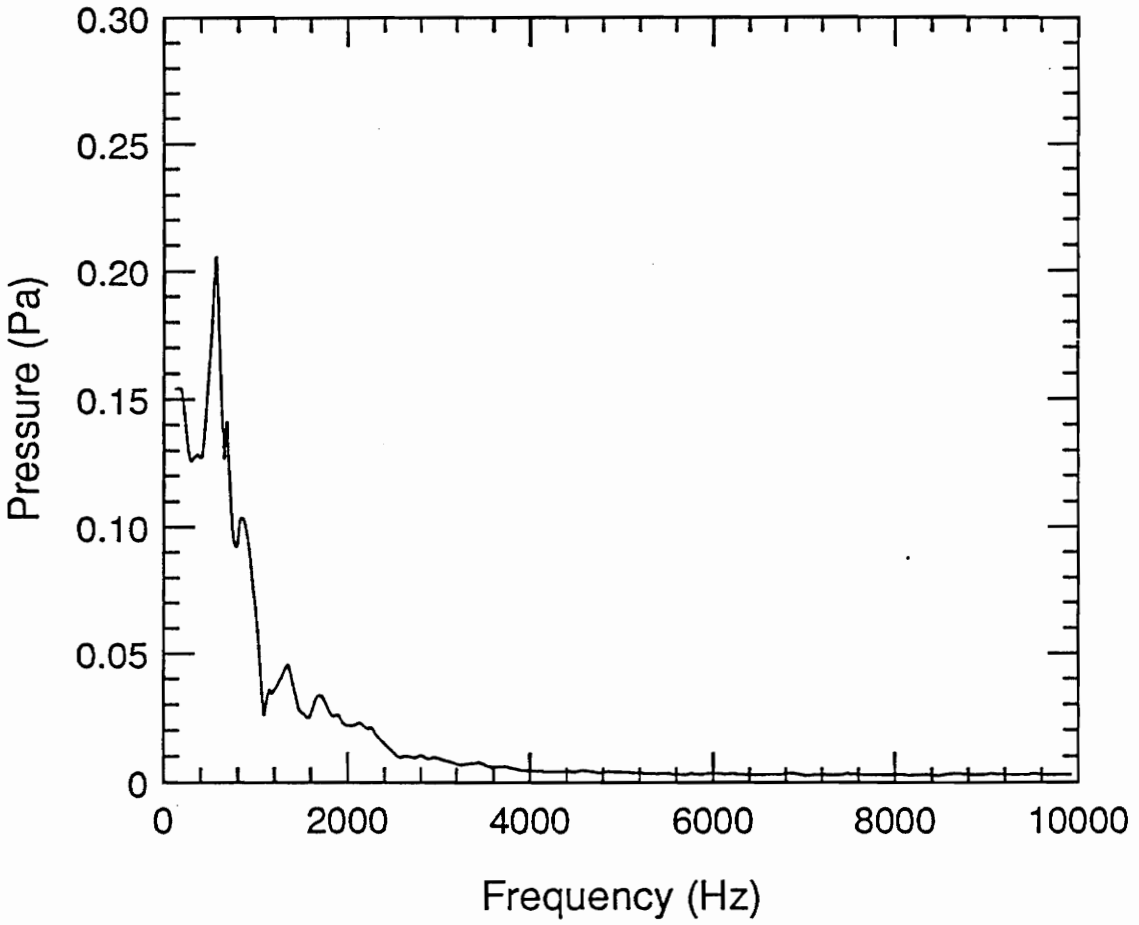

Figure 21. Spectrum for Methane: U = 25 m/s, D = 0.414 cm

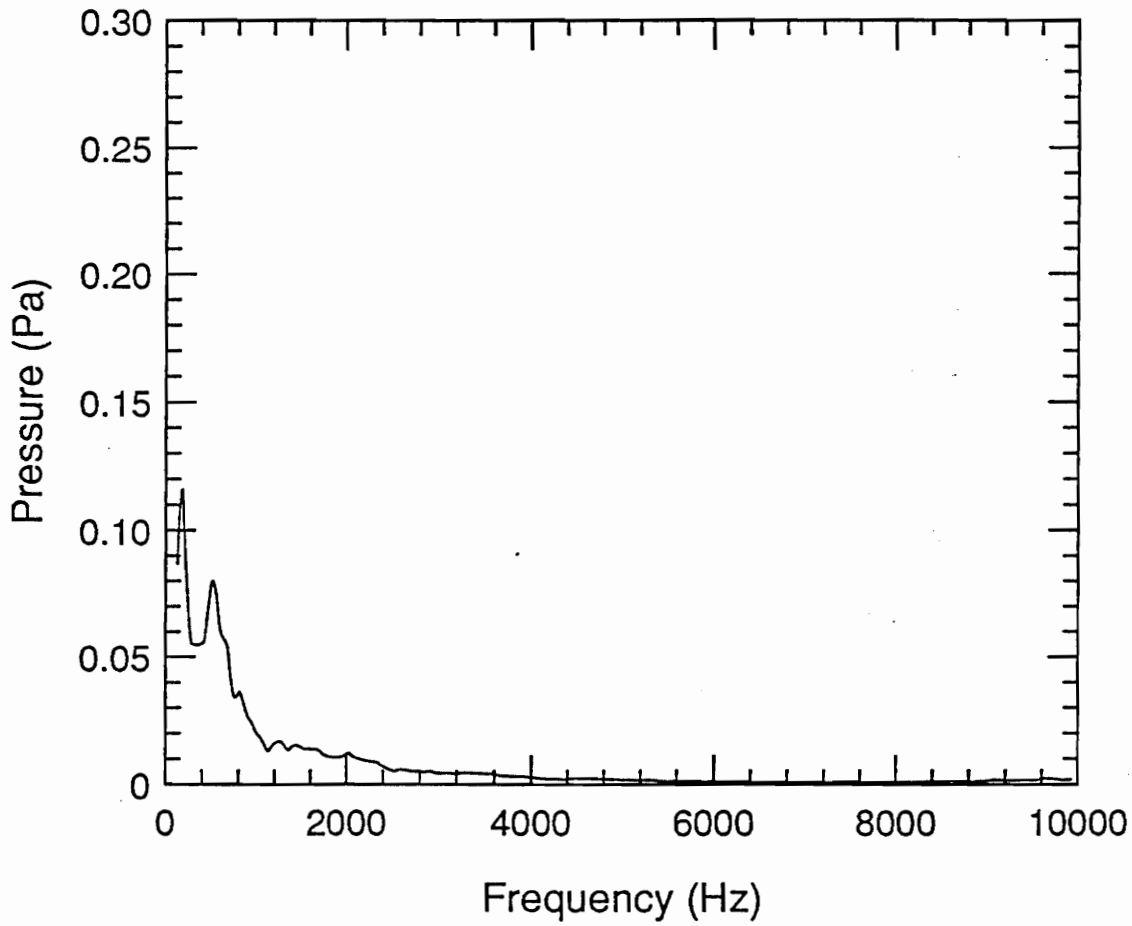

Figure 22. Spectrum for Methane: U = 10 m/s, D = 0.541 cm

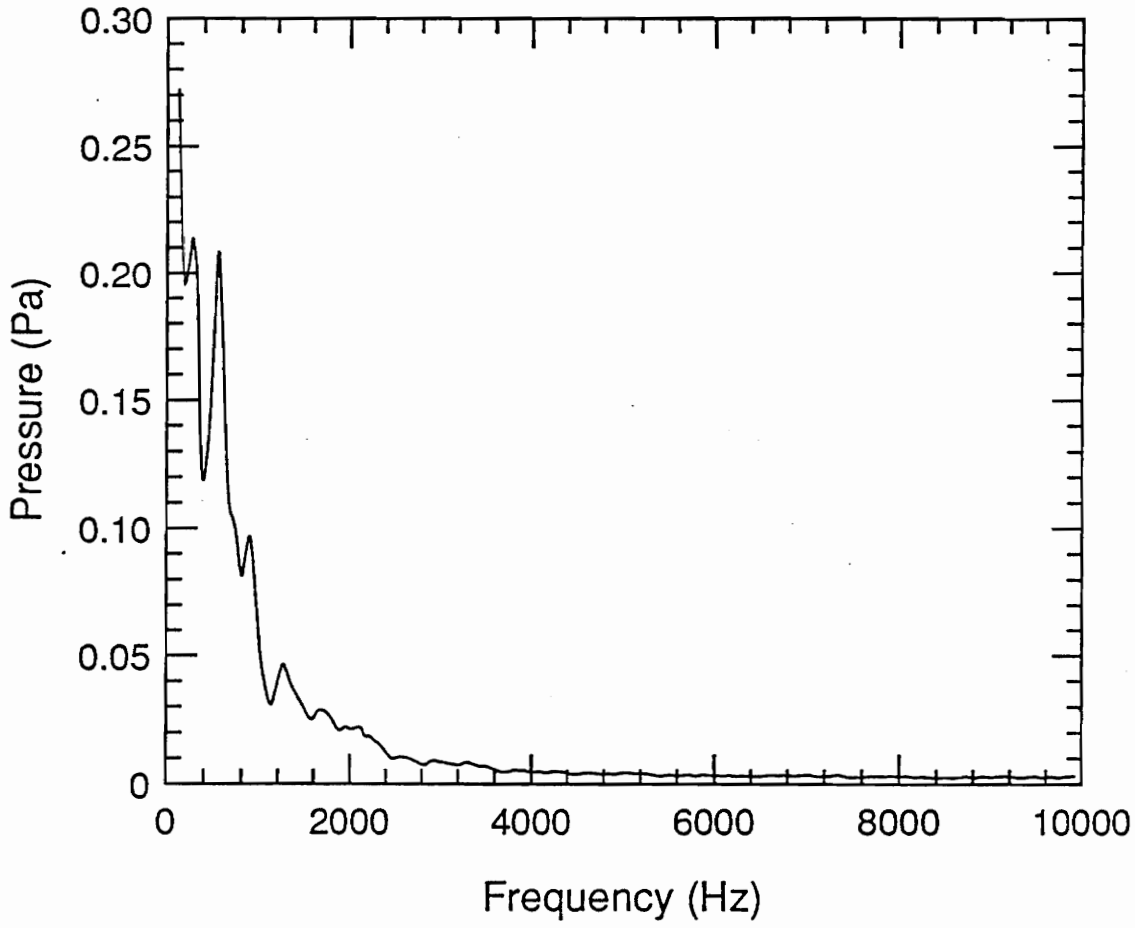

Figure 23. Spectrum for Methane: U = 20 m/s, D = 0.541 cm

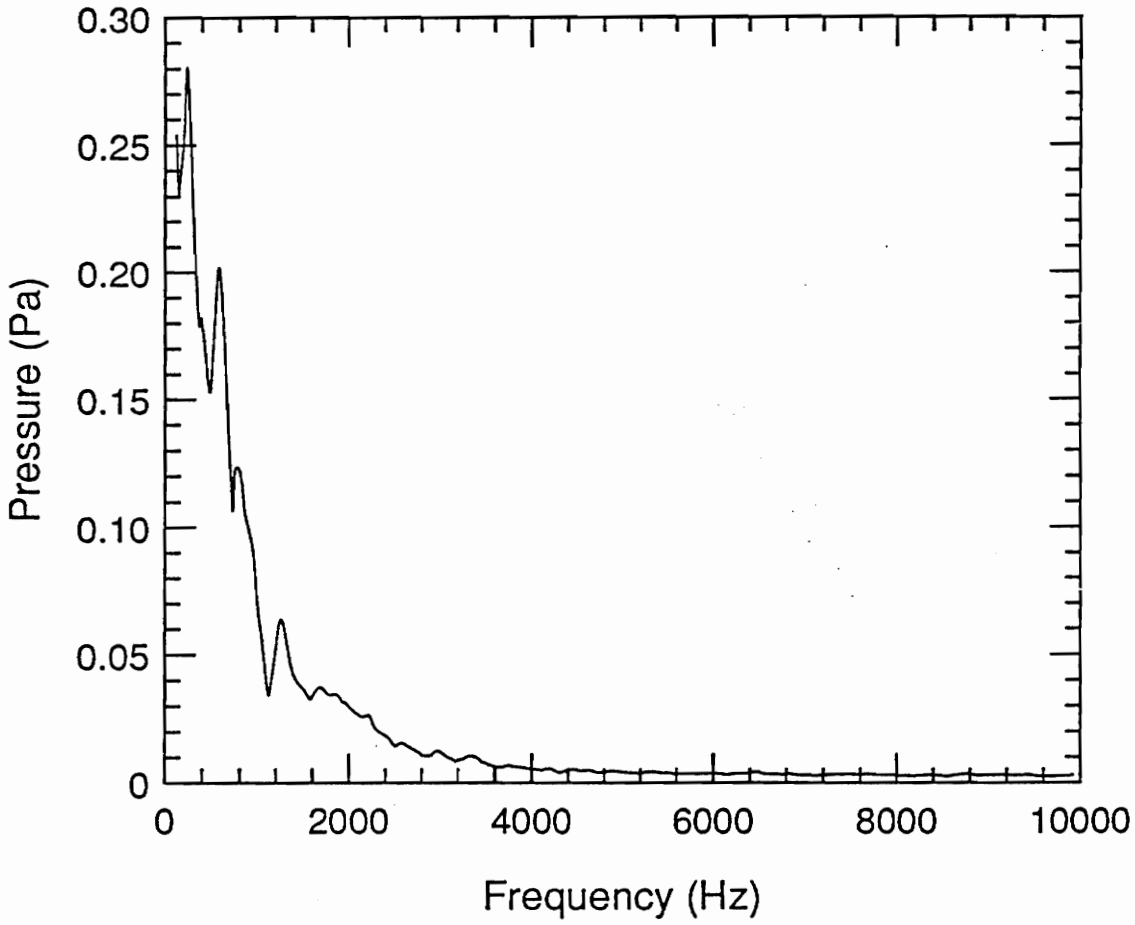

Figure 24. Spectrum for Methane: U = 25 m/s, D = 0.541 cm

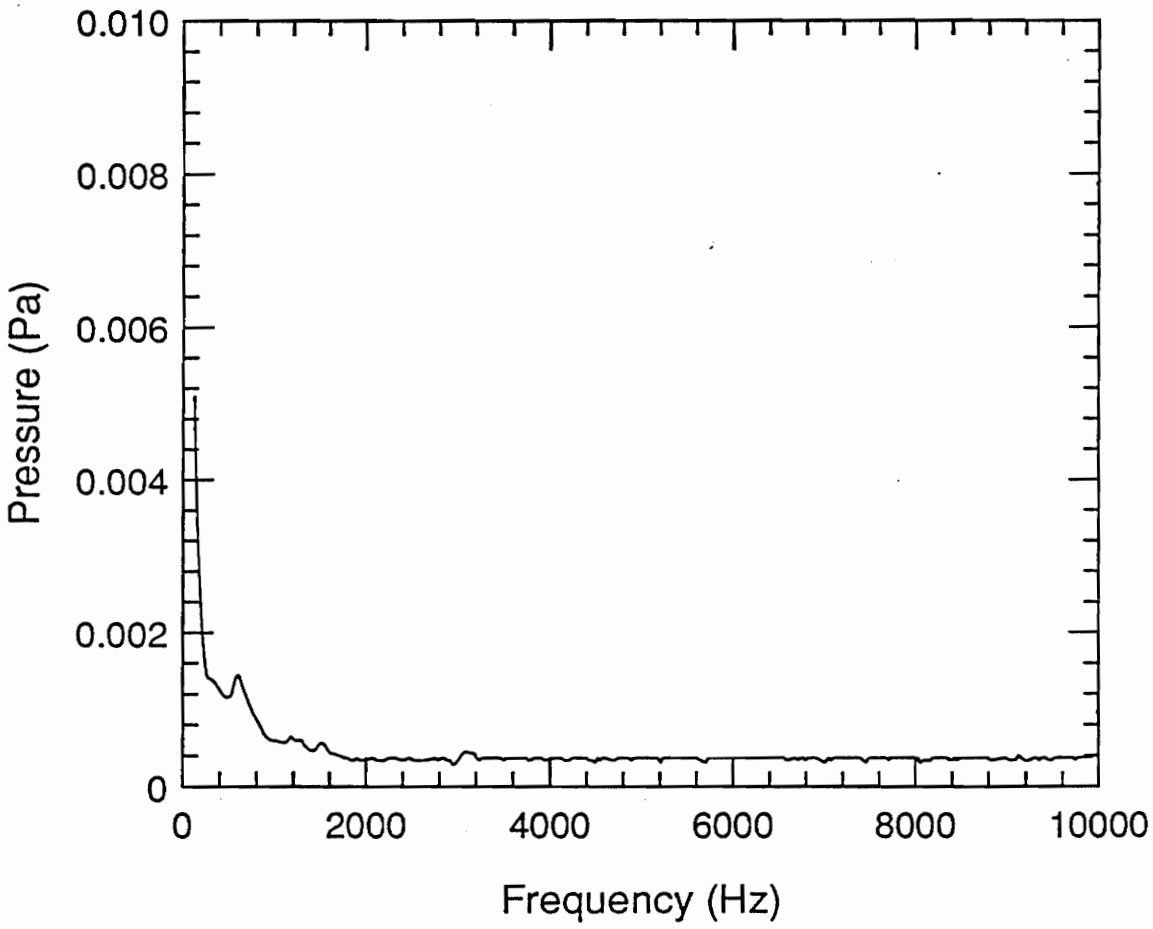

Figure 25. Spectrum for Propane: U = 20 m/s, D = 0.117 cm

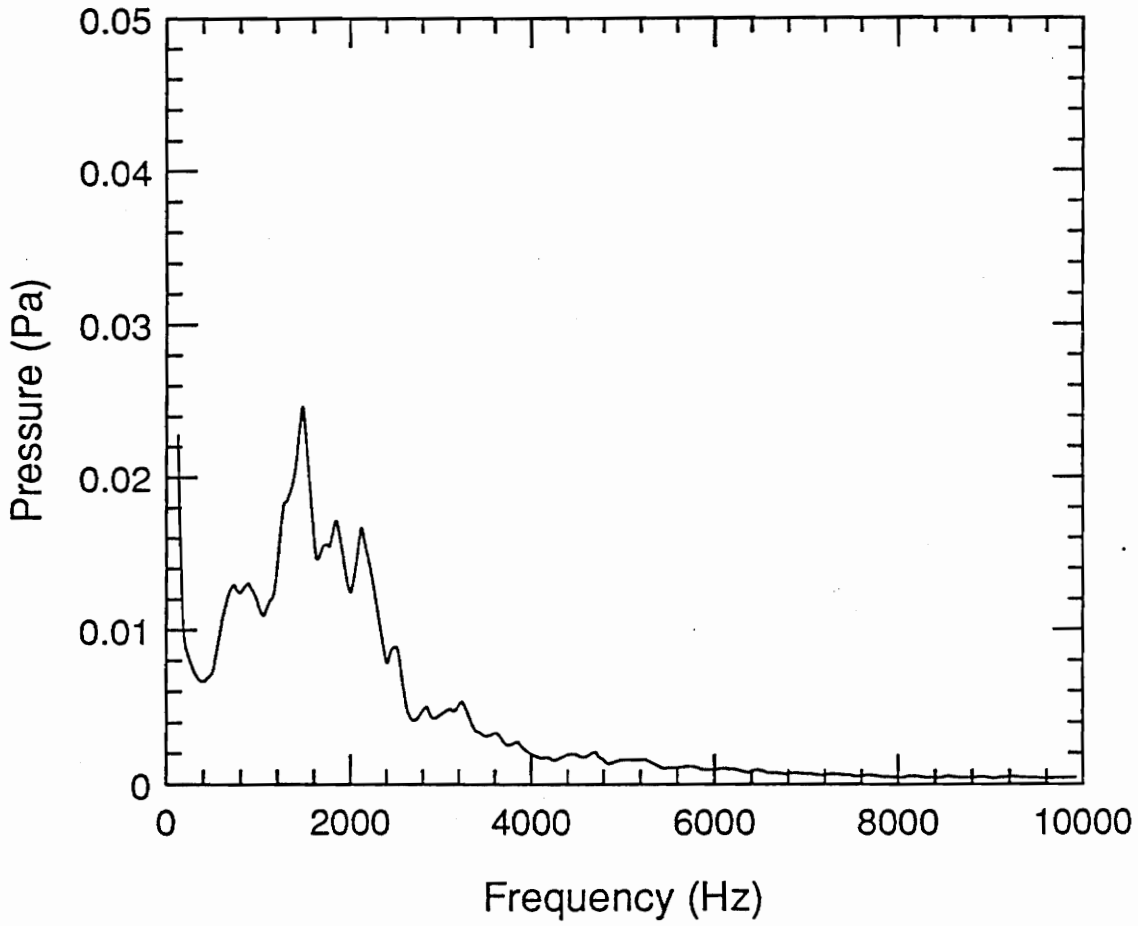

Figure 26. Spectrum for Propane: U = 30 m/s, D = 0.117 cm

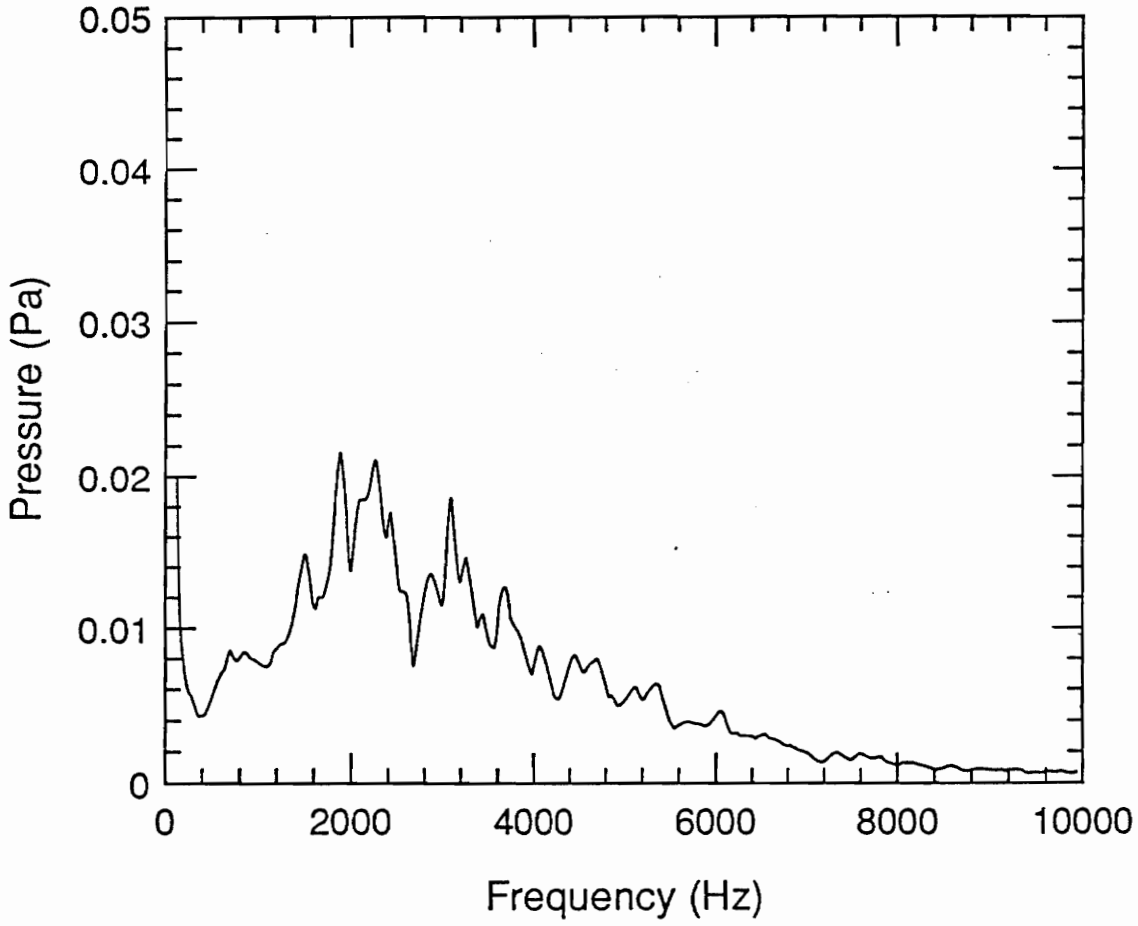

Figure 27. Spectrum for Propane: U = 40 m/s, D = 0.117 cm

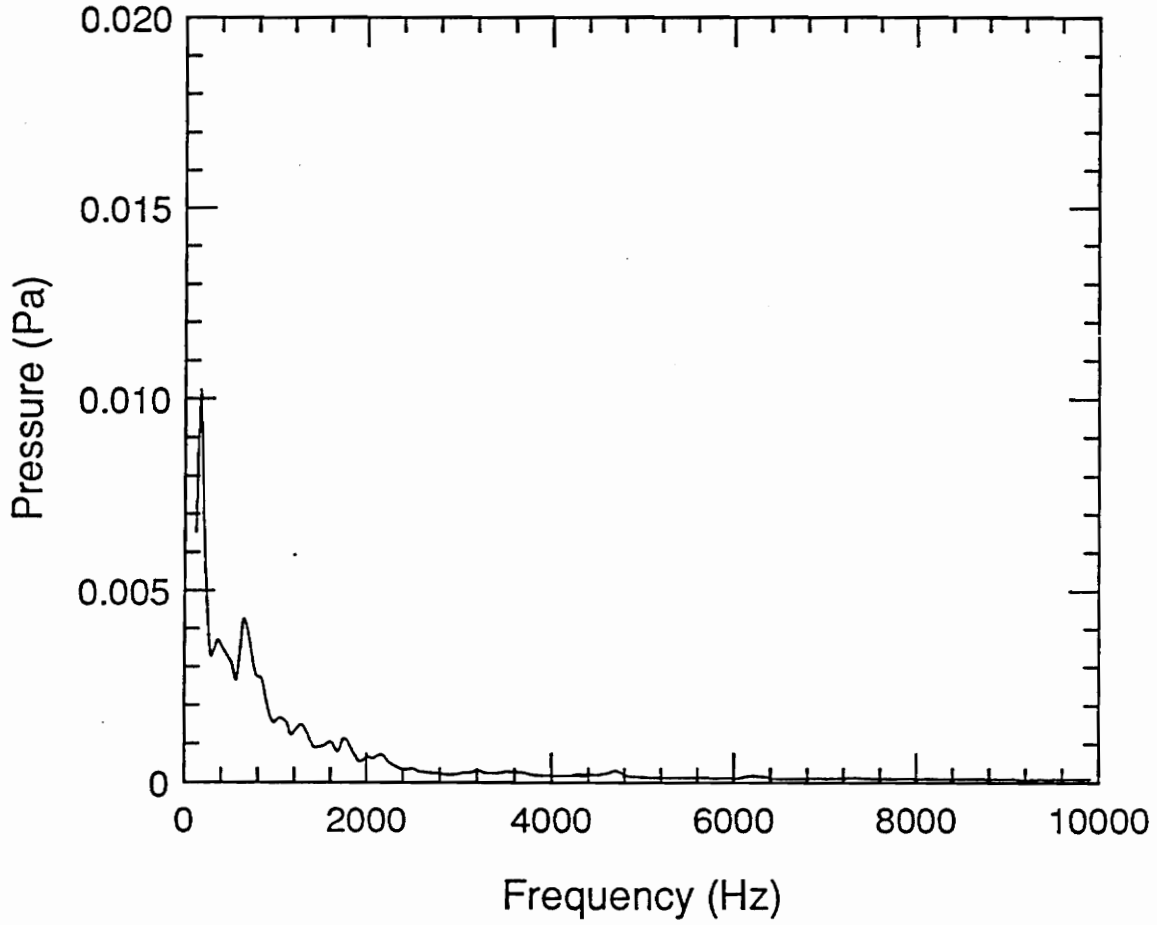

Figure 28. Spectrum for Propane: U = 20 m/s, D = 0.165 cm

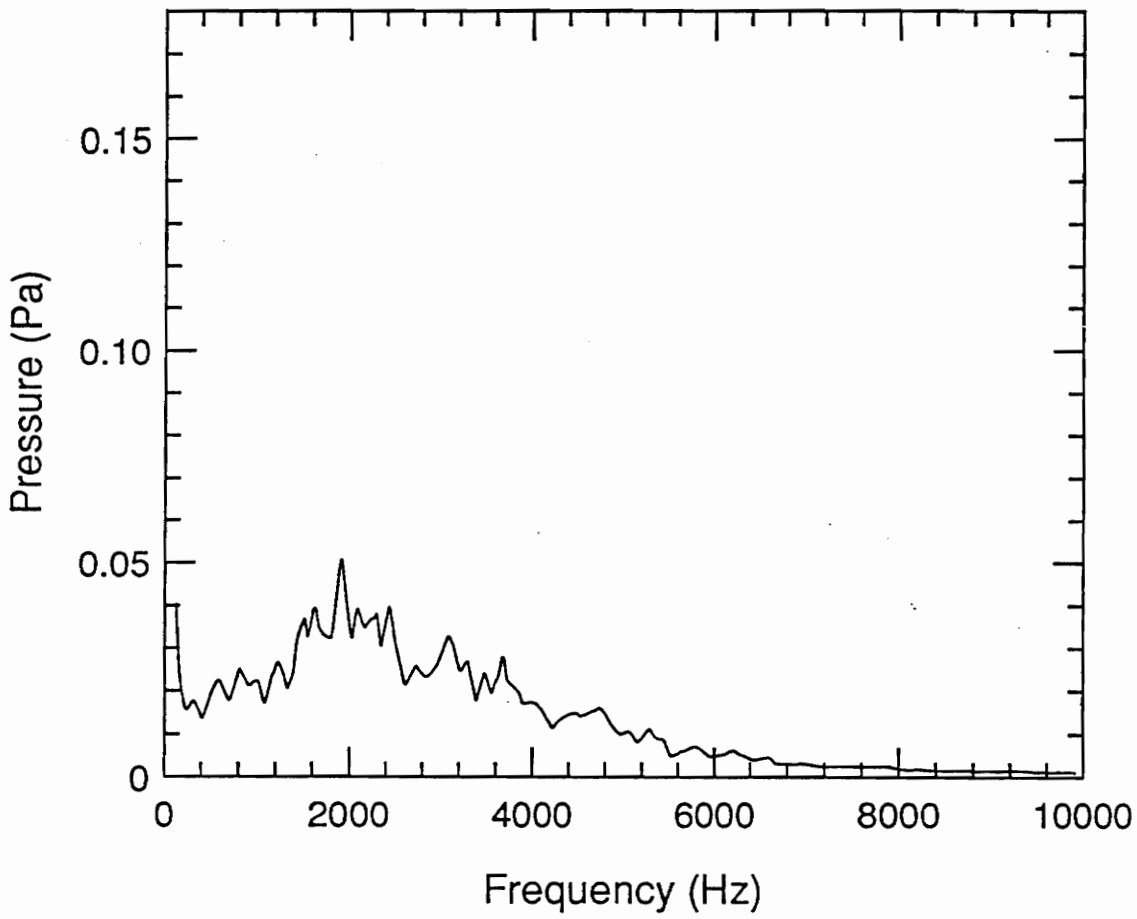

Figure 29. Spectrum for Propane: U = 30 m/s, D = 0.165 cm

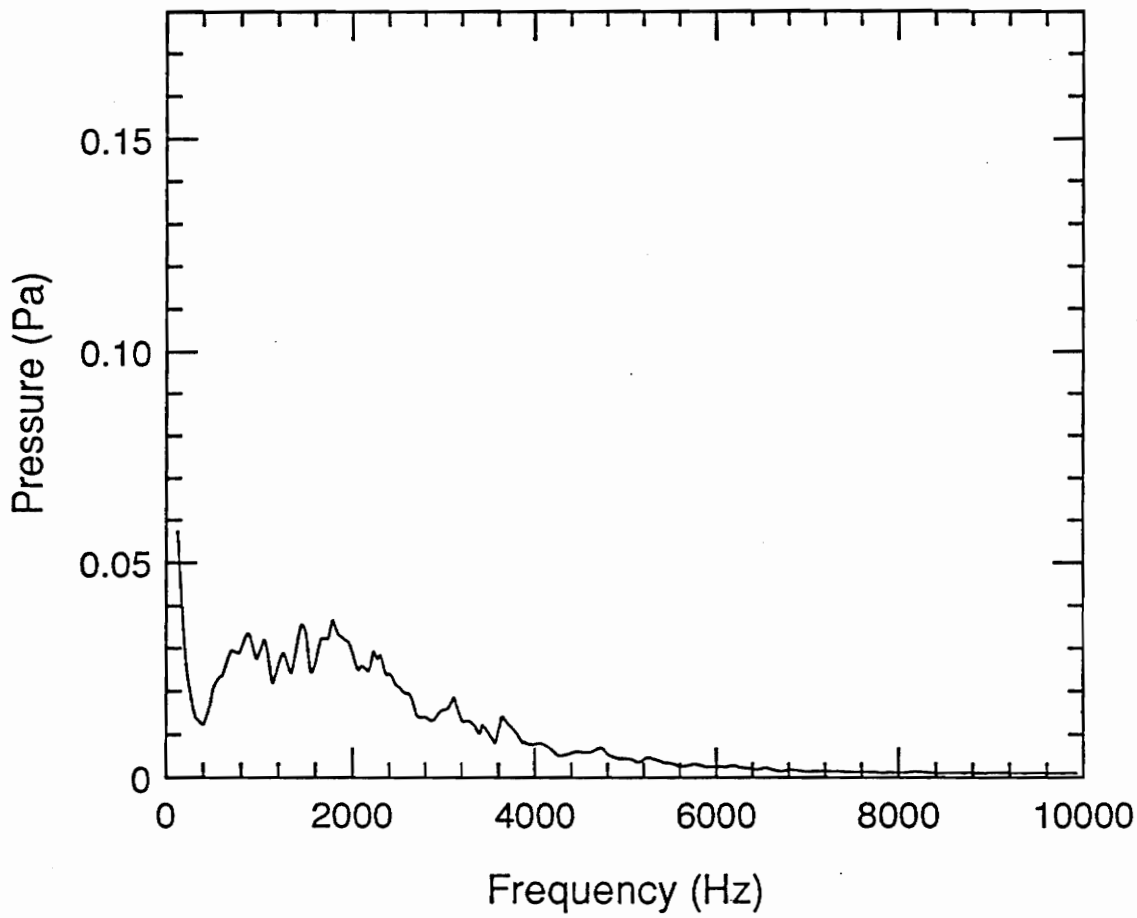

Figure 30. Spectrum for Propane: U = 30 m/s, D = 0.165 cm

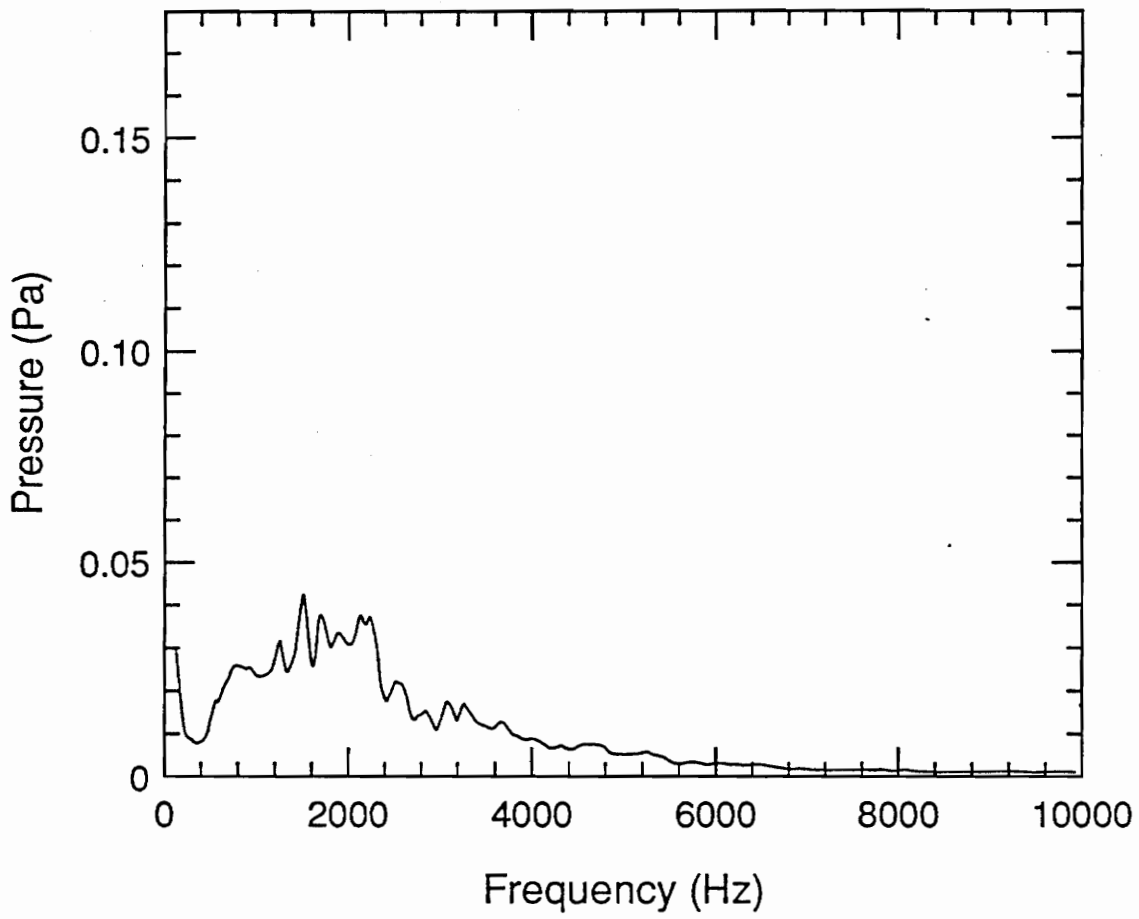

Figure 31. Spectrum for Propane: U = 30 m/s, D = 0.165 cm

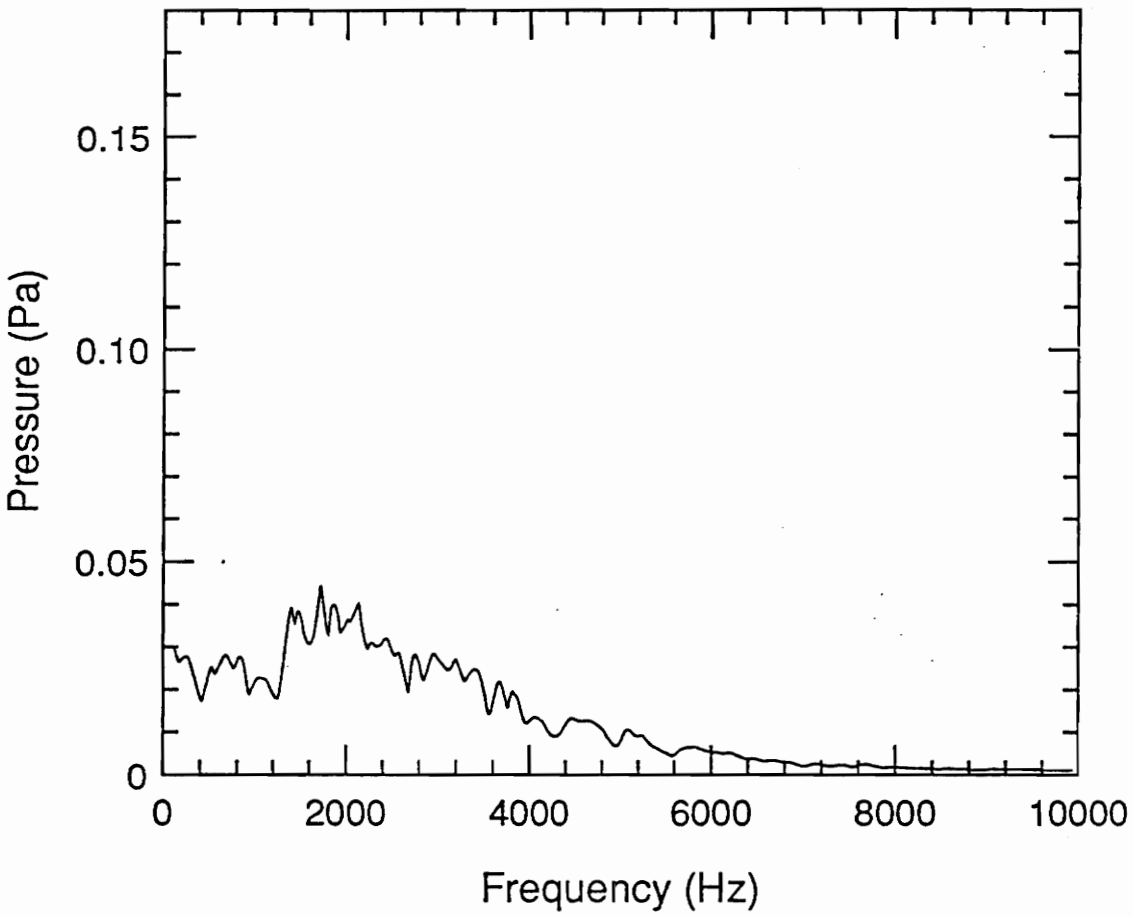

Figure 32. Spectrum for Propane: U = 40 m/s, D = 0.165 cm

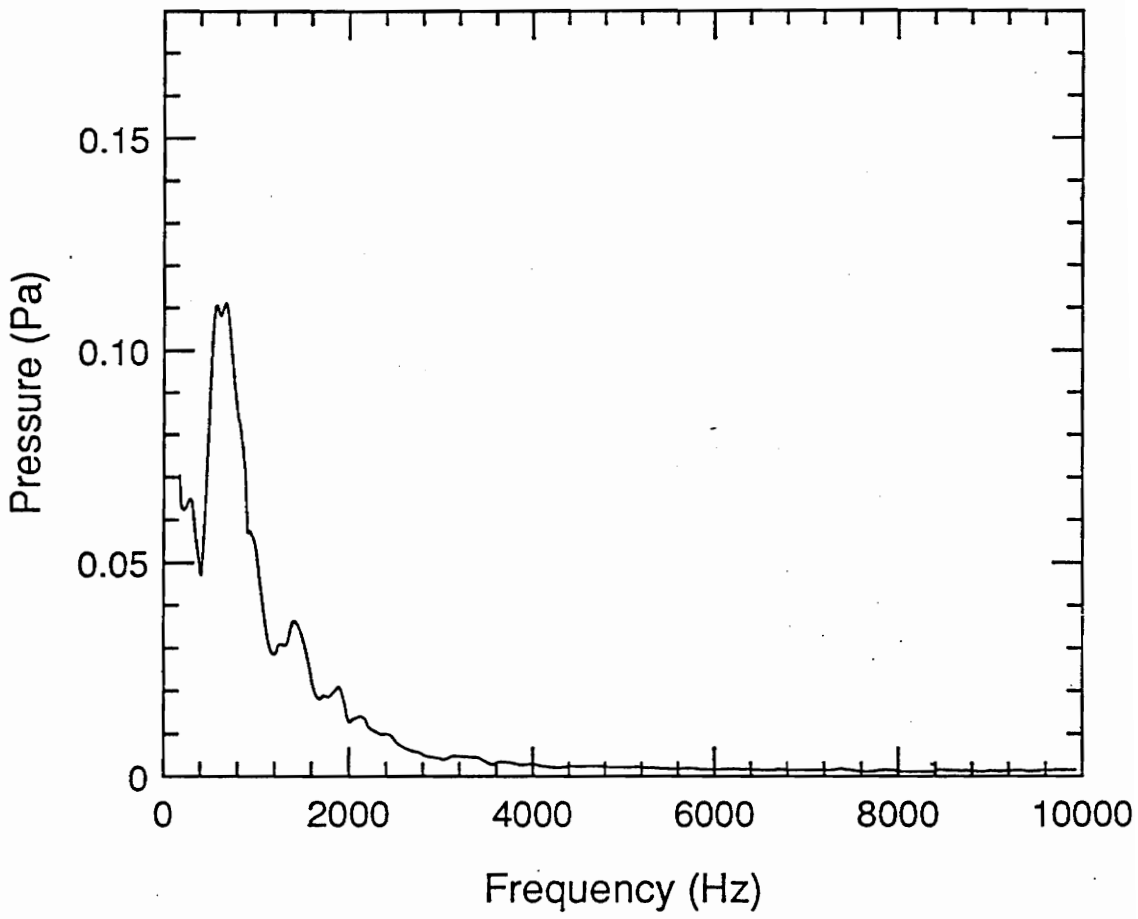

Figure 33. Spectrum for Propane: U = 20 m/s, D = 0.356 cm

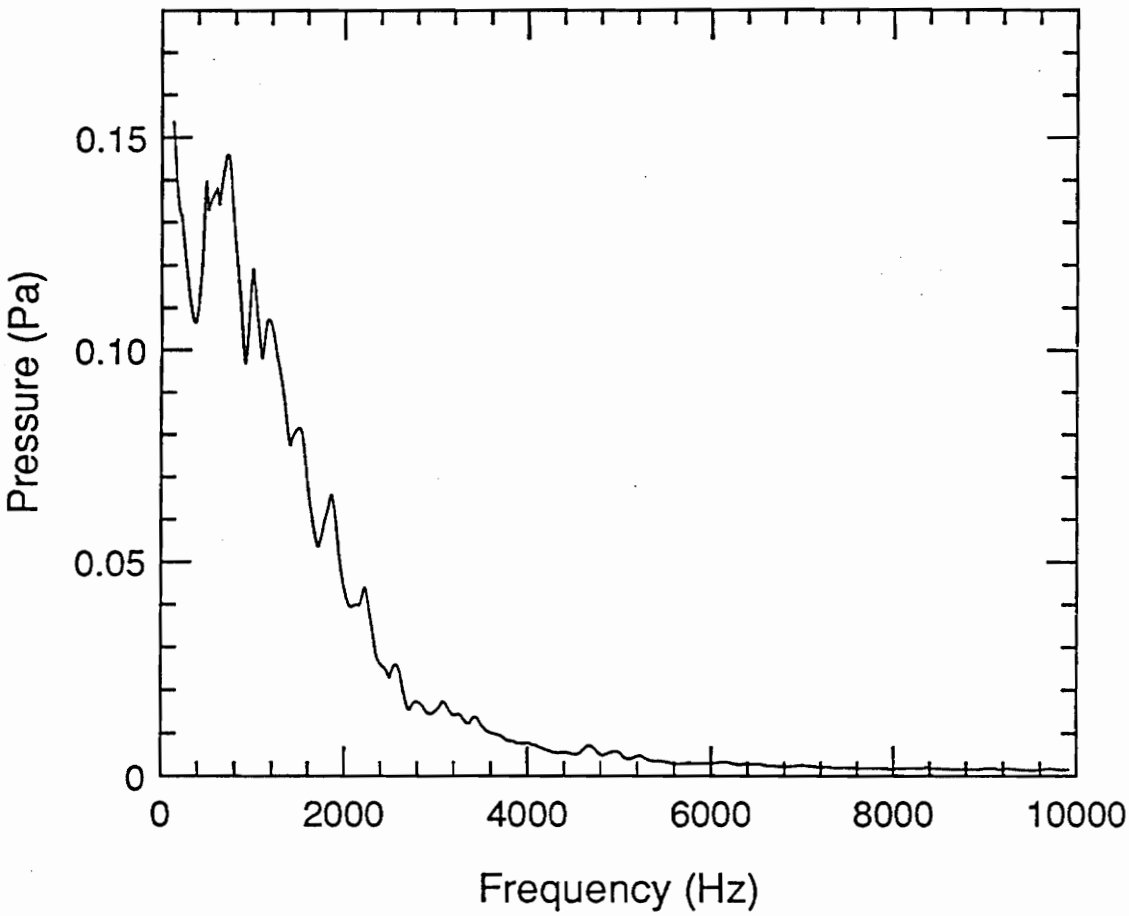

Figure 34. Spectrum for Propane: U = 30 m/s, D = 0.356 cm

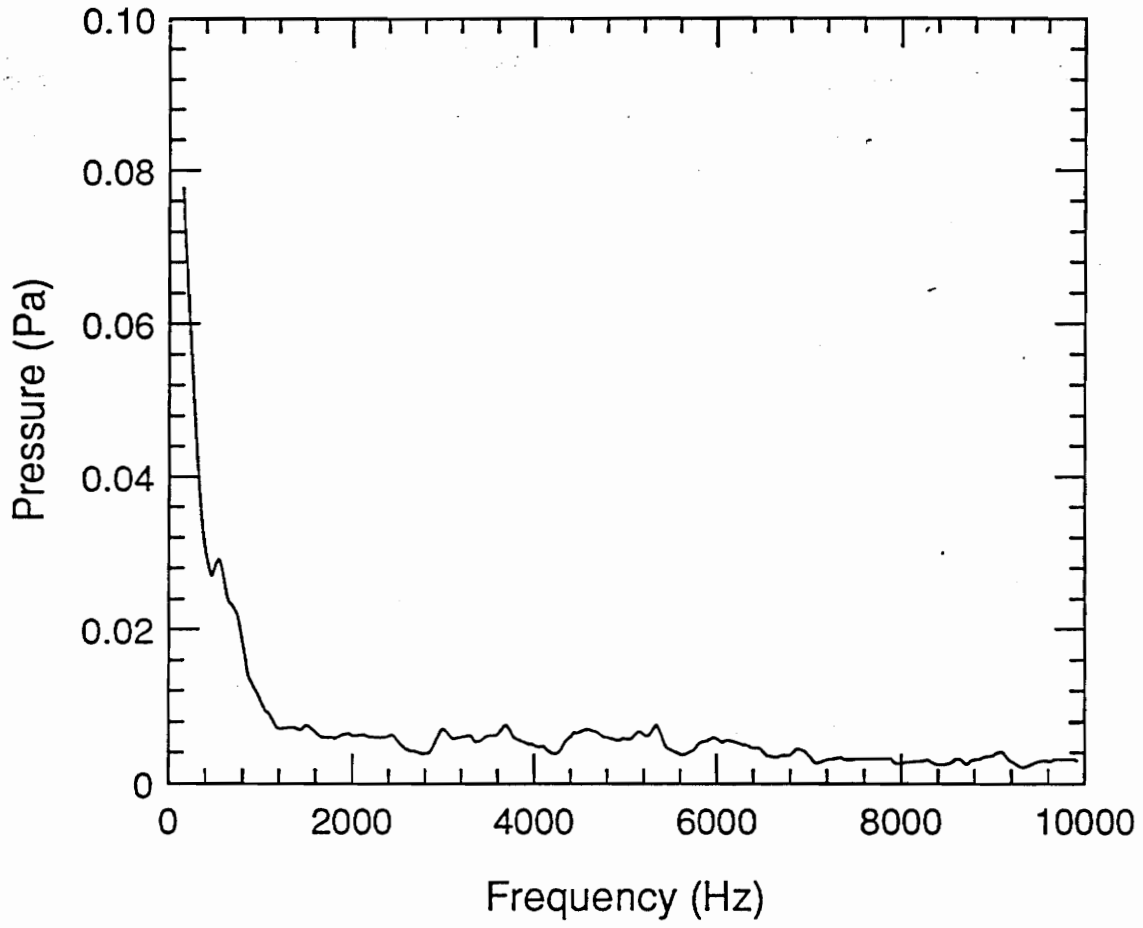

Figure 35. Spectrum for Acetylene: U = 50 m/s, D = 0.117 cm

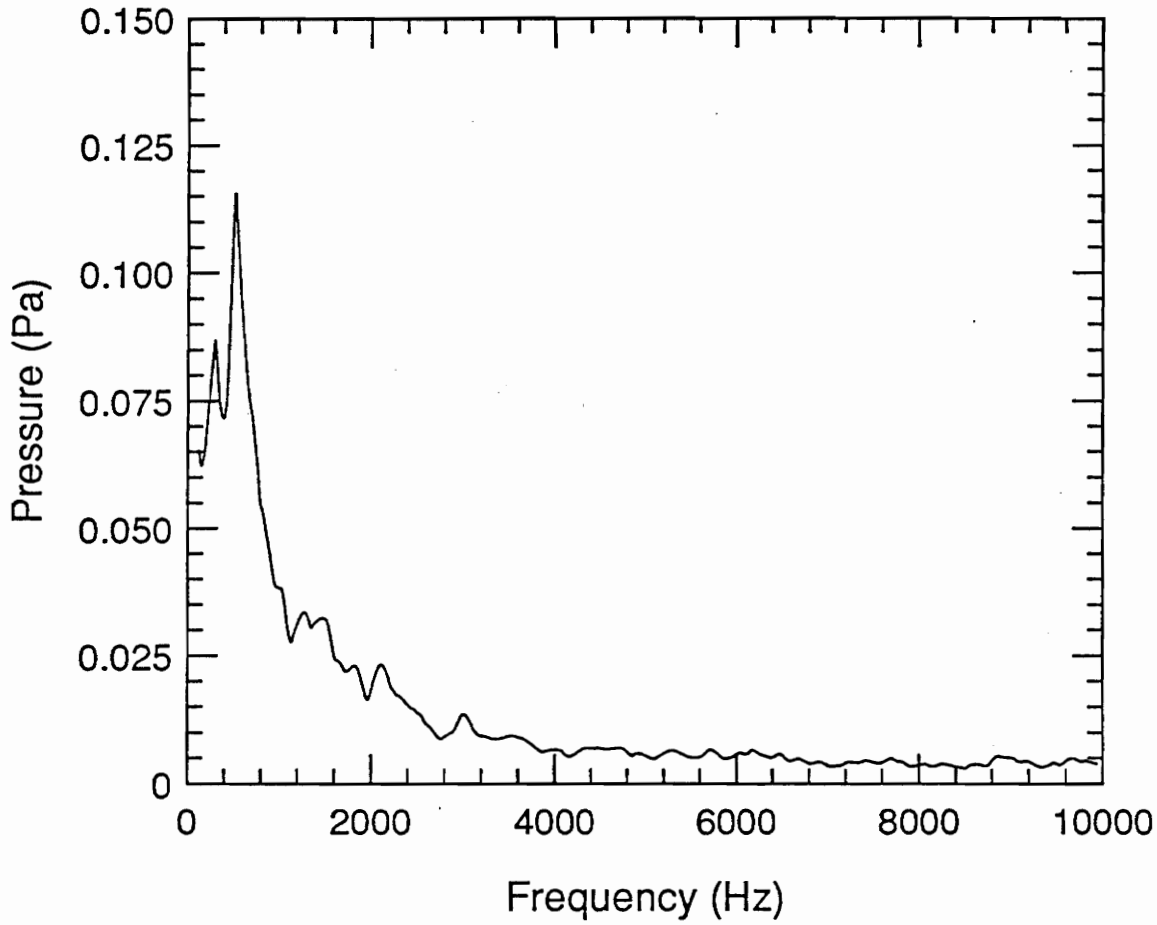

Figure 36. Spectrum for Acetylene: U = 75 m/s, D = 0.117 cm

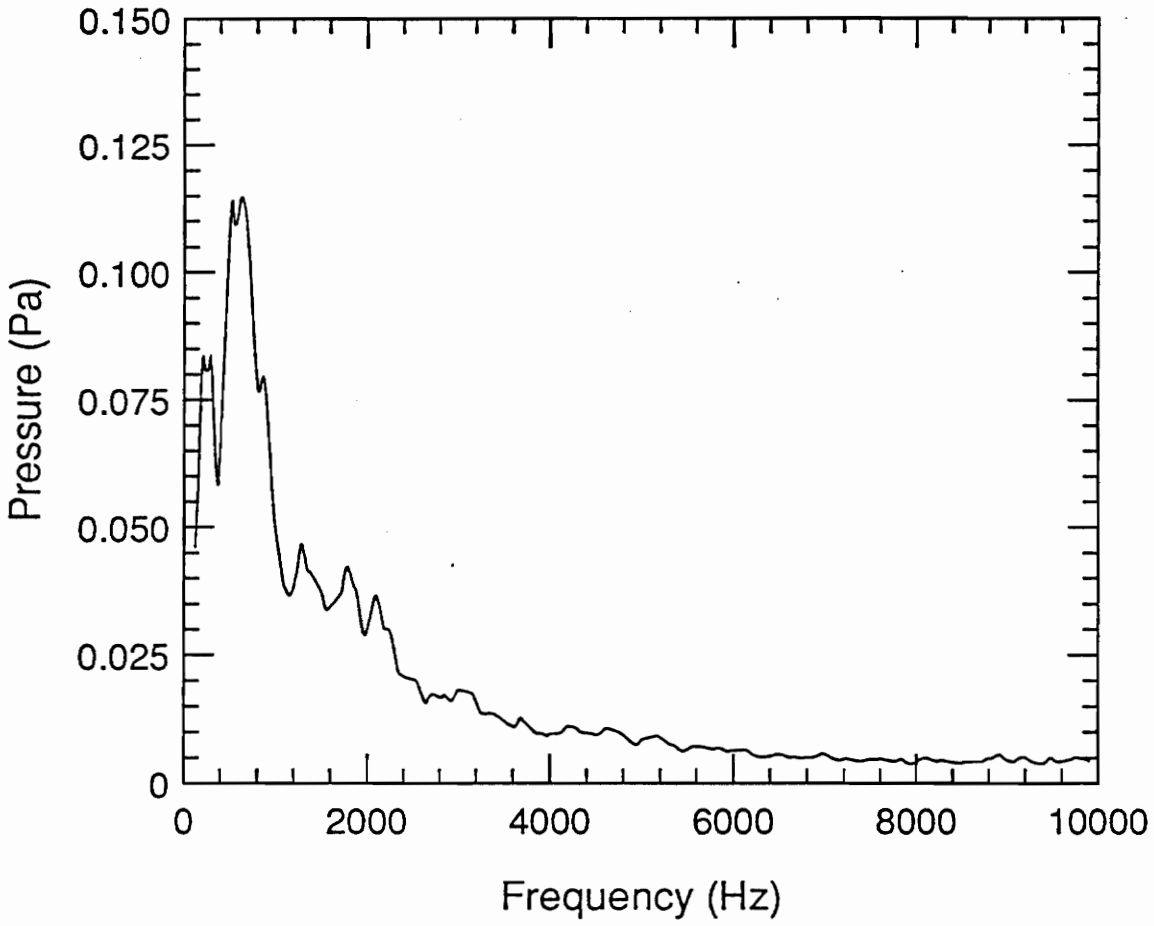

Figure 37. Spectrum for Acetylene: U = 100 m/s, D = 0.117 cm

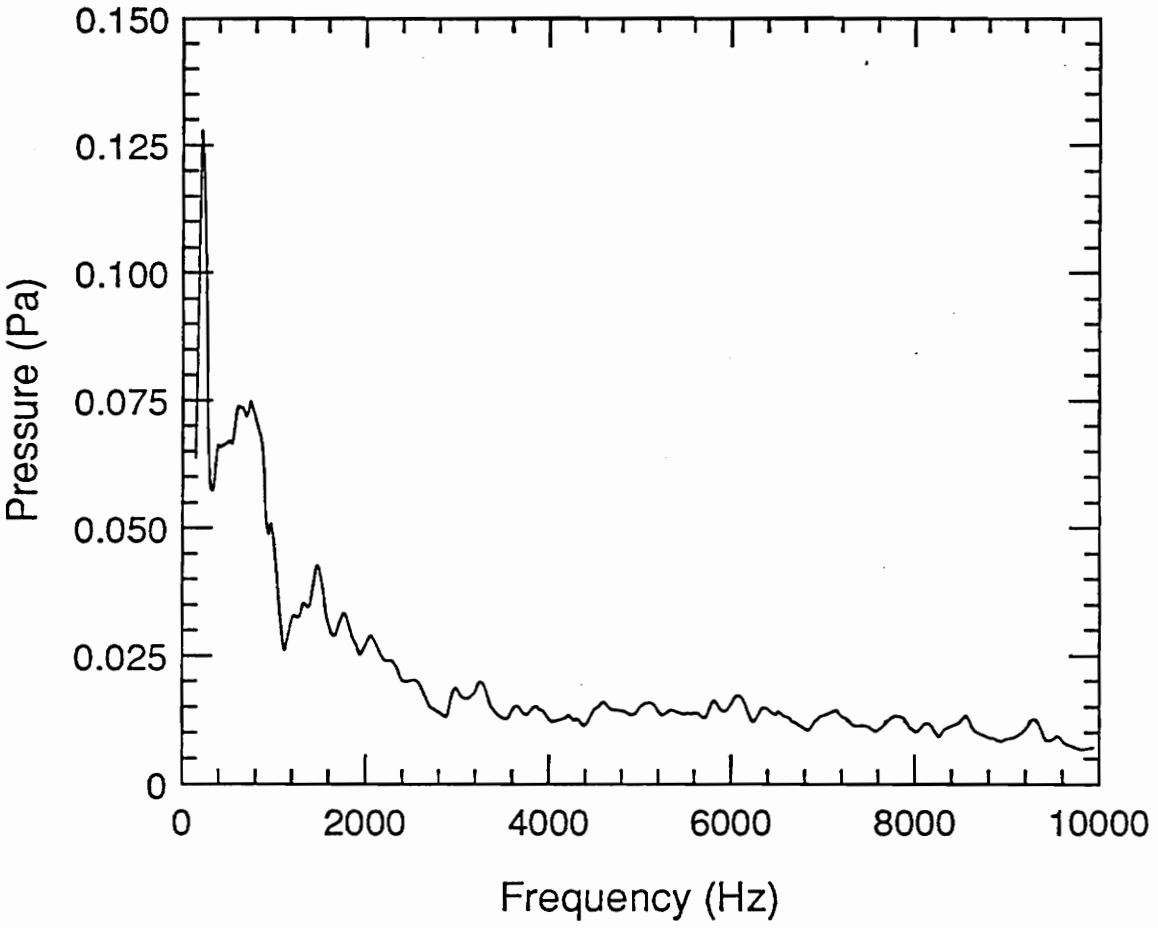

Figure 38. Spectrum for Acetylene: U = 50 m/s, D = 0.165 cm

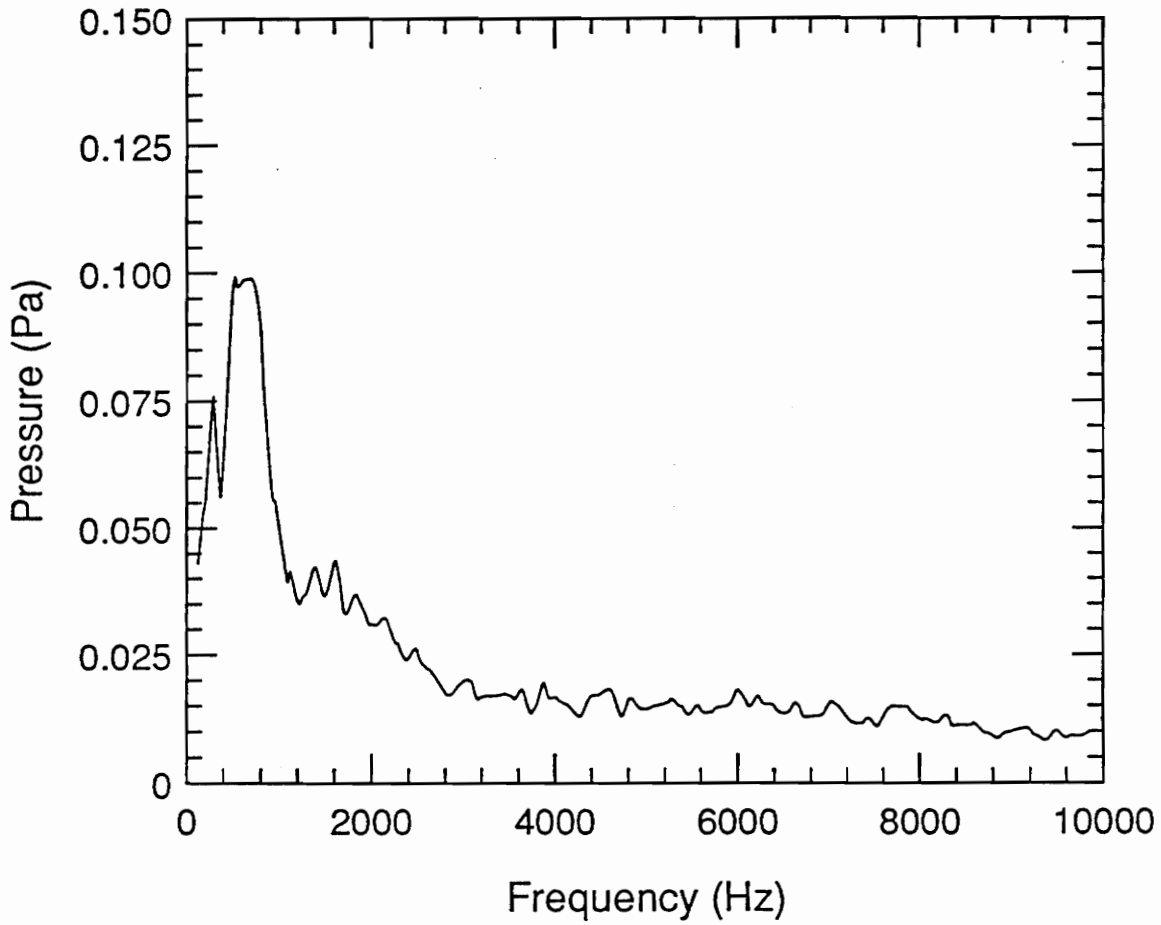

Figure 39. Spectrum for Acetylene: U = 75 m/s, D = 0.165 cm

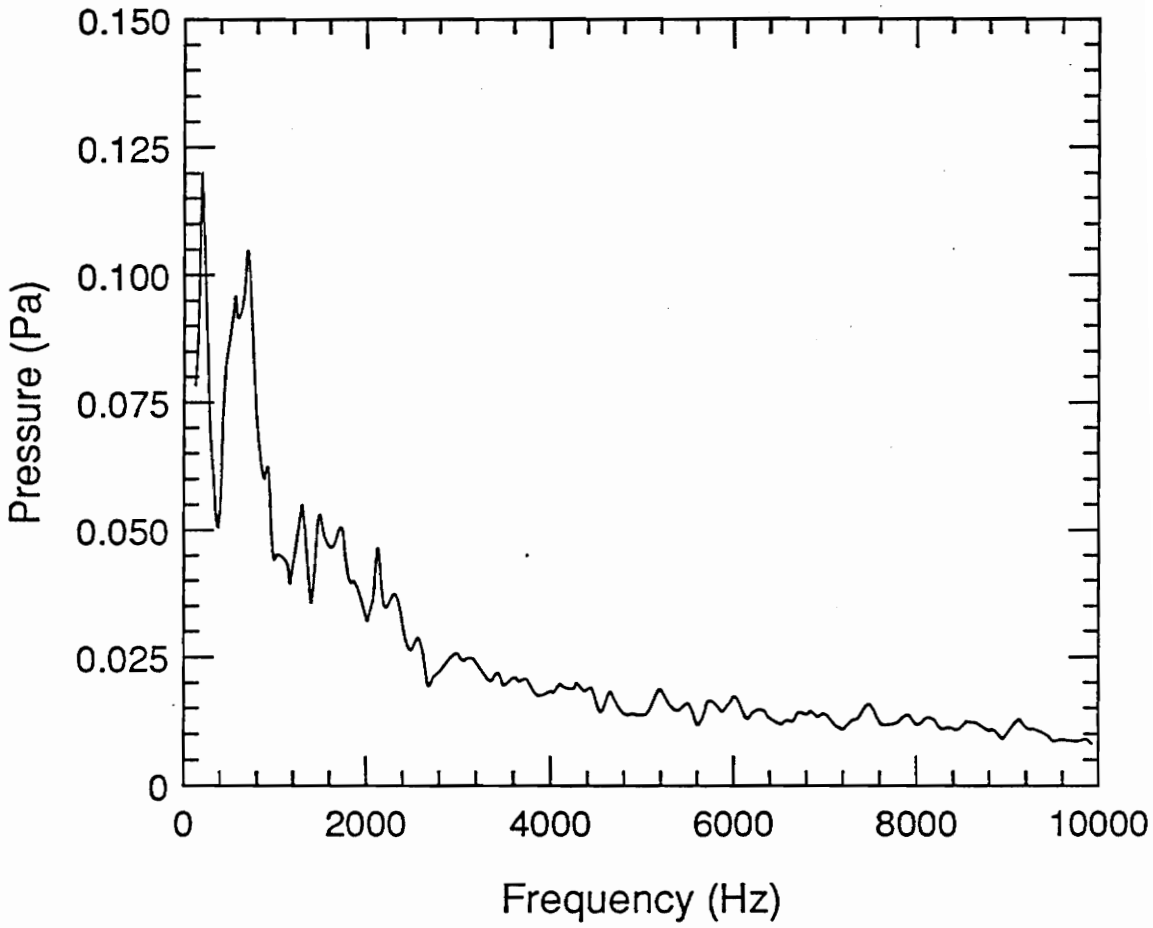

Figure 40. Spectrum for Acetylene: U = 100 m/s, D = 0.165 cm

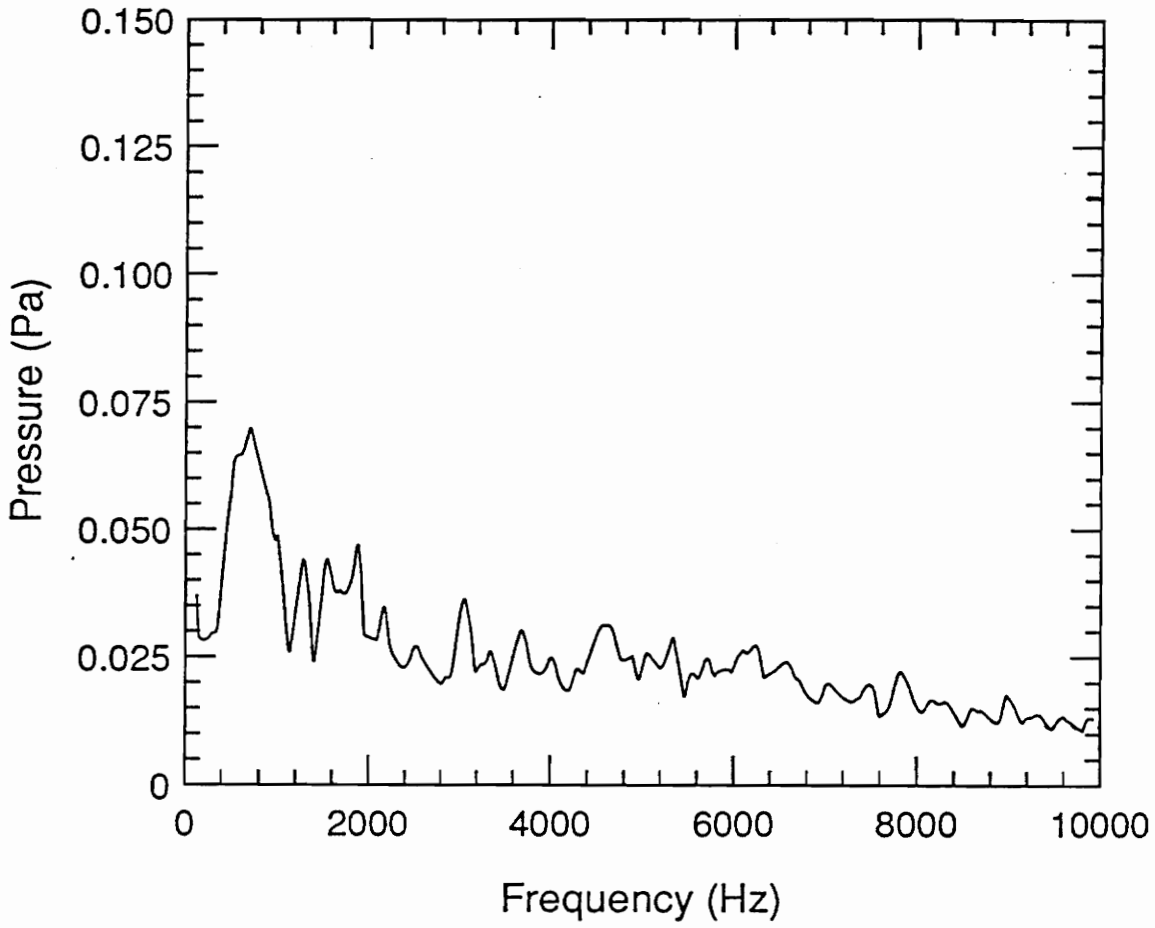

Figure 41. Spectrum for Acetylene: U = 50 m/s, D = 0.356 cm

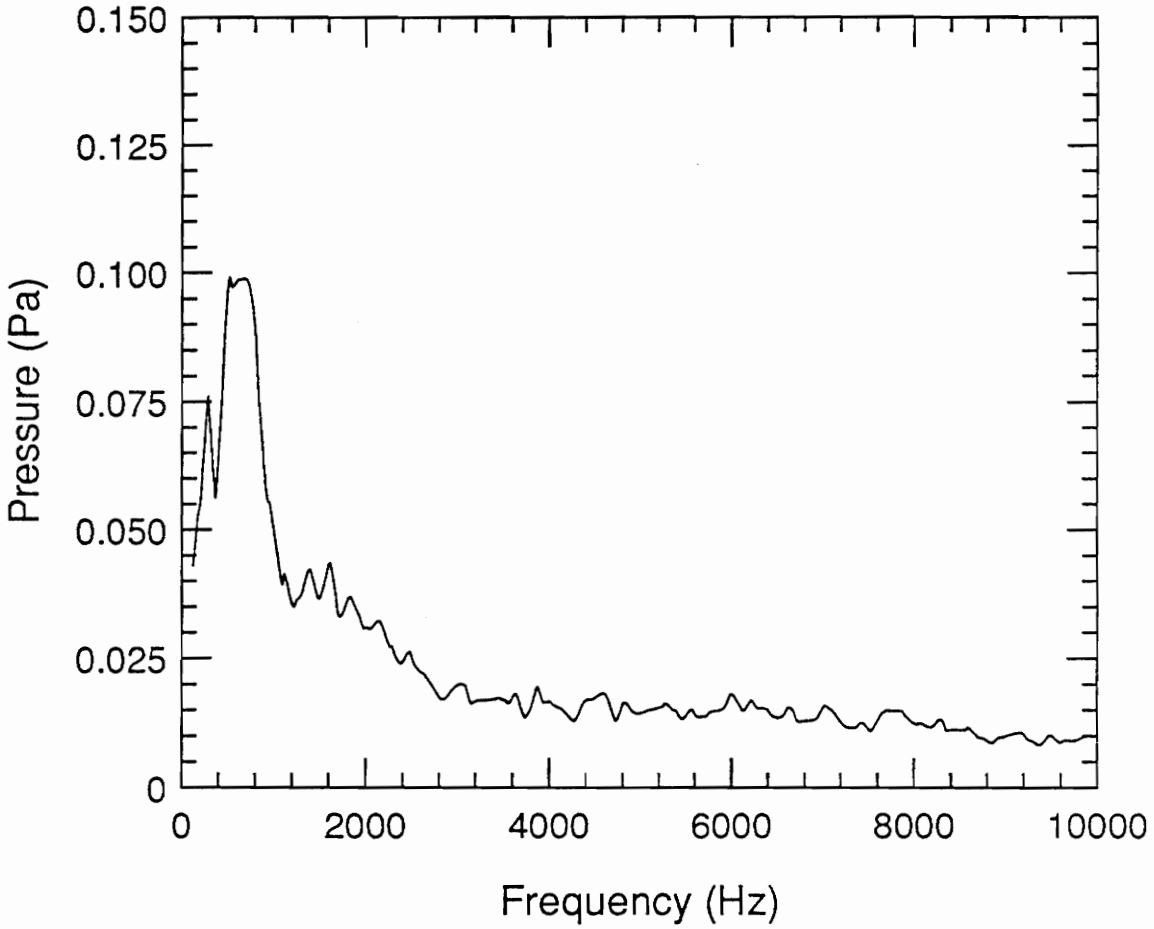

Figure 42. Spectrum for Acetylene: U = 75 m/s, D = 0.356 cm

Appendix E. Third-Octave-Band Data

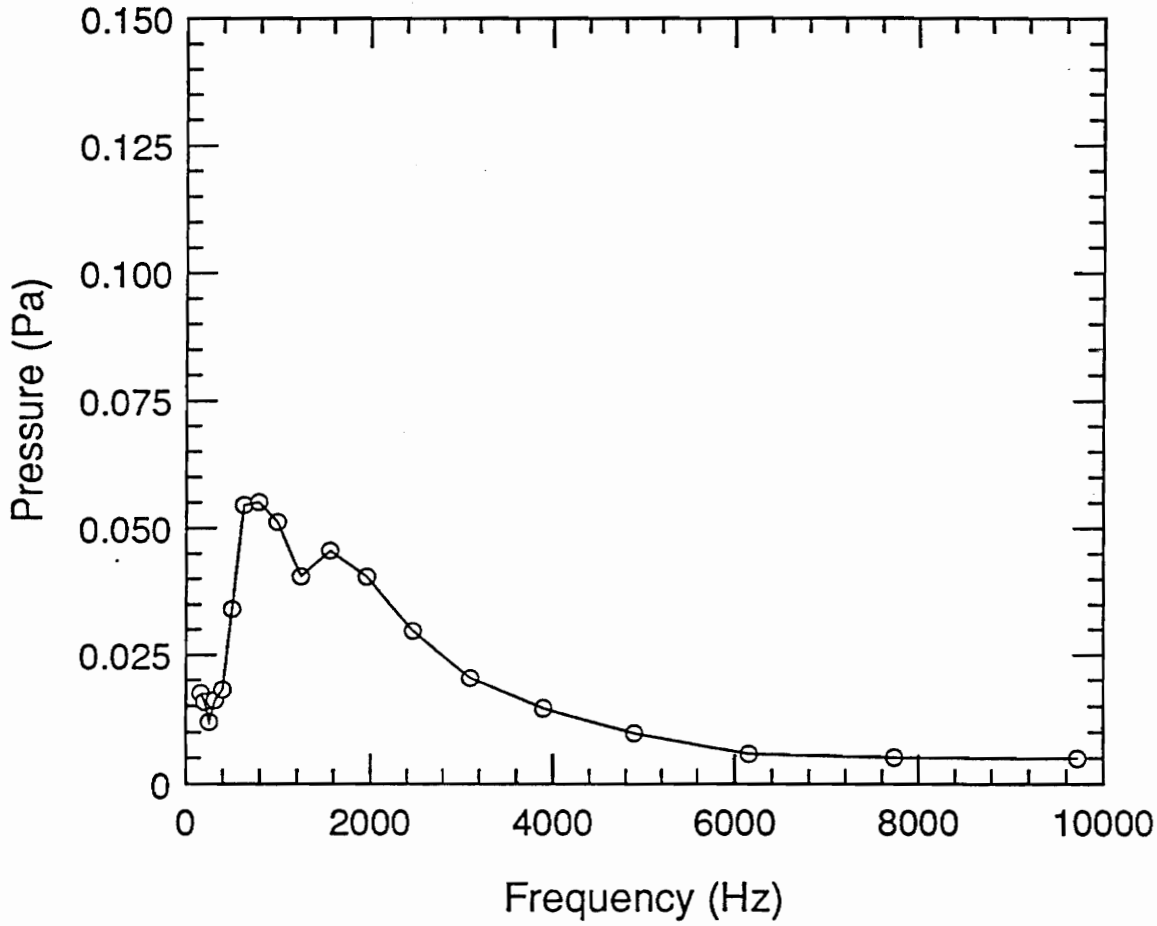

Figure 43. 1/3-Octave Spectrum for Methane: U = 10 m/s, D = 0.356 cm

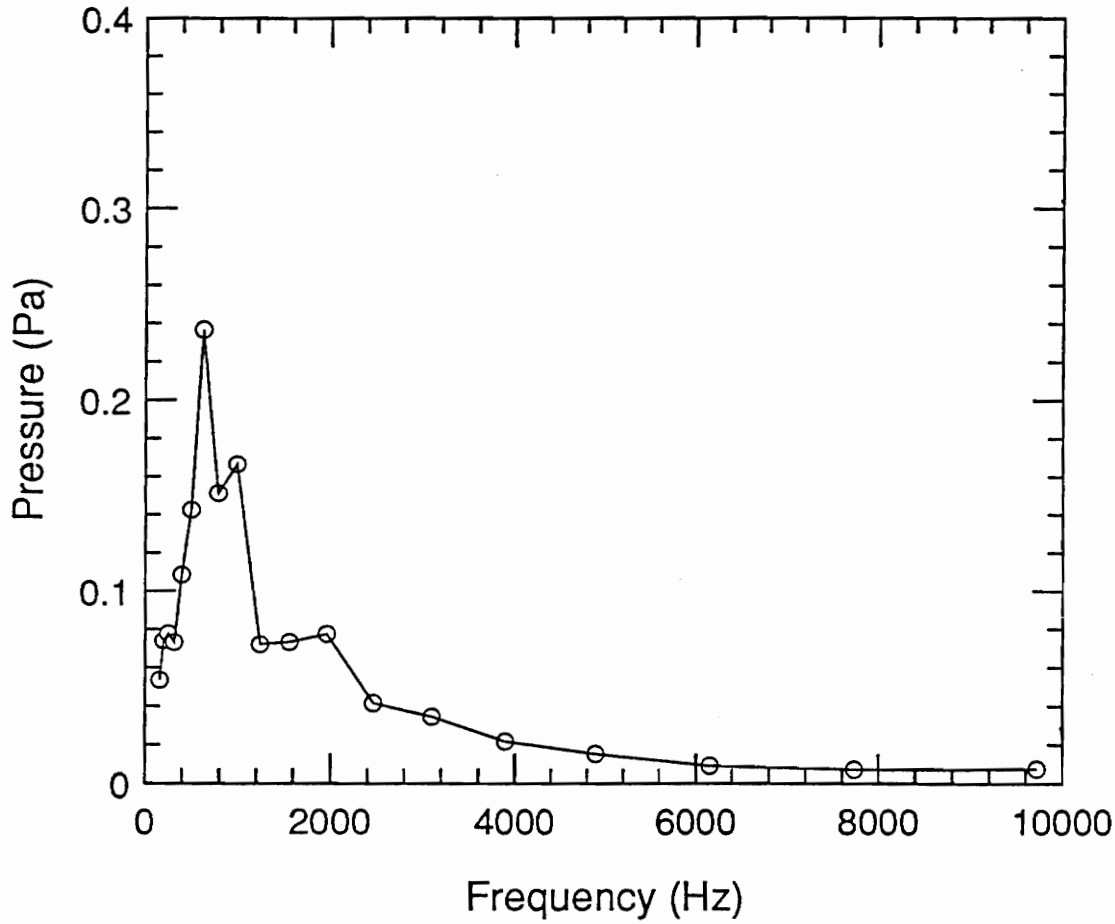

Figure 44. 1/3-Octave Spectrum for Methane: U = 20 m/s, D = 0.356 cm

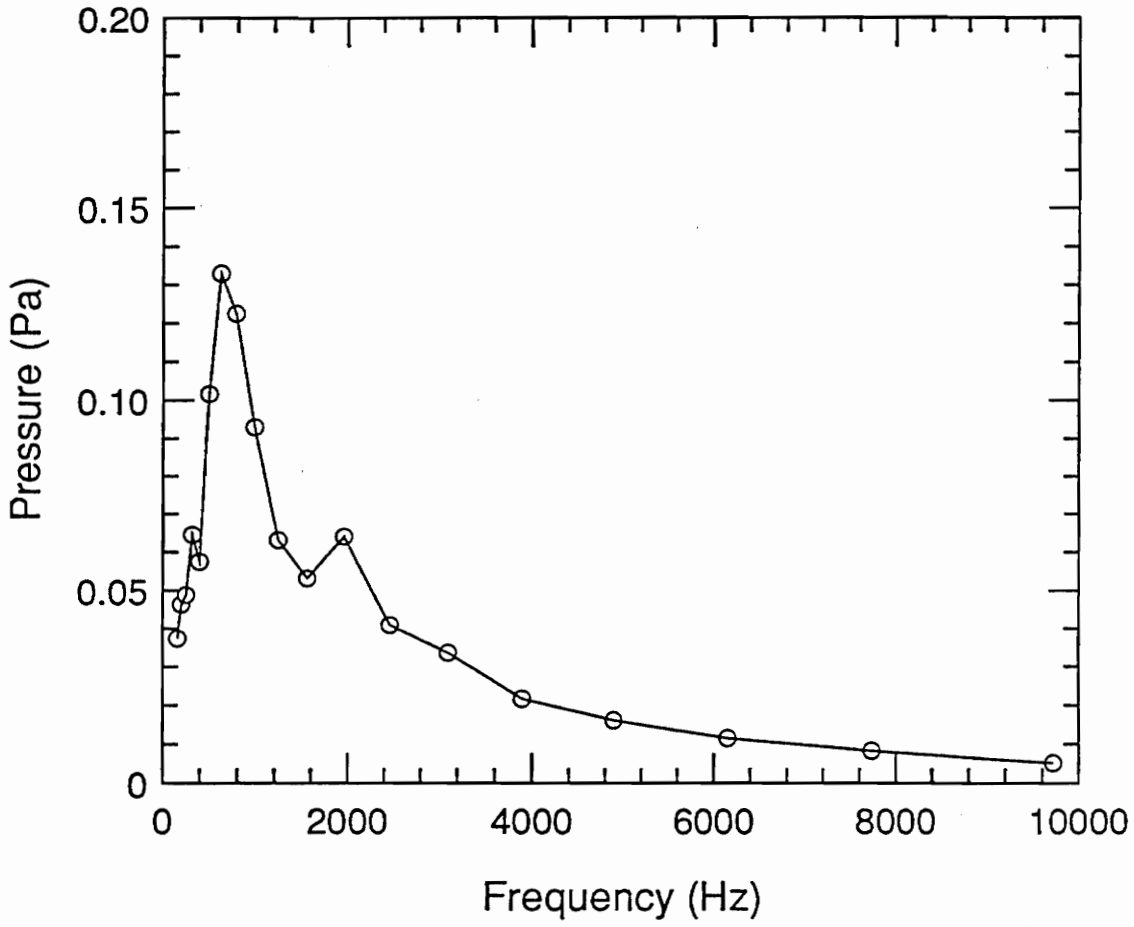

Figure 45. 1/3-Octave Spectrum for Methane: U = 10 m/s, D = 0.414 cm

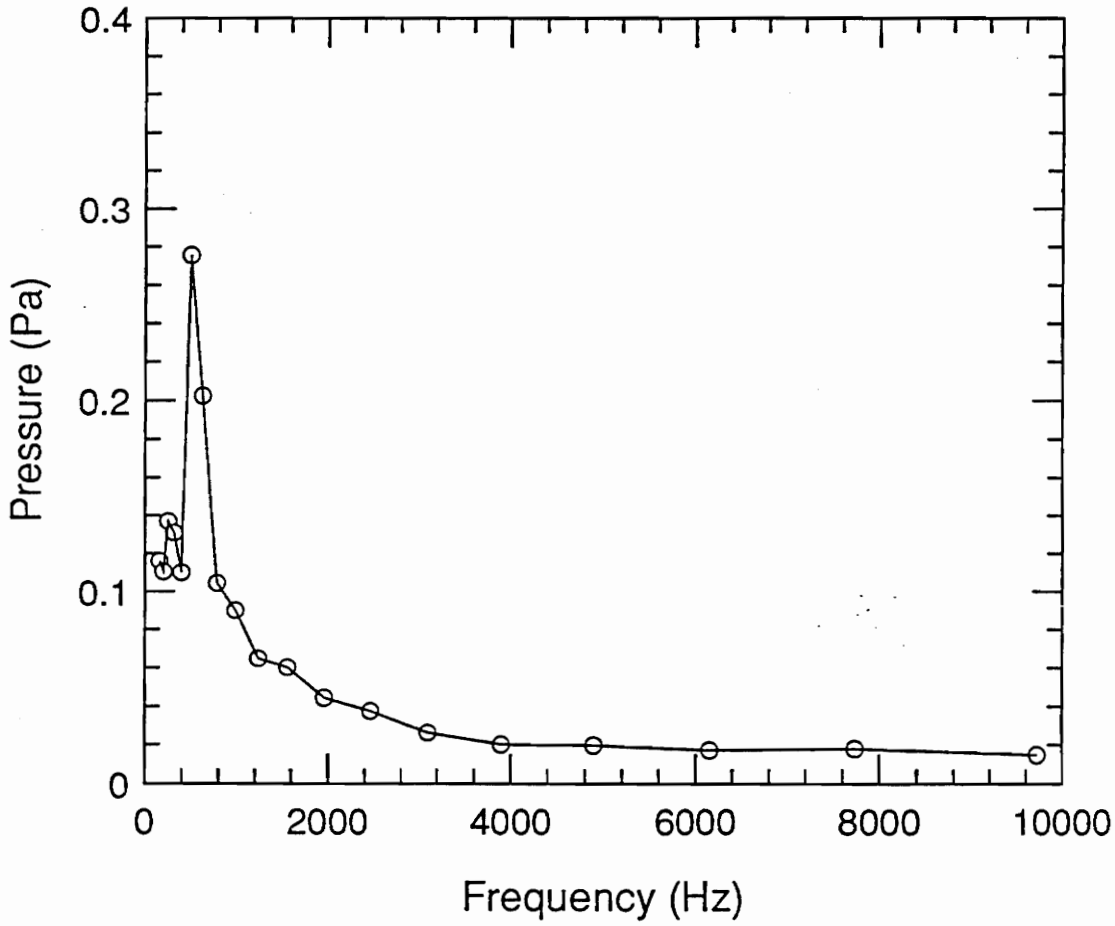

Figure 46. 1/3-Octave Spectrum for Methane: U = 20 m/s, D = 0.414 cm

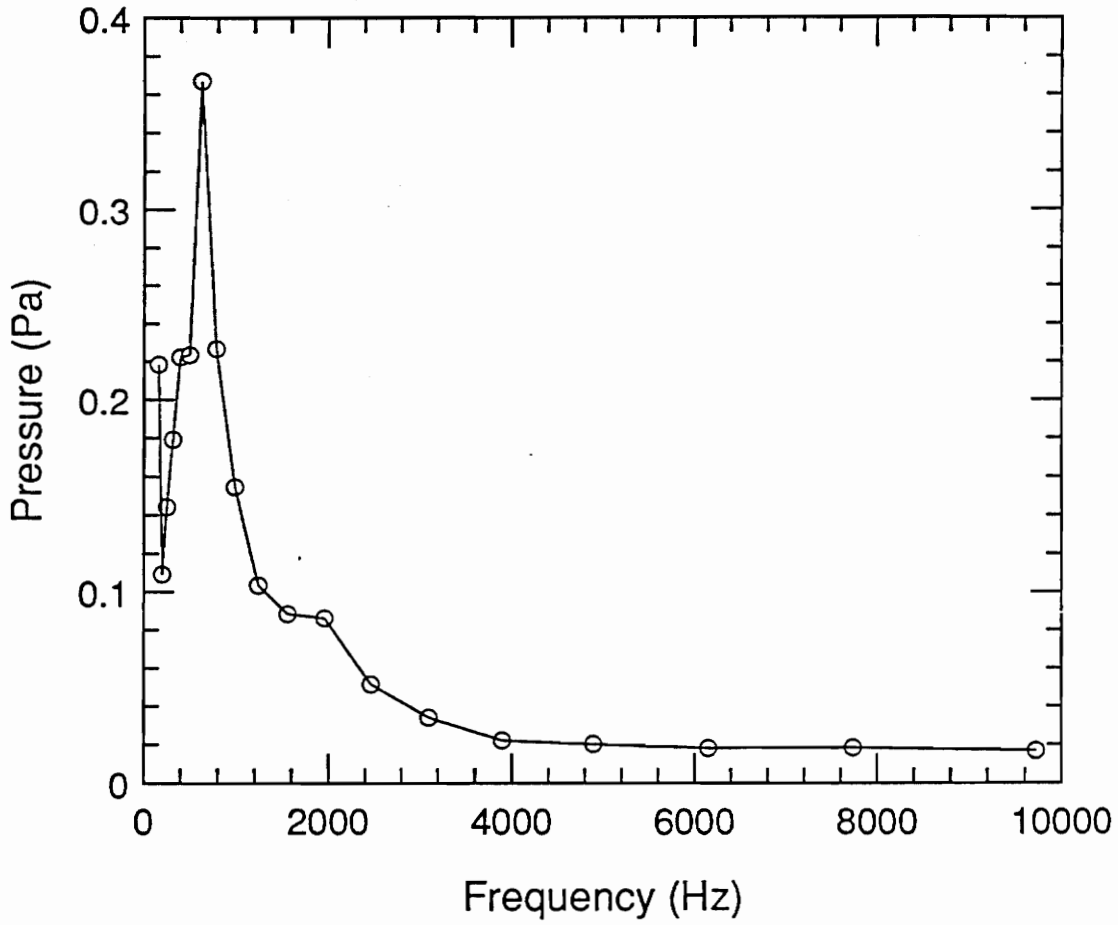

Figure 47. 1/3-Octave Spectrum for Methane: U = 25 m/s, D = 0.414 cm

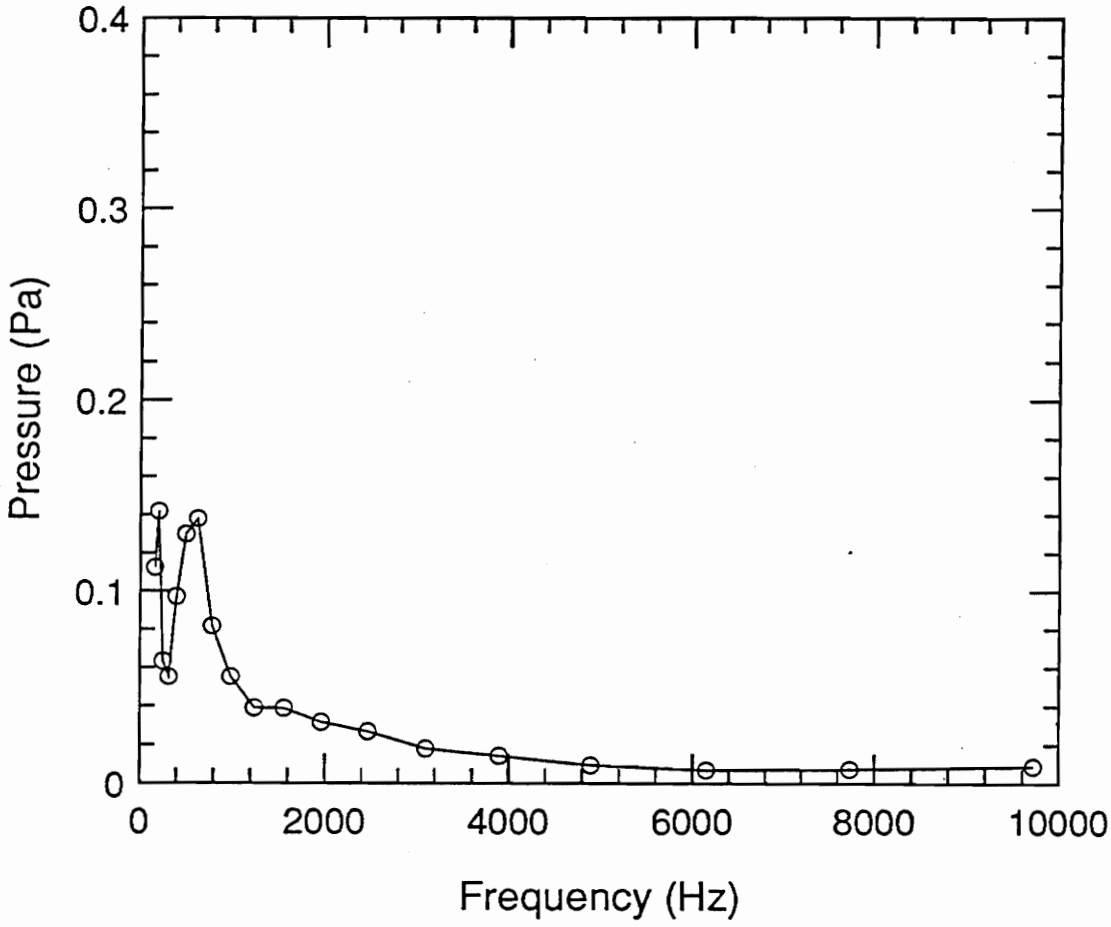

Figure 48. 1/3-Octave Spectrum for Methane: U = 10 m/s, D = 0.541 cm

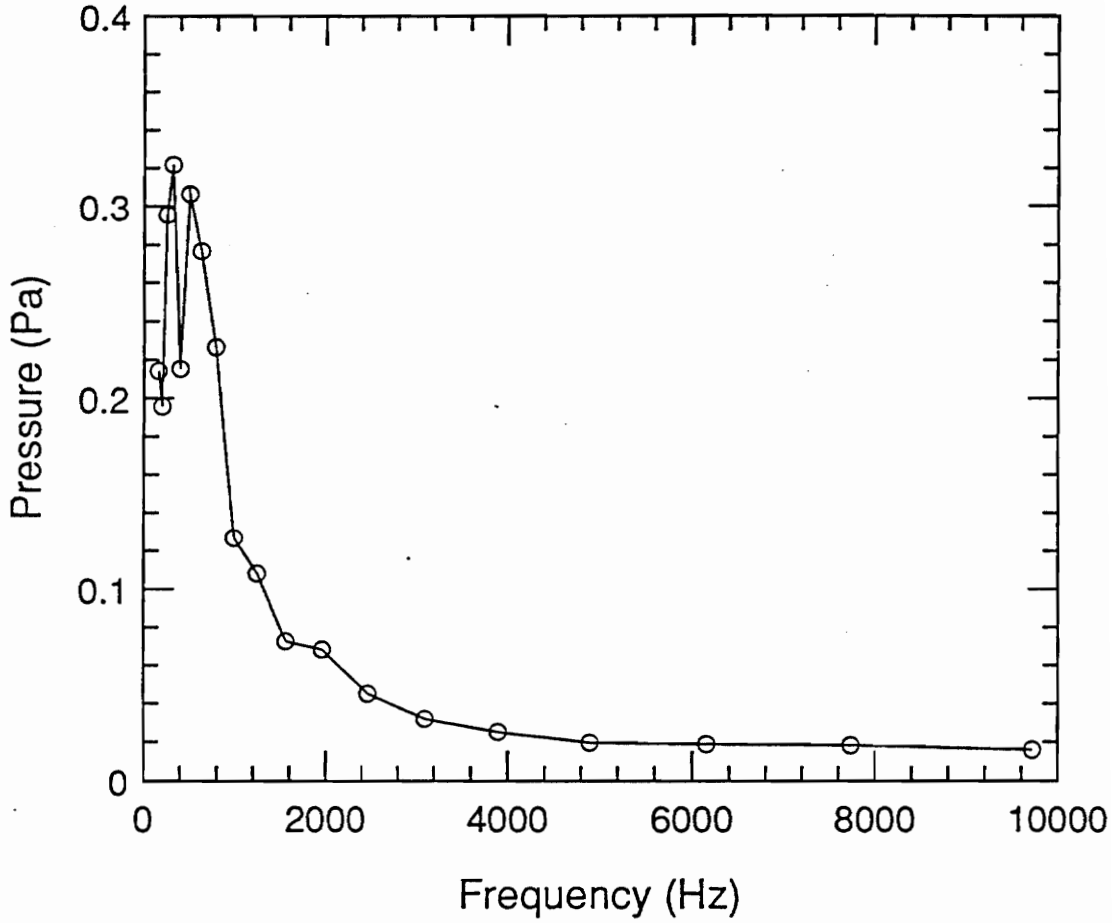

Figure 49. 1/3-Octave Spectrum for Methane: U = 20 m/s, D = 0.541 cm

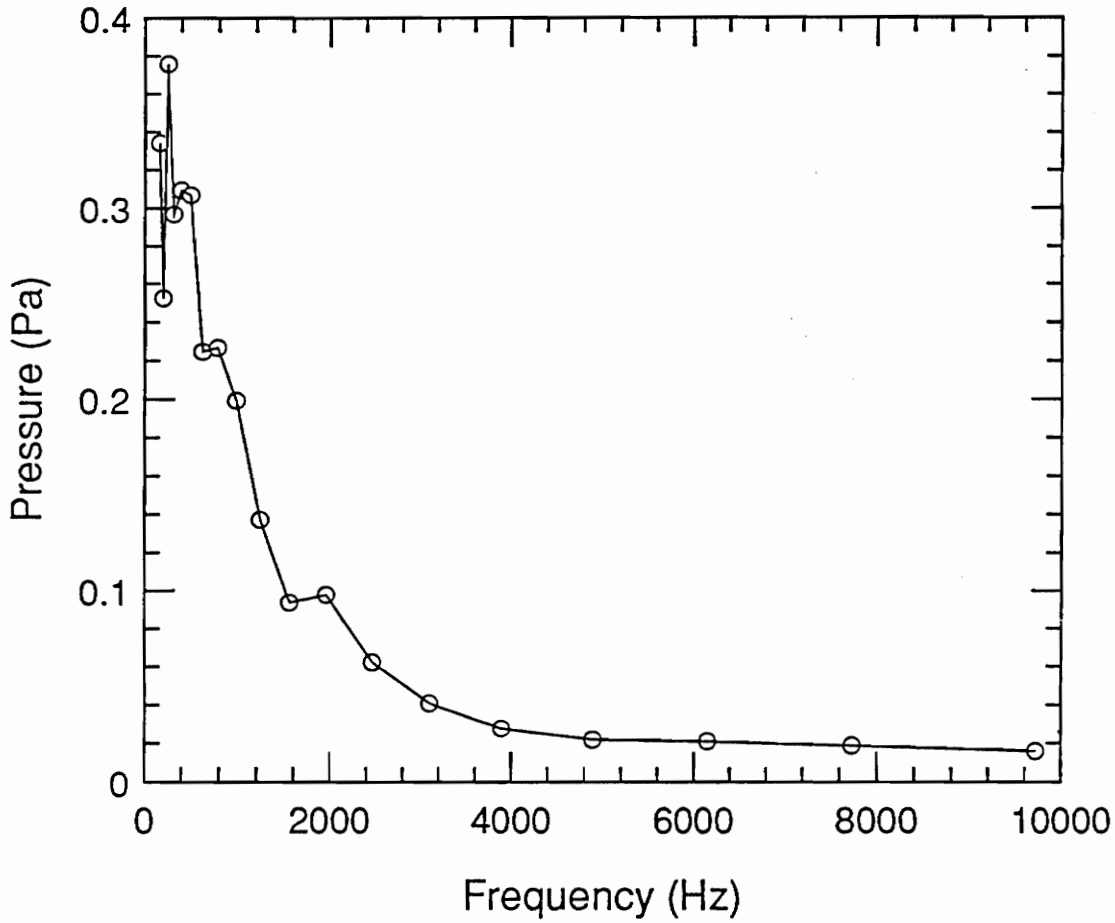

Figure 50. 1/3-Octave Spectrum for Methane: U = 25 m/s, D = 0.541 cm

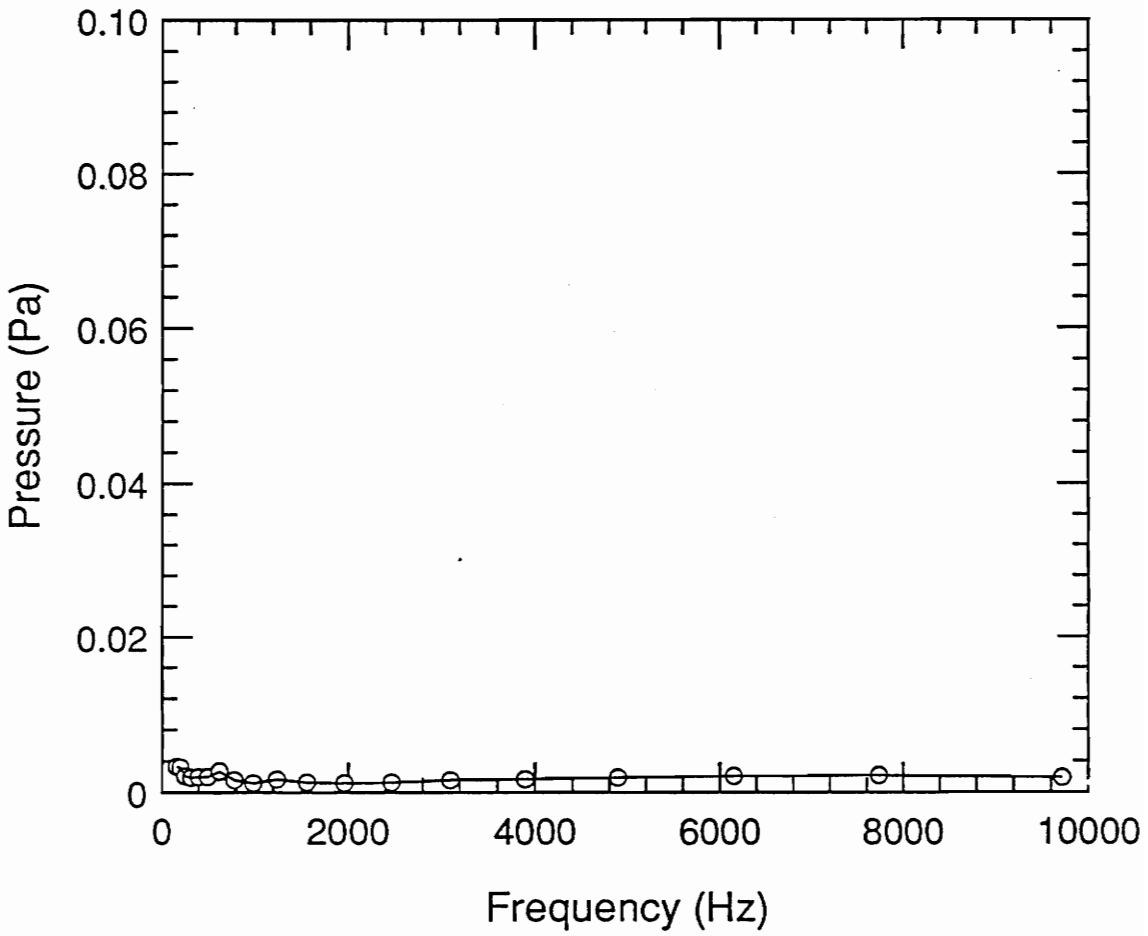

Figure 51. 1/3-Octave Spectrum for Propane: U = 20 m/s, D = 0.117 cm

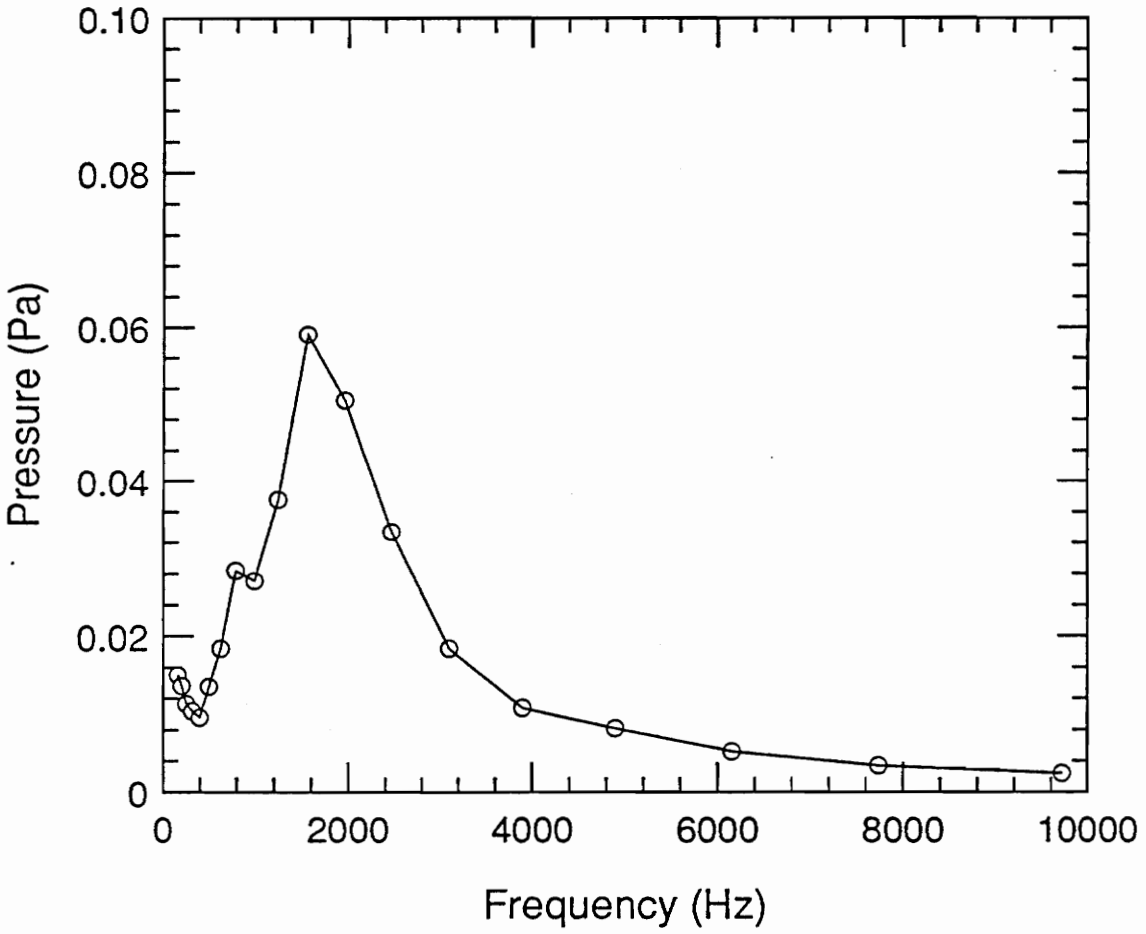

Figure 52. 1/3-Octave Spectrum for Propane: U = 30 m/s, D = 0.117 cm

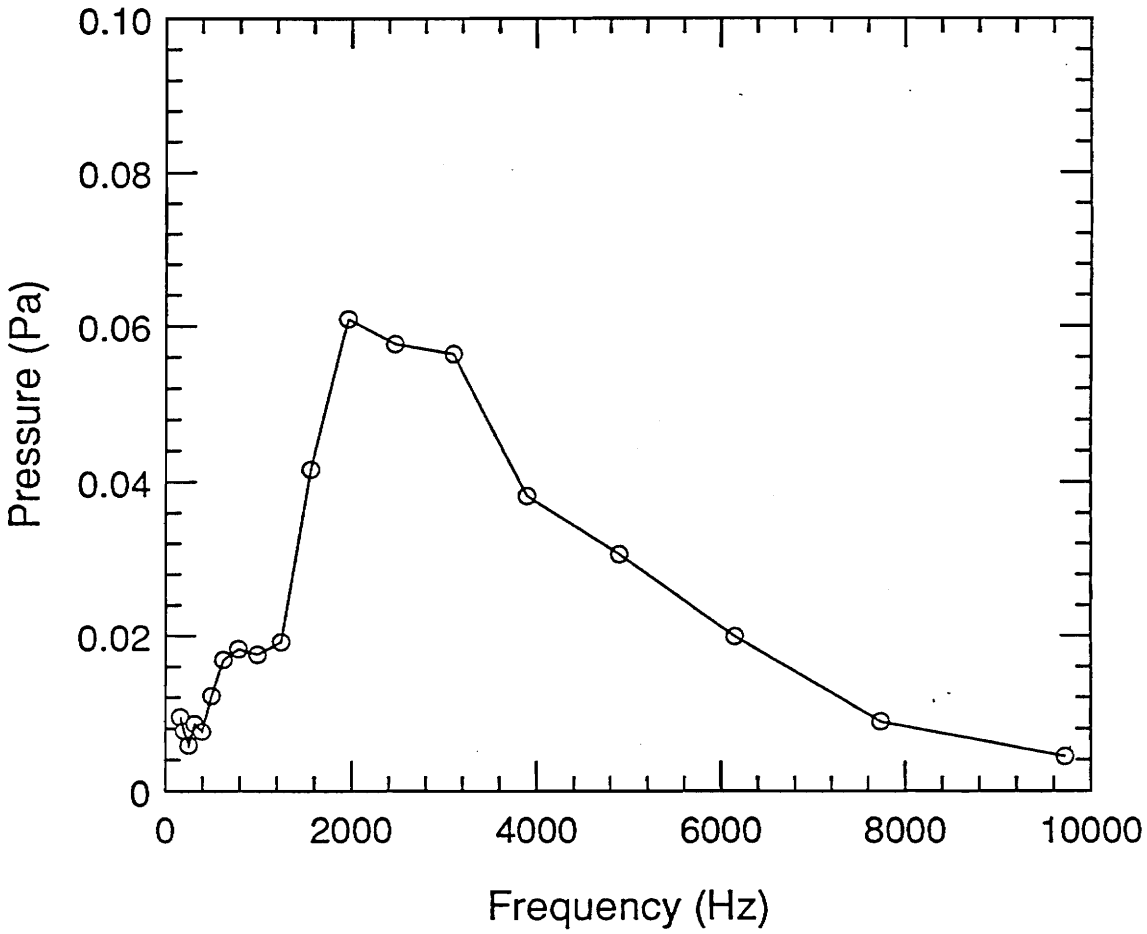

Figure 53. 1/3-Octave Spectrum for Propane: U = 40 m/s, D = 0.117 cm

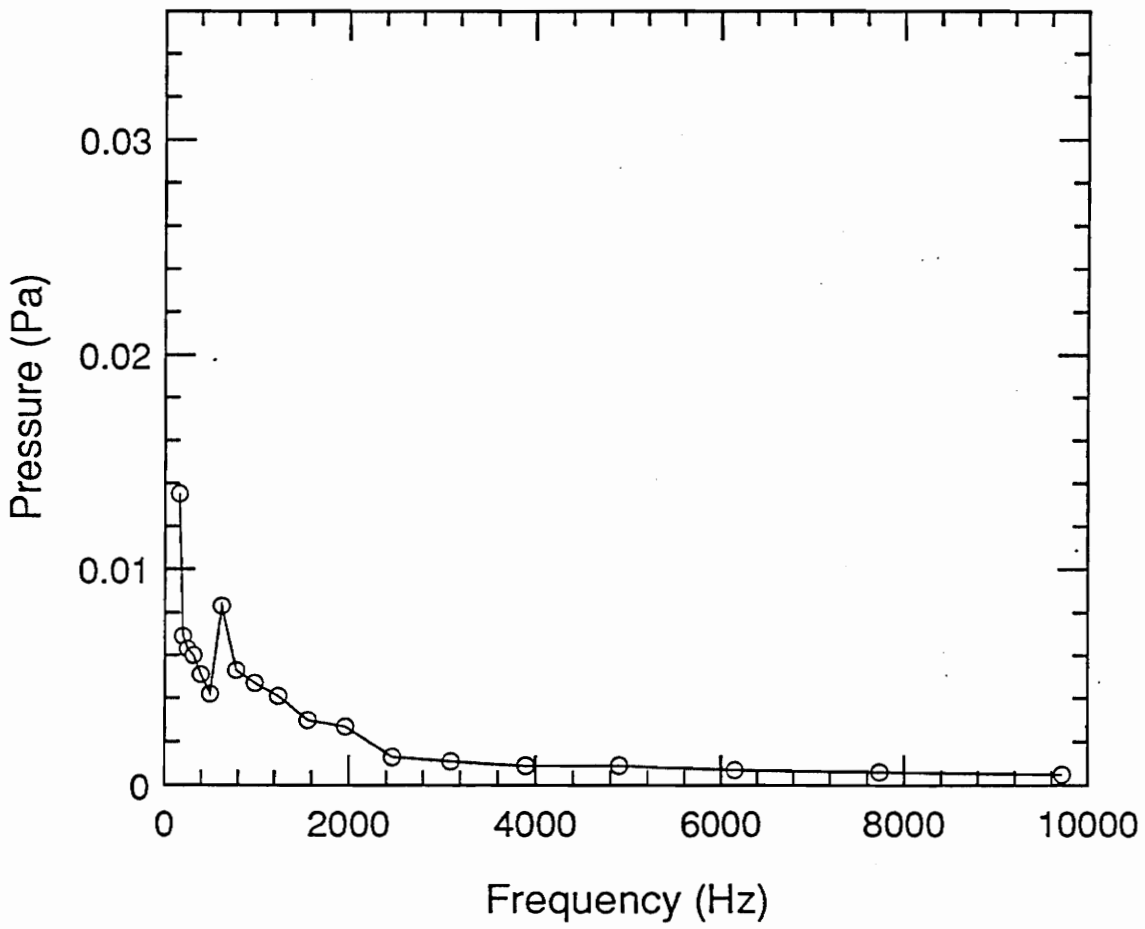

Figure 54. 1/3-Octave Spectrum for Propane: U = 20 m/s, D = 0.165 cm

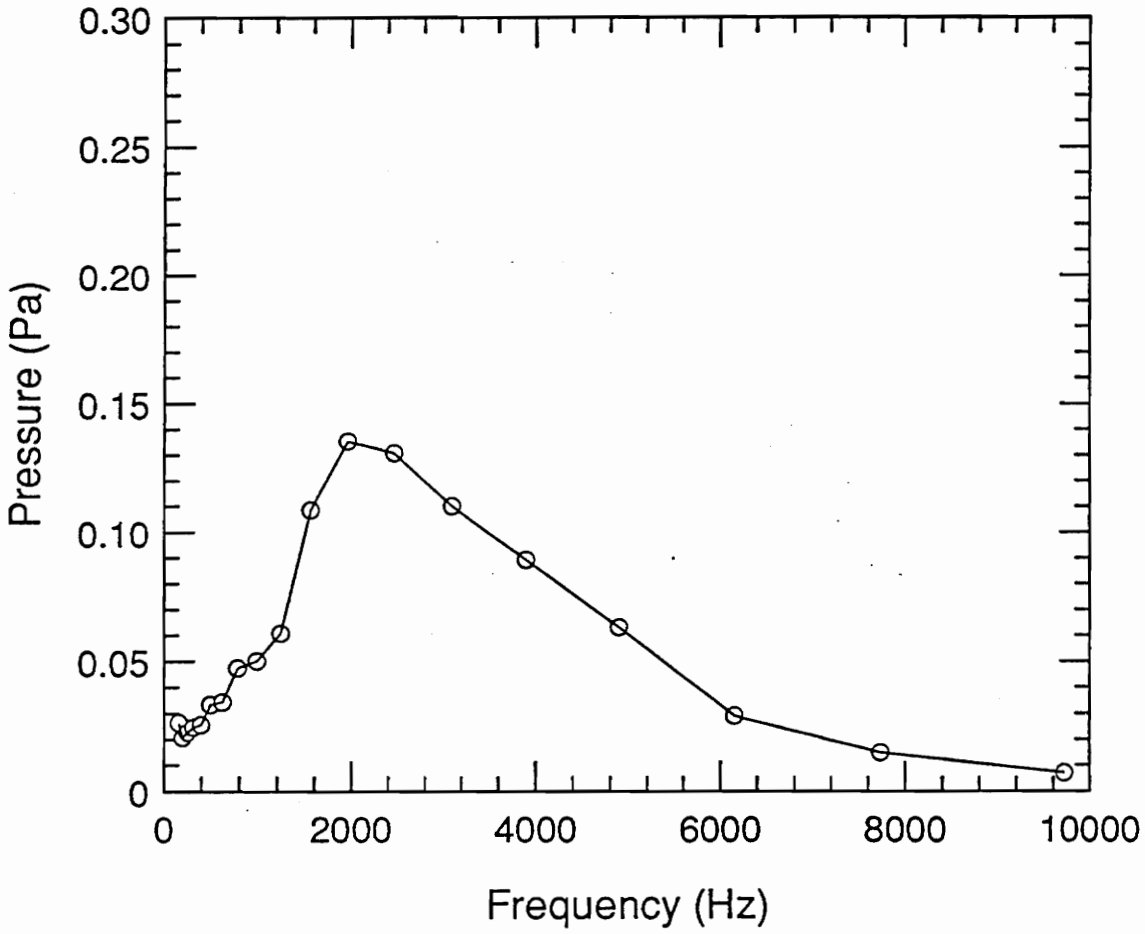

Figure 55. 1/3-Octave Spectrum for Propane: U = 30 m/s, D = 0.165 cm

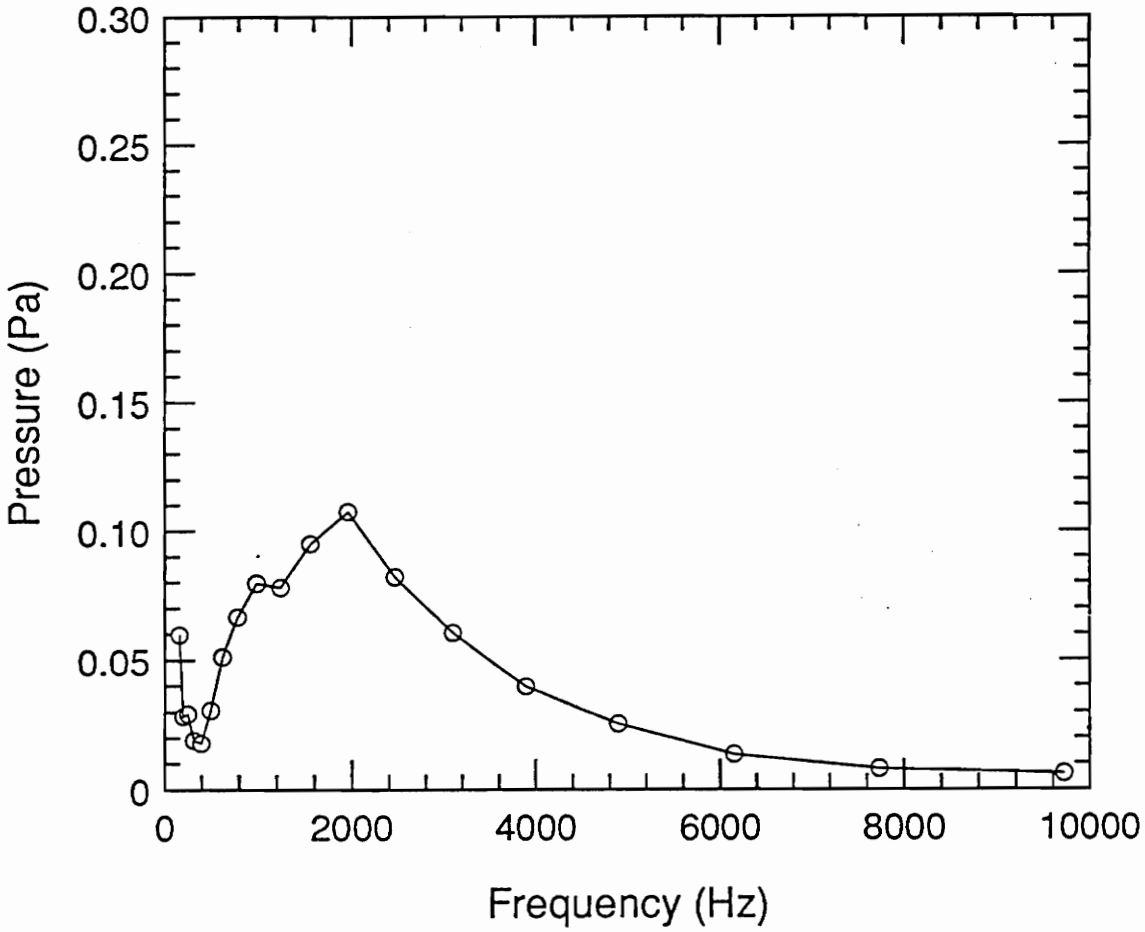

Figure 56. 1/3-Octave Spectrum for Propane: U = 30 m/s, D = 0.165 cm

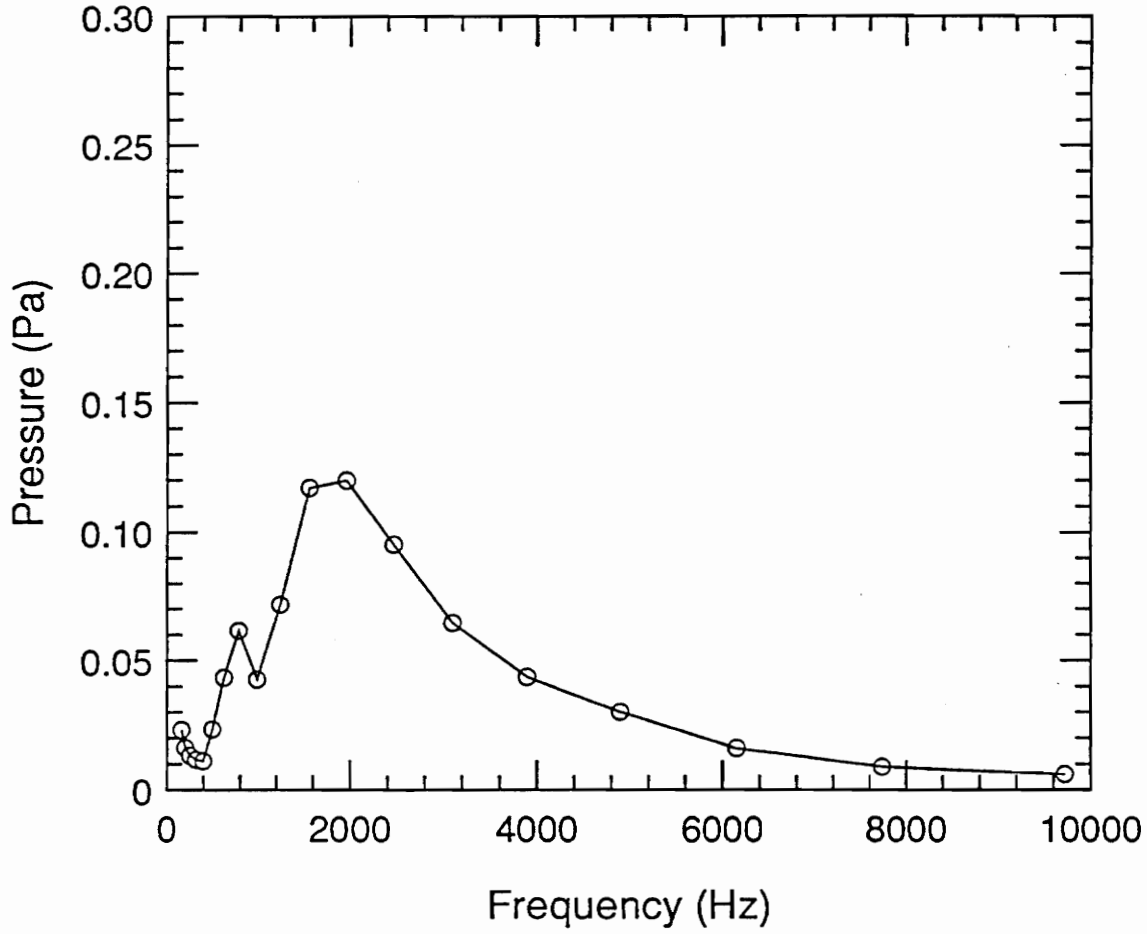

Figure 57. 1/3-Octave Spectrum for Propane: U = 30 m/s, D = 0.165 cm

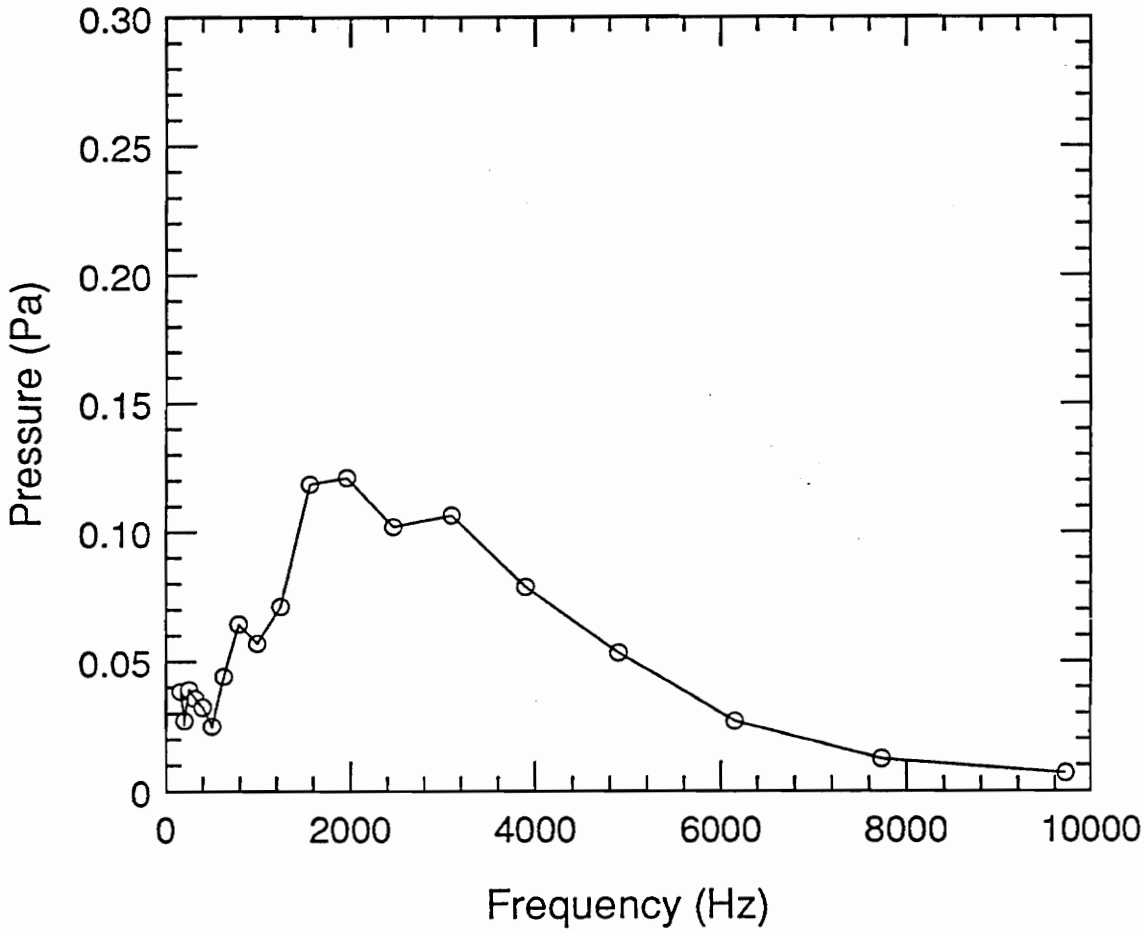

Figure 58. 1/3-Octave Spectrum for Propane: U = 40 m/s, D = 0.165 cm

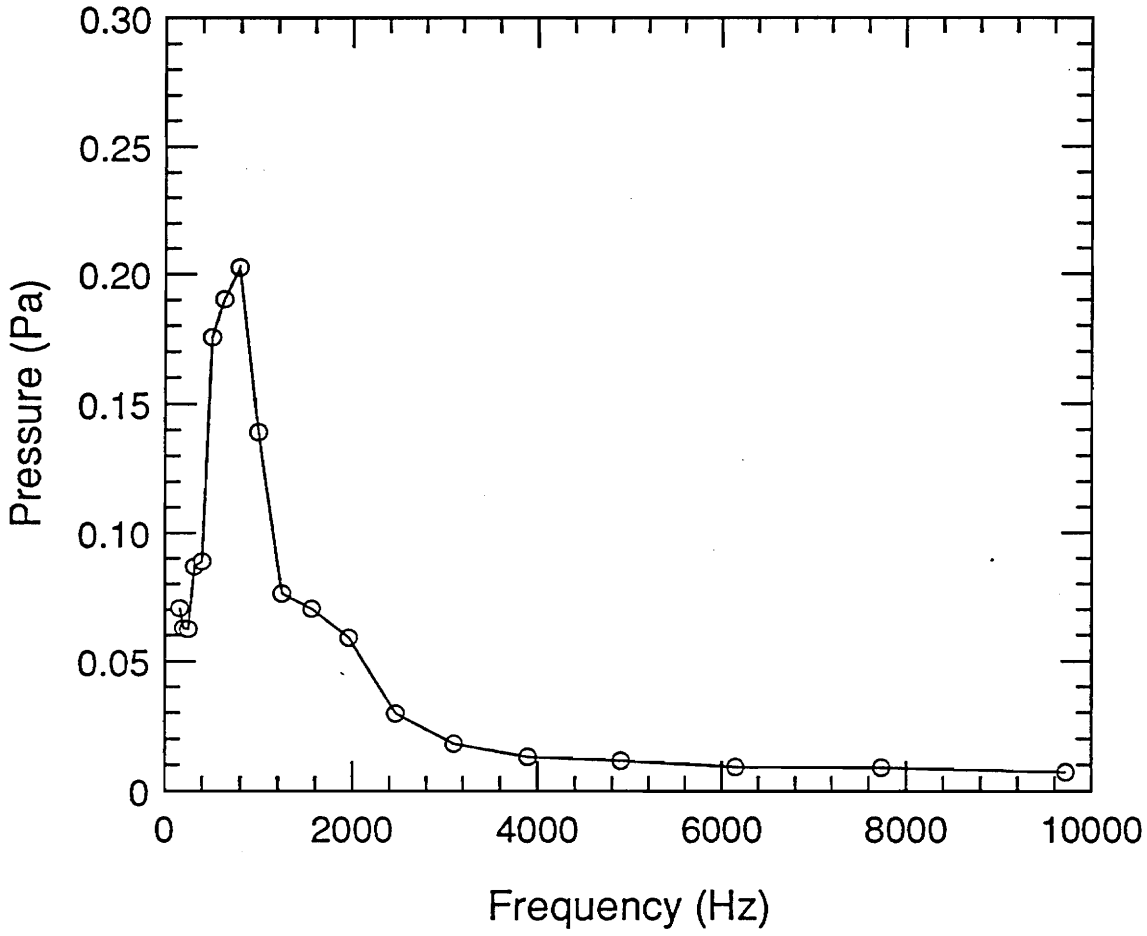

Figure 59. 1/3-Octave Spectrum for Propane: U = 20 m/s, D = 0.356 cm

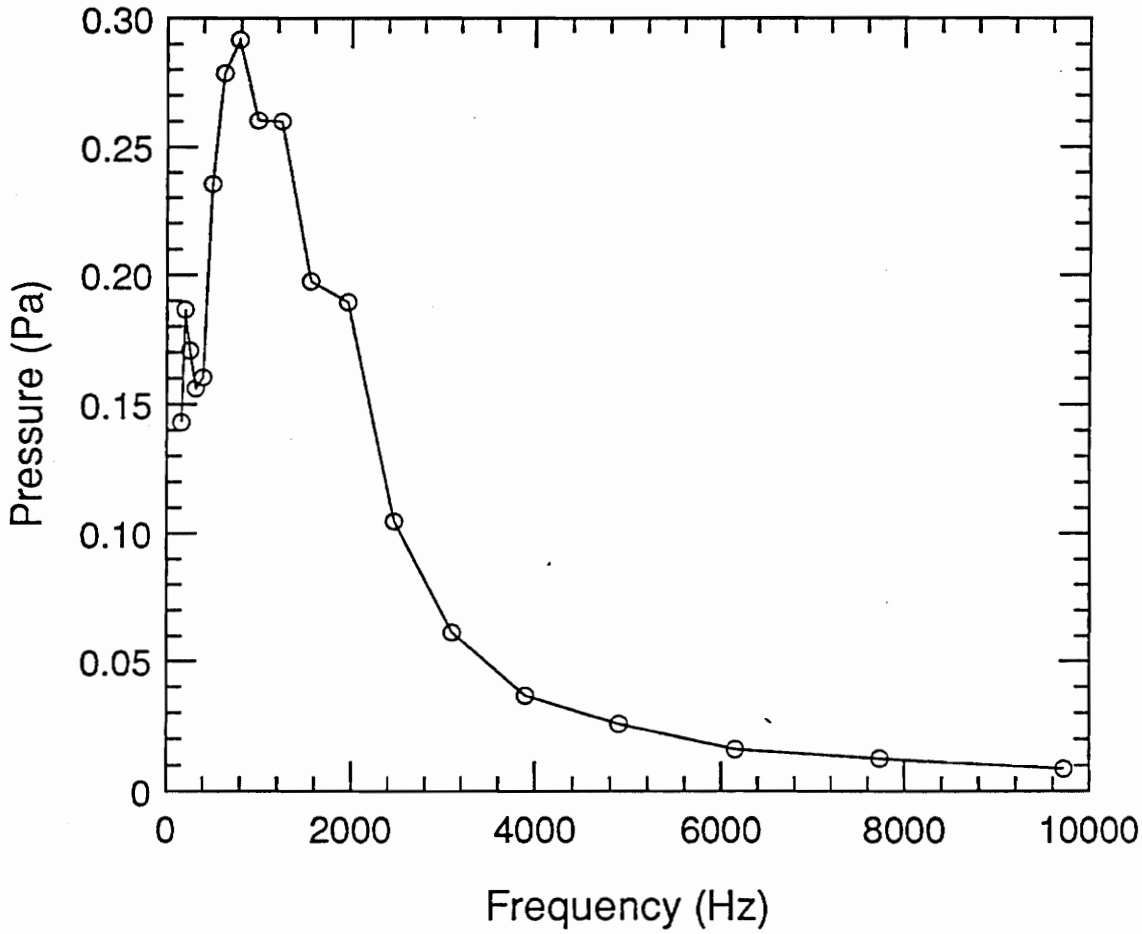

Figure 60. 1/3-Octave Spectrum for Propane: U = 30 m/s, D = 0.356 cm

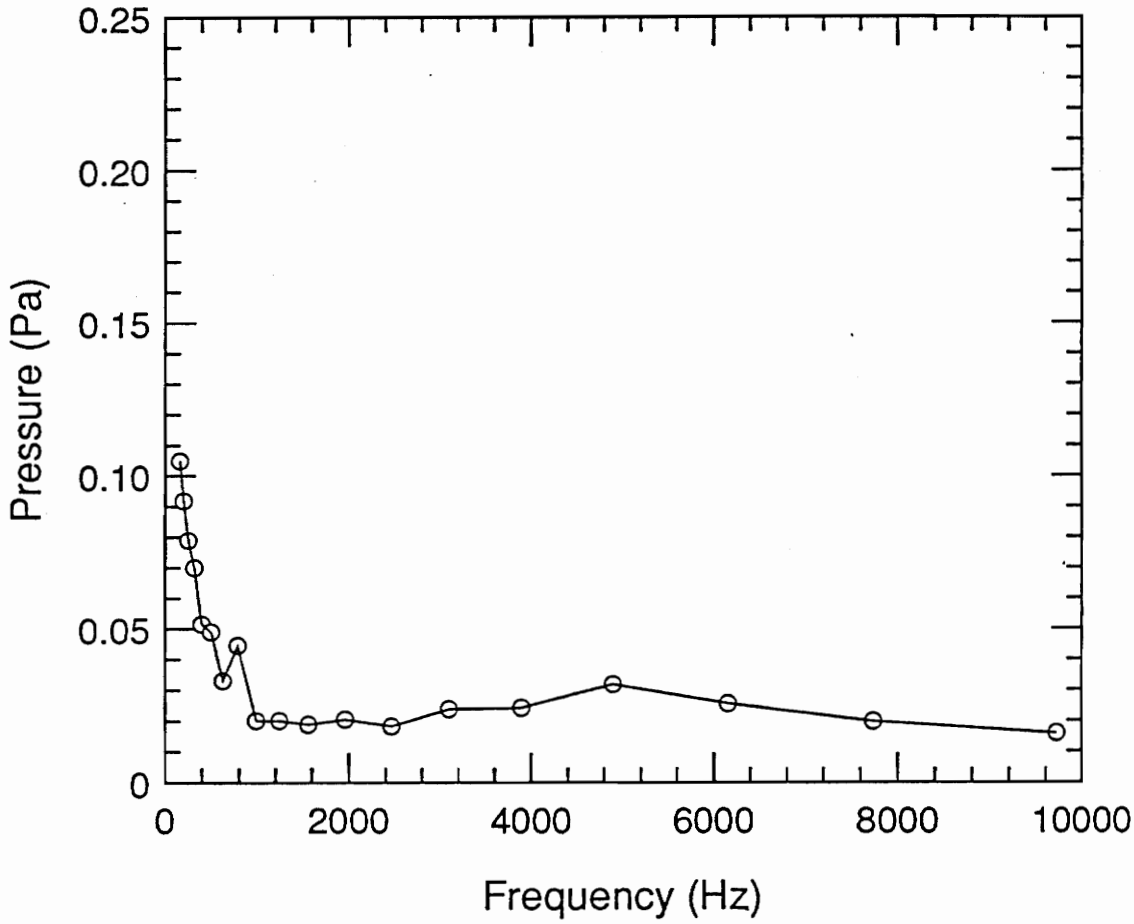

Figure 61. 1/3-Octave Spectrum for Acetylene: U = 50 m/s, D = 0.117 cm

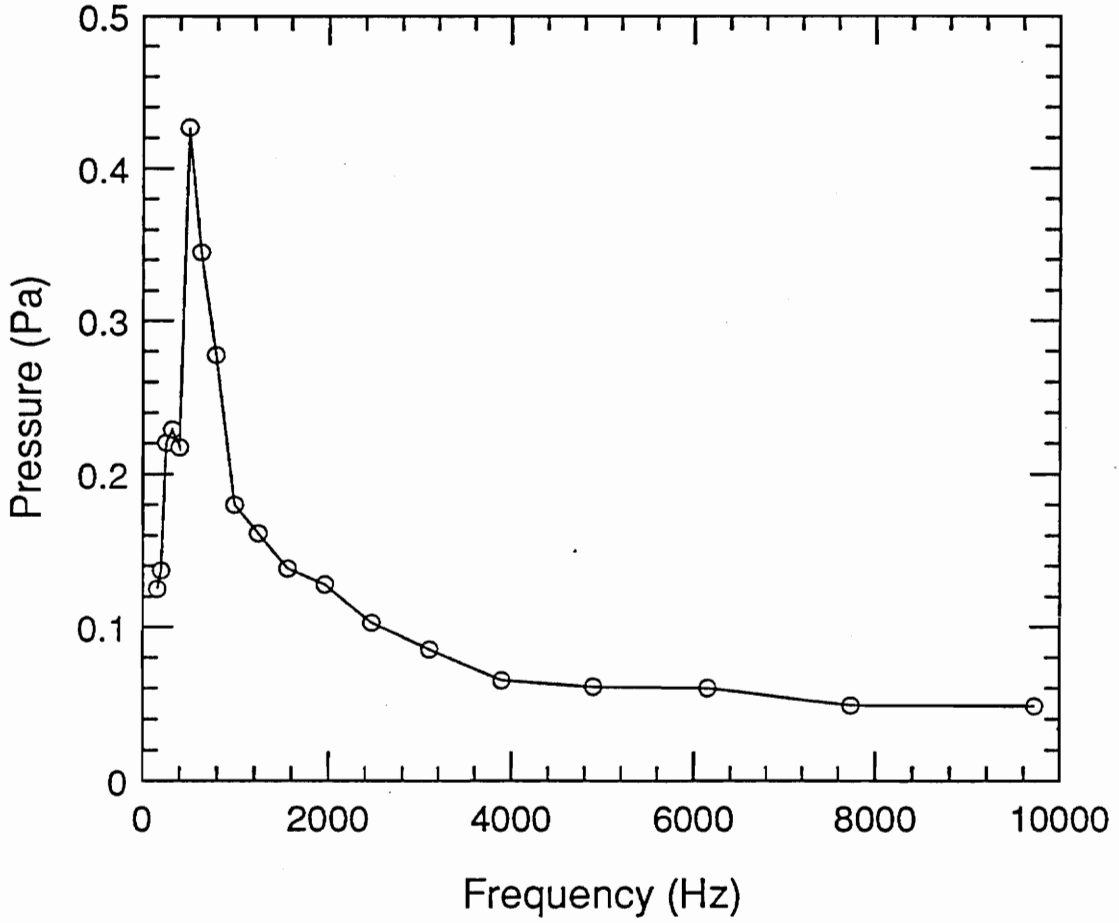

Figure 62. 1/3-Octave Spectrum for Acetylene: U = 75 m/s, D = 0.117 cm

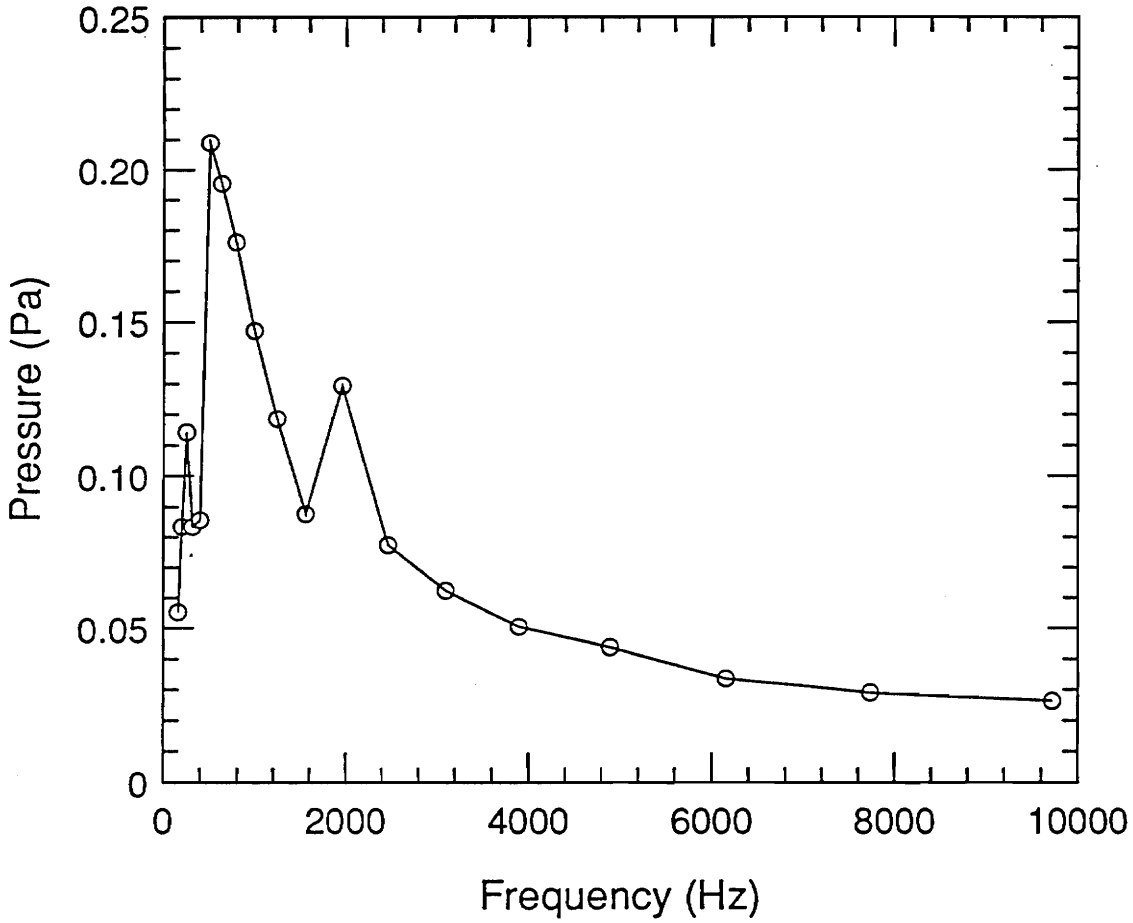

Figure 63. 1/3-Octave Spectrum for Acetylene: U = 100 m/s, D = 0.117 cm

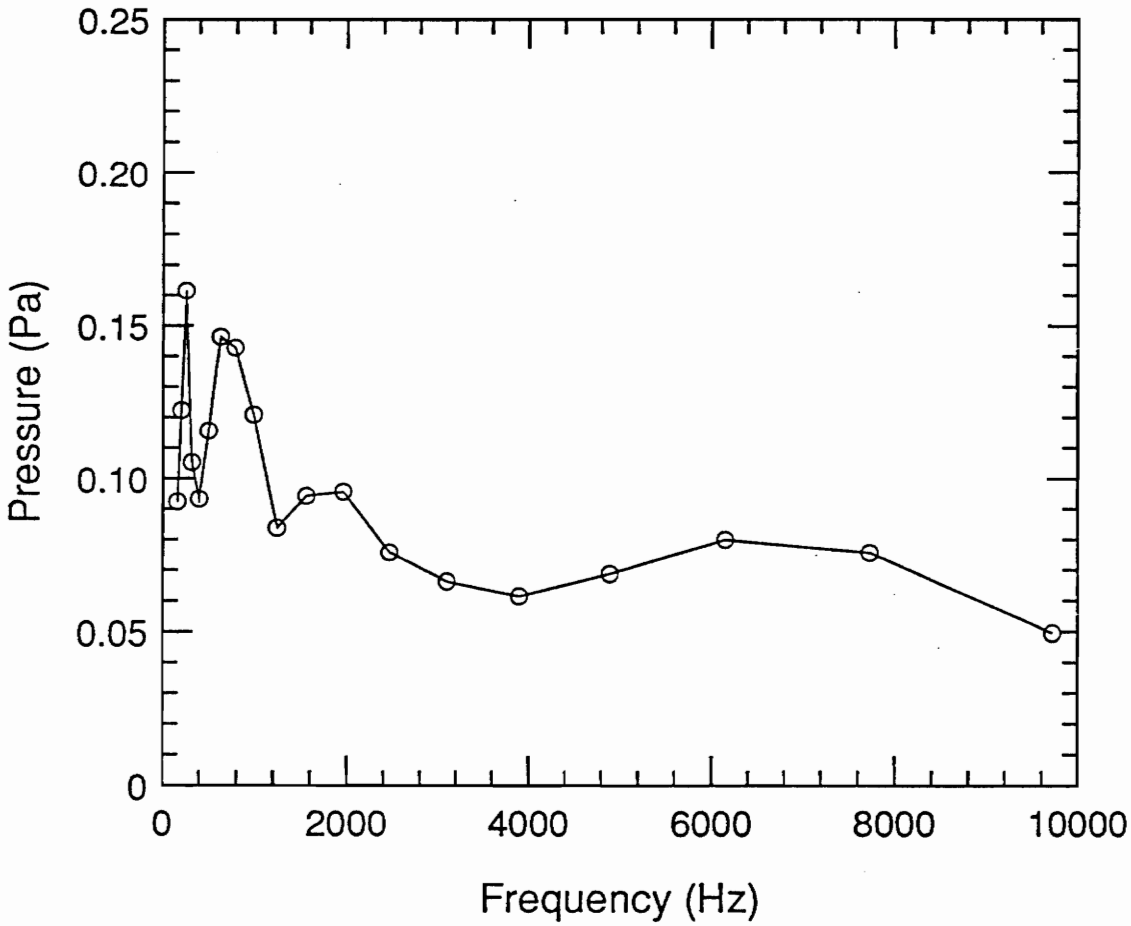

Figure 64. 1/3-Octave Spectrum for Acetylene: U = 50 m/s, D = 0.165 cm

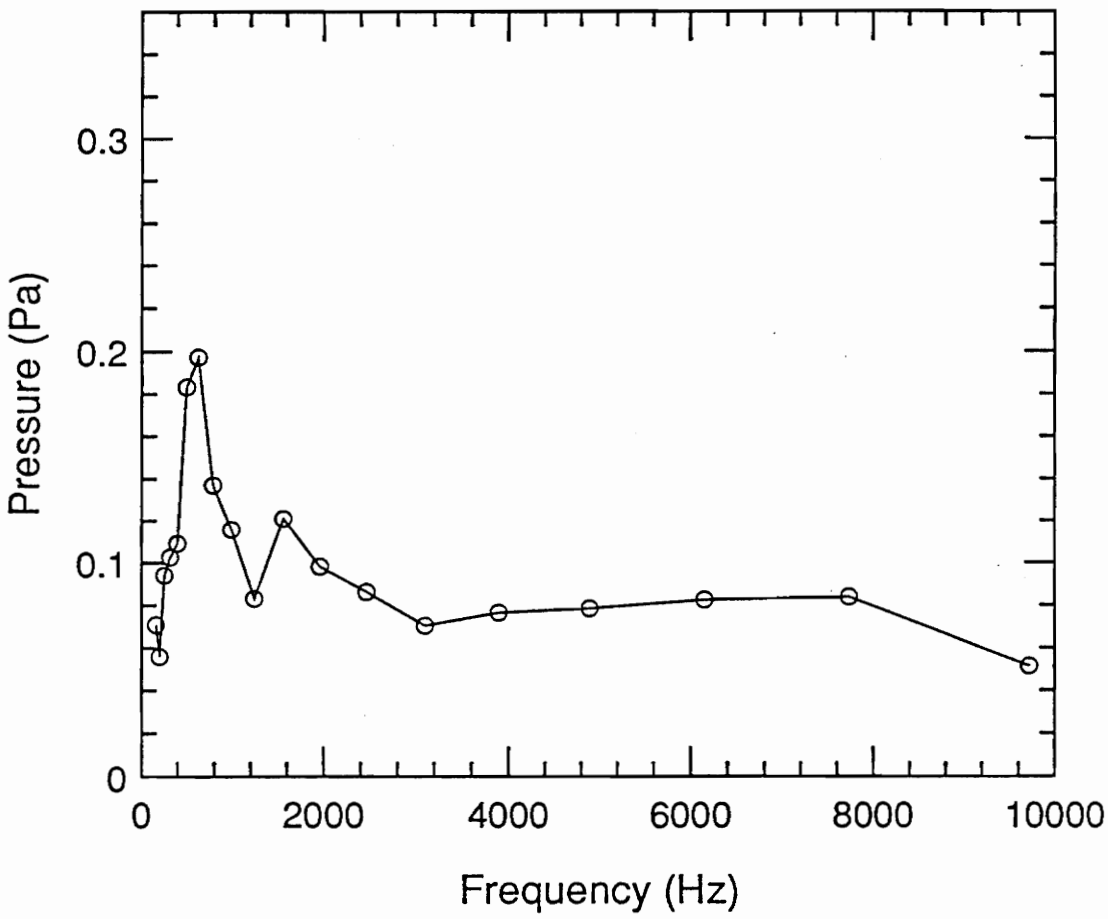

Figure 65. 1/3-Octave Spectrum for Acetylene: U = 75 m/s, D = 0.165 cm

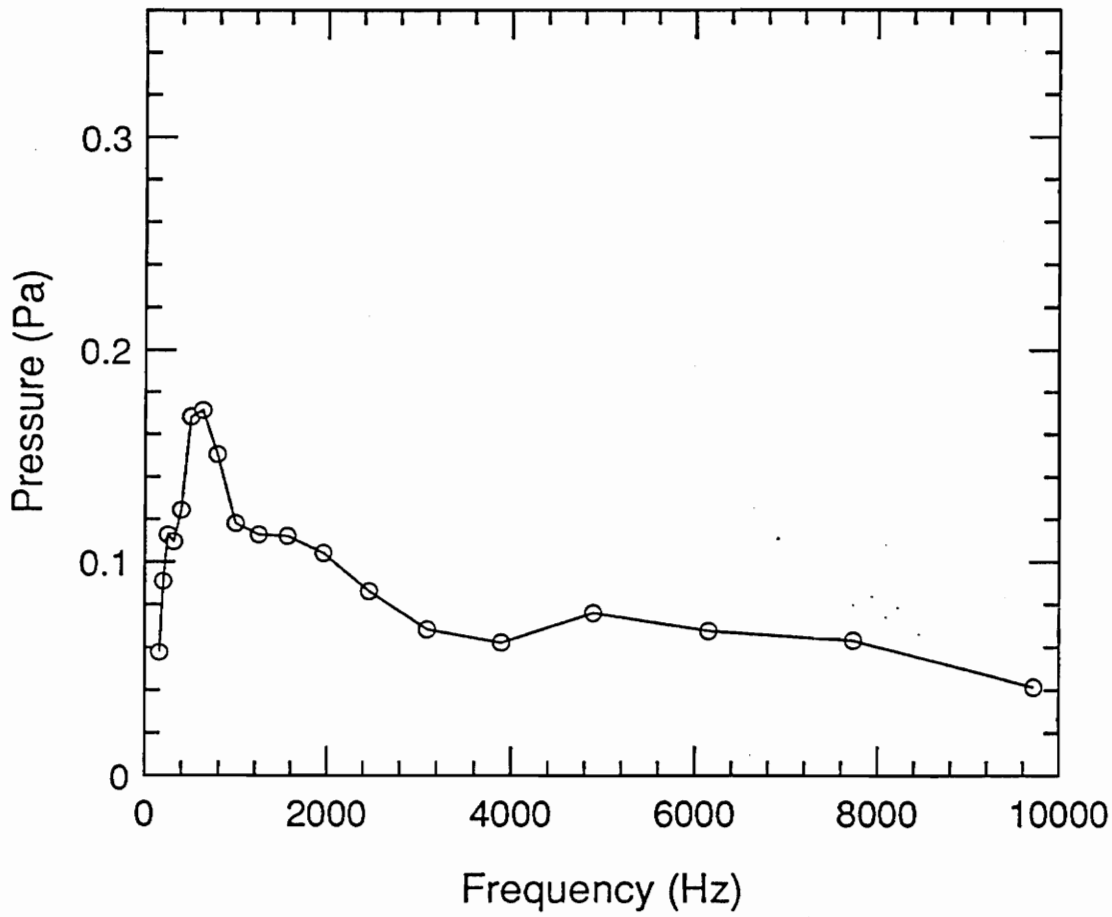

Figure 66. 1/3-Octave Spectrum for Acetylene: U = 75 m/s, D = 0.165 cm

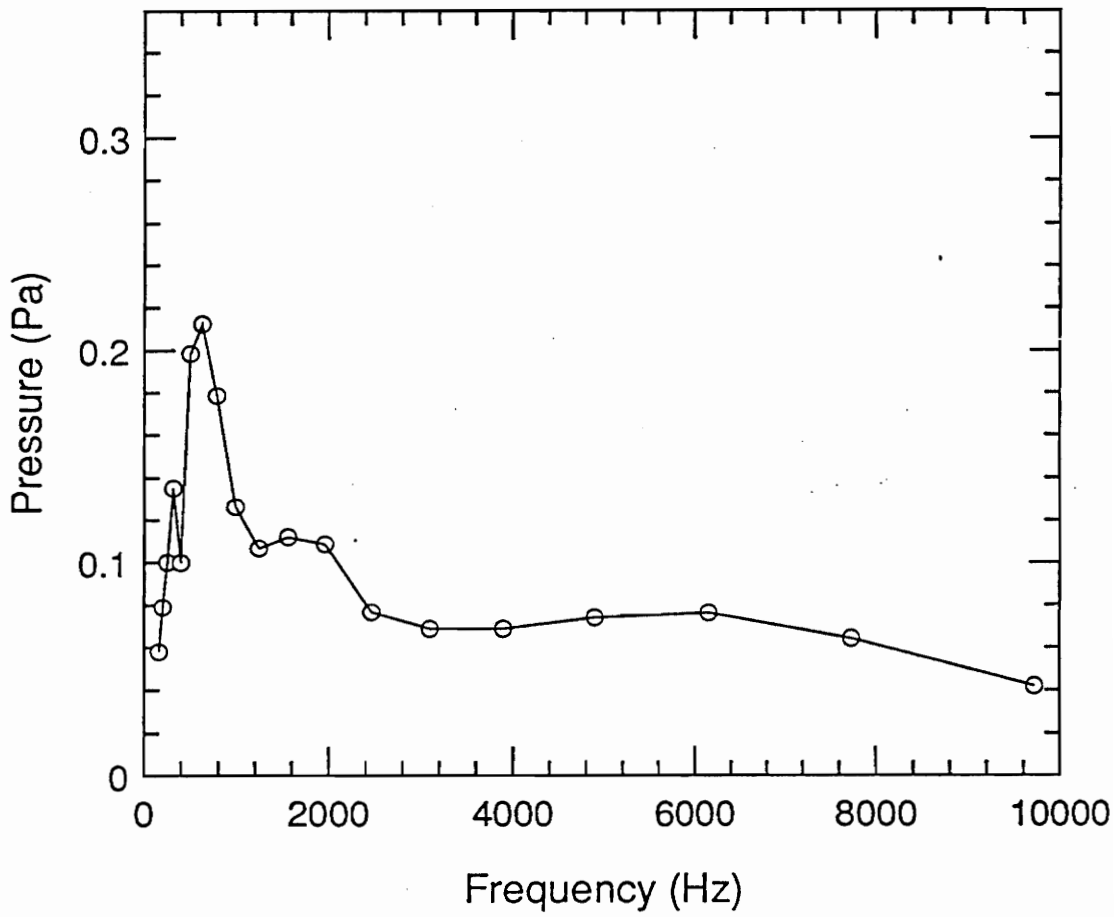

Figure 67. 1/3-Octave Spectrum for Acetylene: U = 75 m/s, D = 0.165 cm

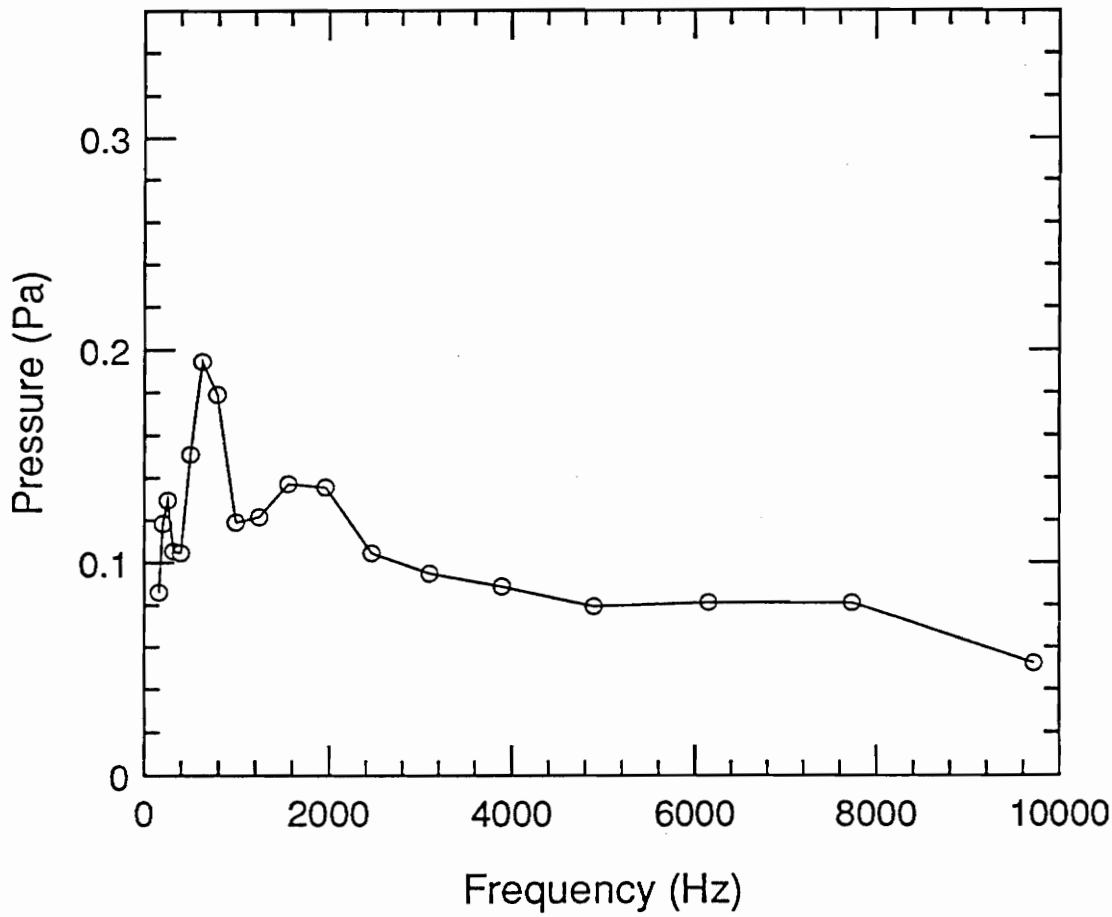

Figure 68. 1/3-Octave Spectrum for Acetylene: U = 100 m/s, D = 0.165 cm

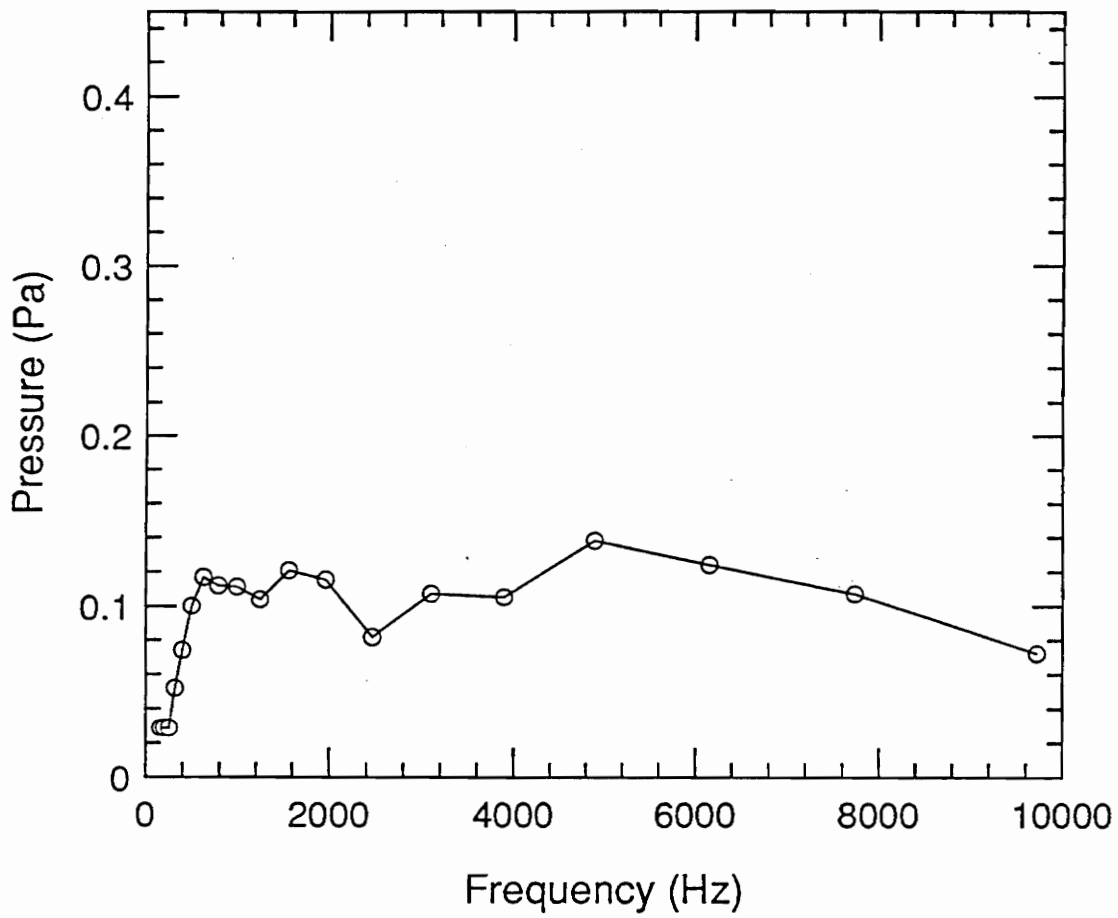

Figure 69. 1/3-Octave Spectrum for Acetylene: U = 50 m/s, D = 0.356 cm

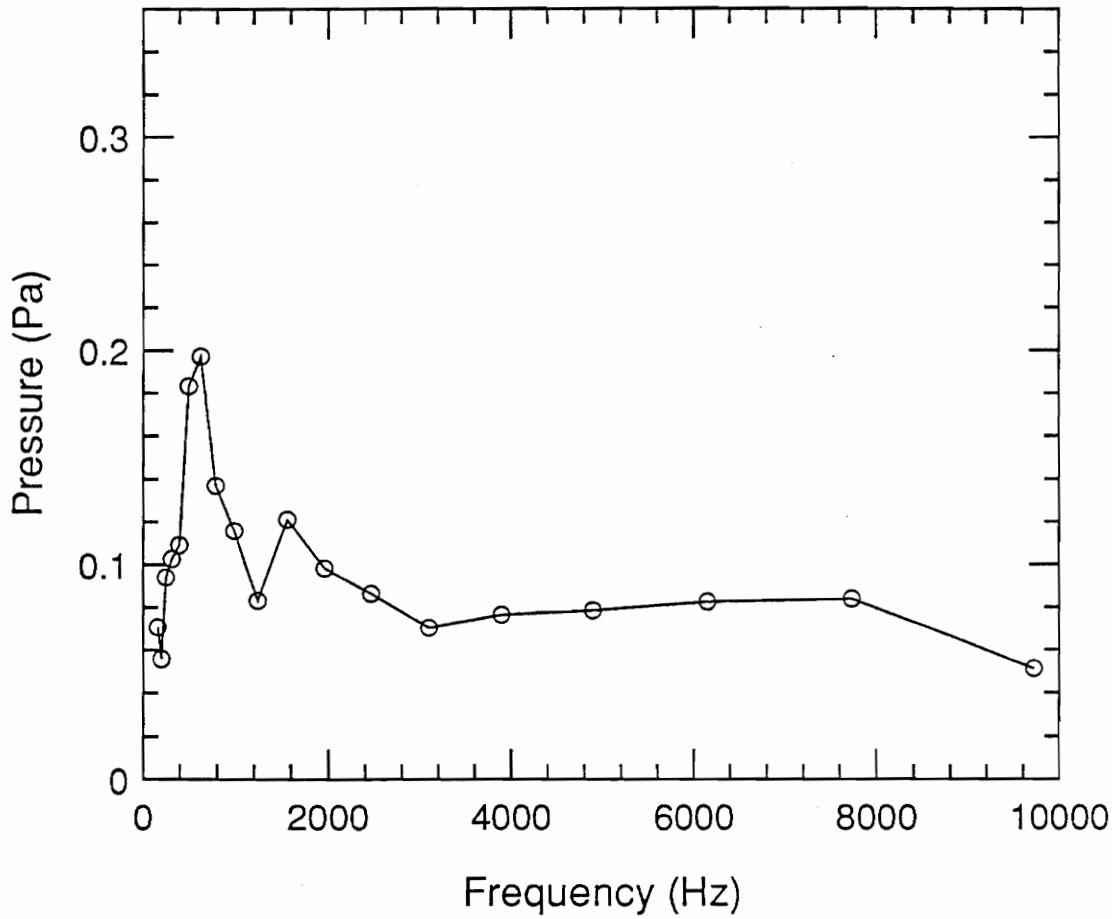

Figure 70. 1/3-Octave Spectrum for Acetylene: U = 75 m/s, D = 0.356 cm

Vita

The author was born in Winter Park, Florida on August 1, 1966 and graduated from Spring Valley High School, in Columbia South Carolina, in June of 1984. In September of that year, the author enrolled in the college of Engineering at the University of Miami and subsequently earned the degree of Bachelor of Science in Mechanical Engineering in May of 1988.

In September of 1988, the author entered the Graduate School at Virginia Polytechnic Institute and State University to begin work on the degree of Master of Science in Mechanical Engineering. Upon completion of this degree, he plans on "selling out" in pursuing a Masters in Business Administration.

William J. Westerman III